IOWA STATE UNIVERSITY
Digital Repository

Graduate Theses and Dissertations | Graduate College

2014

Function of class one nonsymbiotic plant hemoglobins

Xiaoguang Wang
Iowa State University

Follow this and additional works at: http://lib.dr.iastate.edu/etd

 Part of the Agriculture Commons, Biochemistry Commons, Microbiology Commons, and the Plant Sciences Commons

Recommended Citation
Wang, Xiaoguang, "Function of class one nonsymbiotic plant hemoglobins" (2014). *Graduate Theses and Dissertations*. Paper 14253.

This Dissertation is brought to you for free and open access by the Graduate College at Digital Repository @ Iowa State University. It has been accepted for inclusion in Graduate Theses and Dissertations by an authorized administrator of Digital Repository @ Iowa State University. For more information, please contact digirep@iastate.edu.

Function of class one nonsymbiotic plant hemoglobins

by

Xiaoguang Wang

A dissertation submitted to the graduate faculty

in partial fulfillment of the requirements for the degree of

DOCTOR OF PHILOSOPHY

Major: Genetics

Program of Study Committee:
Mark Hargrove, Co-Major Professor
Thomas Bobik, Co-Major Professor
Alan DiSpirito
Basil Nikolau
Gregory Phillips

Iowa State University

Ames, Iowa

2014

Copyright © Xiaoguang Wang, 2014. All rights reserved.

TABLE OF CONTENTS

ACKNOWLEDGEMENTS iv

CHAPTER 1. INTRODUCTION: REACTIONS BETWEEN HEMOGLOBINS AND INORGANIC NITROGEN COMPOUNDS 1

Reactions with Nitrite 2
Reactions with Nitric Oxide 5
References 7
Abbreviations 9
Figures and Legends 10

CHAPTER 2. NITRIC OXIDE IN PLANTS: THE ROLES OF ASCORBATE AND HEMOGLOBIN 11

Abstract 11
Introduction 12
Materials and Methods 16
Results 20
Discussion 26
References 30
Tables 35
Figures and Legends 37

CHAPTER 3. GROWTH PHENOTYPES OF *E. COLI* NITRITE REDCUTASE MUTANTS REVEAL A ROLE FOR NIR NITRIE ASSIMILATION DURING ANAEROBIC NITRATE RESPIRATION 43

Introduction 43
Materials and Methods 49
Results 52
Discussion 62
References 65
Tables 68
Figures and Legends 70

CHAPTER 4. STUDY OF S-NITROSOGLUTATHIONE REDUCTASE AS A POSSIBLE COFACTOR OF CLASS 1 NONSYMBIOTIC HEMOGLOBIN FOR PLANT HYPOXIC NITRITE REDUCTION 81

Introduction 81
Materials and Methods 83
Results 85
Discussion 89

References 91
Figures and Legends 94

CHAPTER 5. CONCLUSION 102
References 103

ACKNOWLEDGEMENTS

I would like to thank my major professor Dr. Mark Hargrove, my co-major professor Dr. Thomas Bobik and my program of study committee: Dr. Alan DiSpirito, Dr. Basil Nikolau and Dr. Gregory Phillips. I could never have done any work in this thesis without your guidance and support.

I want to offer my appreciation to all of the faculty and staff in the Roy J. Carver Department of Biochemistry, Biophysics, and Molecular Biology. Thank you for providing an outstanding academic environment and effective administrative services that are crucial for me as a graduate student. I also would like to thank all of lab mates, past and present, for making the lab an awesome place to work. Thank you, Dr. James Trent III, Dr. Smita Kakar and Dr. Ryan Sturms for teaching me all the experimental techniques. Thank you Navjot Singh and Denis Tamiev for your countless favors and all the lunches we went together. Thank you Ashley Spooner for your hard work to organize the whole lab.

Thank you, all of my dear friends I met in Ames. You are the ones who made my 7 years' stay in this small town truly amazing and memorable. I could not go this far without your accompany and encouragement. No matter all those wonderful moments we shared or all those challenges we faced together, are and will always be invaluable treasures in my life.

I would like to thank my family, my uncle Zhenzhuang, aunt Weihuang and aunt Jianhua for their tremendous support. And especially thank you, Mom and Dad, you are the best parents I could ever ask for. Without you, I would never have the chance to study abroad. When life was getting tough, you were the ones who encouraged and showed

faith on me. For all the good times, you were always the first to cheer for me. To me, these have meant so much.

CHAPTER 1

INTRODUCTION: REACTIONS BETWEEN HEMOGLOBINS AND INORGANIC NITROGEN COMPOUNDS

The research topics of this thesis are all related to the reactions between plant class 1 nonsymbiotic hemoblogin (nsHb1) and nitrite and nitric oxide under hypoxic or anoxic conditions. This chapter is a general introduction of reactions between hemoglobins and these two reactive inorganic nitrogen compounds, to help one better understand research chapters 2, 3 and 4.

Reactions of heme proteins with inorganic nitrogen compounds are wide-spread in biology, with hemes involved in both dissimilatory and assimilatory nitrogen metabolism, and ammonium oxidation. In many of these cases the heme cofactors are only transferring elections, but in others they serve as the active site for binding and reacting with the nitrogen metabolite. Less is known about the reactions of Hbs with nitrogenous compounds. Azide and cyanide bind tightly and reversibly to most ferric Hbs [1], and less tightly to the ferrous oxidation states. Exogenous imidazole will also bind to Hbs, and mimic hexacoordination [2]. Nitric oxide binds reversibly to both oxidation states, but tightest to ferrous heme [1]. The reactions described below outline not only the reversible reactions with Hbs, but also those that result in redox changes for the heme and substrate. These include chemical reactions with nitric oxide, nitrite, and hydroxylamine.

Reactions with Nitrite

Hbs react with nitrite in both the deoxyferrous and oxyferrous oxidation states, with markedly different outcomes. The reaction between oxyhemoglobin (oxy-rbcHb) and nitrite was first reported by Arthur Gamgee in 1868 [3], who observed the oxidation of oxy-rbcHb upon addition of nitrite. Although the products of this reaction were firmly identified as methemoglobin (met-rbcHb) and nitrate [4], and the reaction is recognized as a nitrite-induced autooxidation [5], the actual mechanism is still unclear. Keszler *et al.* proposed a model involving H_2O_2 and the ferrylhemoglobin (ferrylHb) radical in which nitrite is involved in the faster propagation-phase of the reaction [6]. Nevertheless, this reaction explains the toxicity of nitrite to humans due to hemoglobinemia resulting from heme oxidation and dissociation [7, 8].

Surprisingly, all of the studies concerning nitrite reactions with oxyHb involve pxHbs (mostly human blood Hb and muscle myoglobins), and not hxHbs. The fact that many hxHbs are often unstable with oxygen is certainly to blame, but others, such as nsHb1 from plants, can form relatively stable oxy complexes [9, 10]. Class 1 nsHbs are expressed during hypoxia, which is also associated with elevated levels of nitrite [11, 12] Thus, if oxygen concentrations were high enough to bind the Hb, there would be a potential for the reaction.

The second reaction of Hbs with nitrite is much more relevant to hxHbs. At the beginning of 1900s, John Haldane reported the reaction between deoxyhemoglobin (deoxy-rbcHb) and nitrite while researching the chemistry of meat curing [13]. He found that the red color of salted meat results from nitric oxide (NO) binding to deoxyferrous Hb, forming a ferrous-nitrosyl rbcHb complex (which to the eye resembles the color of

fresh oxygenated meat more than the brown color associated with oxidation). NO is produced by the reaction of nitrite with deoxyHb in the absence of oxygen. The bimolecular reaction passes one electron from ferrous heme to nitrite, making NO and ferric heme (Reaction 3). Since binding of NO to ferrous Hb (reaction 2) is extremely rapid (k_{NO} ~ 100 μM^{-1} s^{-1}) [14], the NO formed in the reaction rapidly binds the remaining ferrous Hb making the stable ferrous-NO complex associated with red color.

$$Hb^{Fe(II)} + NO_2^- + H^+ \xrightarrow{k_{NO_2^-}} Hb^{Fe(III)} + NO + OH^- \quad \text{(Reaction 1)}$$

$$Hb^{Fe(II)} + NO \xrightarrow{k_{NO}} Hb^{Fe(II)}NO \quad \text{(Reaction 2)}$$

$$2Hb^{Fe(II)} + NO_2^- + H^+ \xrightarrow{k_{obs}} Hb^{Fe(III)} + Hb^{Fe(III)}NO + OH^- \quad \text{(Reaction 3)}$$

Nitrite reductase activity only occurs with the deoxyferrous form of Hbs and is common in both pxHbs and hxHbs **(**Table 2**)**. The speed of the reaction varies between different Hbs, and does not correlate with coordination state or strength of coordination in hxHbs. Human rbcHb is not a good nitrite reductase in the deoxyferrous form (T state). But when it is saturated by 40-60% oxygen (about half T state, half R state), it shows the maximum nitrite reductase activity (6 M^{-1} s^{-1}) [15-17]. Deoxy Mb reduces nitrite with a bimolecular rate constant of 11 M^{-1} s^{-1}, reportedly protecting heart cells from myocardial ischemia-reperfusion injury [18, 19].

Plant class 1 nsHbs and *Syn*Hb react relatively rapidly with nitrite (~ 160 M^{-1} s^{-1}) [20], compared to rbcHb and Mb, which are slower (~ 2 M^{-1} s^{-1}), and animal hxHbs (Ngb and Cgb), which are slower still (< 1 M^{-1} s^{-1}) [21, 22]. In the case of Ngb, the wild type protein reduces nitrite very slowly, but when the distal histidine is mutated to leucine or

glutamine, the rate increase dramatically to ~ 250 M^{-1} s^{-1}, on par with the plant nsHbs [21]. Thus, hexacoordination is not required for rapid rates of nitrite reduction, and in fact hexacoordination in wild type Ngb clearly inhibits the reaction.

The reduction of nitrite by both pxHbs and hxHbs is thought to play important roles in the diverse tissues where these different proteins are located. In plants and cyanobacteria, nitrate and nitrite concentration can increase to high (millimolar) levels, especially under hypoxic conditions [11, 12]. In this case, plant nsHbs could effectively reduce nitrite to aid in nitrogen assimilation to produce ammonium, or dissimilation to aid the regeneration of NAD^+. In support of this mechanism is the fact that nsHb1 also reduces hydroxylamine to ammonia, another reaction on this pathway. Along these lines, the hexacoordinate hemoglobin from the cyanobacterium *synechococcus* aids in growth on high concentrations of nitrate, possibly by detoxifying peroxynitrite that resulting from NO production by nitrate or nitrite reductase [23].

In animals, nitrite reductase activity of Ngb is proposed to be important in regulating NO metabolism for the protection of neurons during hypoxia [24-26]. Petersen *et al.* studied the reaction between murine deoxy Ngb and nitrite [27] reporting a second order rate constant of 5.1 M^{-1} s^{-1} for the reaction. They found that ferric Ngb was the main product, and ferrous nitrosyl Ngb was present in smaller amounts (less than 20% of total product). This high product ratio of ferric to ferrous nitrosyl Ngb was explained as being due to the lower affinity of Ngb for NO compared to Mb and Hb [14]. A recent study of deoxyferrous human Ngb nitrite reduction by Tiso *et al.* [21] measured a rate constant of 0.12 M^{-1} s^{-1} resulting in a 1:1 ratio of ferric Ngb and ferrous nitrosyl Ngb. Tiso *et al.* also proposed that the nitrite reductase activity of Ngb is correlated with

coordination state, based on the fact that the pentacoordinate Ngb mutant proteins H64L and H64Q speed up nitrite reduction ~2000 times compared to the wild type protein. Mutations that strengthen coordination (C55A and C46A) were shown to slow the reaction.

Cgb is a hxHb that is expressed in almost all tissues [28, 29]**.** Despite its slow rate of nitrite reduction (0.14 M^{-1} s^{-1}), Li *et al* have recently suggested its function as a nitrite reductase might be significant [22]. Nitrite reduction by deoxy ferrous Cgb produces a slightly smaller ratio of nitrosyl Cgb than ferric Cgb, and nM scale NO release from this reaction was measured by EPR and a gas phase chemilluminescence NO analyzer. Together with Cgb's up-regulation during hypoxia [30], these results support a hypothesis involving NO metabolism during hypoxia.

Reactions with Nitric Oxide

Just as the reactions of Hbs with nitrite depends greatly on the starting oxidation and ligand state of the heme iron, so do those with NO. Deoxy Hbs generally reversibly bind NO with very high affinity constants, which are in the picomolar range for blood Hb and Mb [31]. Ferric Hbs will also reversibly bind NO with much lower affinity, and can be slowly reduced by NO. In general, hexacoordination lowers NO affinity in both oxidations states [14, 32], and has no clear effect on NO-induced reduction of the ferric proteins [33].

If NO contacts the oxyferrous form of Hb, a very rapid chemical reaction called "NO dioxygenation" (NOD) occurs, in which NO reacts with bound oxygen eventually making nitrate and oxidizing the heme iron (Reaction 4). NOD is the function of

bacterial and fungal "flavohemoglobins" (flavoHbs), who use it to detoxify NO in their surroundings or resulting from endogenous sources [34-37]. As implied by their name, flavoHbs have a heme domain and a flavin domain [38]. In the NOD reaction, the oxyferrous heme domain reacts with NO to make nitrate and ferric heme. The flavin domain then shuttles an electron from NADH to the heme to re-reduce it so that it can bind oxygen to start the cycle again.

$$Hb^{Fe(II)}O_2 + NO \longrightarrow Hb^{Fe(III)}\text{–}OONO \longrightarrow Hb^{Fe(III)} + NO_3^- \qquad \text{(Reaction 4)}$$

While NOD activity was first found in *E.coli* flavoHb [35], most Hbs (both hexa- and pentacoordinate) can carry out the oxidative NOD reaction very effectively [33]. However, flavoHb can rapidly finish the reductive half of the NOD reaction by using NADH to reduce the ferric heme back to the ferrous form (Figure 1-1). For Hbs to scavenge NO using the NOD mechanism, there must be an effective mechanism for heme reduction. NOD activity has been ascribed to plant nsHbs, and three mechanisms of reduction have been proposed including specific enzymes, free flavins [39] and ascorbic acid [40]. In the ascorbic acid mechanism, it was proposed that monodehydroascorbate reductase (MDHAR)-mediated ascorbate reduction of metHb might facilitate NO scavenging. However, it has been shown that ascorbic acid reduction of ferric rice nsHb1 is very slow (0.01 $mM^{-1}min^{-1}$) compared to NADH reduction of flavoHb [36], and that hemoglobin reduction by ascorbate is not affected by MDHAR *in vitro*.

References

1. Antonini, E., Brunori, M., *Hemoglobin and myoglobin in their reactions with ligands*. 1971, Amsterdam: North-Holland Pub. Co.
2. Barrick, D., *Replacement of the proximal ligand of sperm whale myoglobin with free imidazole in the mutant His-93-->Gly.* Biochemistry, 1994. **33**(21): p. 6546-54.
3. Gamgee, A., *Researches on the Blood. On the Action of Nitrites on Blood.* Philos. Trans. R. Soc. London, 1868. **158**: p. 589-625.
4. Kim-Shapiro, D.B., et al., *The reaction between nitrite and hemoglobin: the role of nitrite in hemoglobin-mediated hypoxic vasodilation.* J Inorg Biochem, 2005. **99**(1): p. 237-46.
5. Kosaka, H., K. Imaizumi, and I. Tyuma, *Mechanism of autocatalytic oxidation of oxyhemoglobin by nitrite. An intermediate detected by electron spin resonance.* Biochim Biophys Acta, 1982. **702**(2): p. 237-41.
6. Keszler, A., et al., *The Reaction between Nitrite and Oxyhemoglobin: A MECHANISTIC STUDY.* Journal of Biological Chemistry, 2008. **283**(15): p. 9615-9622.
7. Smith, R.P., *The nitrite methemoglobin complex--its significance in methemoglobin analyses and its possible role in methemoglobinemia.* Biochem Pharmacol, 1967. **16**(9): p. 1655-64.
8. Swann, P.F., *The toxicology of nitrate, nitrite and n-nitroso compounds.* Journal of the Science of Food and Agriculture, 1975. **26**(11): p. 1761-1770.
9. Kundu, S., J.T. Trent, 3rd, and M.S. Hargrove, *Plants, humans and hemoglobins.* Trends Plant Sci, 2003. **8**(8): p. 387-93.
10. Smagghe, B.J., et al., *Review: correlations between oxygen affinity and sequence classifications of plant hemoglobins.* Biopolymers, 2009. **91**(12): p. 1083-96.
11. Ferrari, T.E. and J.E. Varner, *Intact tissue assay for nitrite reductase in barley aleurone layers.* Plant Physiol, 1971. **47**(6): p. 790-4.
12. Gupta, K.J., et al., *On the origins of nitric oxide.* Trends in plant science, 2011. **16**(3): p. 160-8.
13. Haldane, J., *The Red Colour of Salted Meat.* J Hyg (Lond), 1901. **1**(1): p. 115-22.
14. Van Doorslaer, S., et al., *Nitric oxide binding properties of neuroglobin. A characterization by EPR and flash photolysis.* J Biol Chem, 2003. **278**(7): p. 4919-25.
15. Huang, Z., et al., *Enzymatic function of hemoglobin as a nitrite reductase that produces NO under allosteric control.* J Clin Invest, 2005. **115**(8): p. 2099-107.
16. Kozlov, A.V., et al., *Mechanisms of vasodilatation induced by nitrite instillation in intestinal lumen: possible role of hemoglobin.* Antioxid Redox Signal, 2005. **7**(3-4): p. 515-21.
17. Rong, Z. and C.E. Cooper, *Modeling hemoglobin nitrite reductase activity as a mechanism of hypoxic vasodilation?* Adv Exp Med Biol, 2013. **789**: p. 361-8.
18. Hendgen-Cotta, U.B., et al., *Nitrite reductase activity of myoglobin regulates respiration and cellular viability in myocardial ischemia-reperfusion injury.* Proc Natl Acad Sci U S A, 2008. **105**(29): p. 10256-61.

19. Hendgen-Cotta, U.B., M. Kelm, and T. Rassaf, *A highlight of myoglobin diversity: the nitrite reductase activity during myocardial ischemia-reperfusion.* Nitric Oxide, 2010. **22**(2): p. 75-82.
20. Sturms, R., A.A. DiSpirito, and M.S. Hargrove, *Plant and cyanobacterial hemoglobins reduce nitrite to nitric oxide under anoxic conditions.* Biochemistry, 2011. **50**(19): p. 3873-8.
21. Tiso, M., et al., *Human neuroglobin functions as a redox-regulated nitrite reductase.* J Biol Chem, 2011. **286**(20): p. 18277-89.
22. Li, H., et al., *Characterization of the mechanism and magnitude of cytoglobin-mediated nitrite reduction and nitric oxide generation under anaerobic conditions.* J Biol Chem, 2012. **287**(43): p. 36623-33.
23. Scott, N.L., et al., *Functional and structural characterization of the 2/2 hemoglobin from Synechococcus sp. PCC 7002.* Biochemistry, 2010. **49**(33): p. 7000-11.
24. Brown, G.C., *Nitric oxide and mitochondrial respiration.* Biochim Biophys Acta, 1999. **1411**(2-3): p. 351-69.
25. Loke, K.E., et al., *Nitric oxide modulates mitochondrial respiration in failing human heart.* Circulation, 1999. **100**(12): p. 1291-7.
26. Allen, J.D. and A.J. Gow, *Nitrite, NO and hypoxic vasodilation.* Br J Pharmacol, 2009. **158**(7): p. 1653-4.
27. Petersen, M.G., S. Dewilde, and A. Fago, *Reactions of ferrous neuroglobin and cytoglobin with nitrite under anaerobic conditions.* J Inorg Biochem, 2008. **102**(9): p. 1777-82.
28. Trent, J.T., 3rd and M.S. Hargrove, *A ubiquitously expressed human hexacoordinate hemoglobin.* J Biol Chem, 2002. **277**(22): p. 19538-45.
29. Burmester, T., et al., *Cytoglobin: A Novel Globin Type Ubiquitously Expressed inVertebrate Tissues.* Molecular Biology and Evolution, 2002. **19**(4): p. 416-421.
30. Schmidt, M., et al., *Cytoglobin is a respiratory protein in connective tissue and neurons, which is up-regulated by hypoxia.* J Biol Chem, 2004. **279**(9): p. 8063-9.
31. Eich, R.F., et al., *Mechanism of NO-induced oxidation of myoglobin and hemoglobin.* Biochemistry, 1996. **35**(22): p. 6976-83.
32. Herold, S., et al., *Reactivity studies of the Fe(III) and Fe(II)NO forms of human neuroglobin reveal a potential role against oxidative stress.* J Biol Chem, 2004. **279**(22): p. 22841-7.
33. Smagghe, B.J., J.T. Trent, III, and M.S. Hargrove, *NO Dioxygenase Activity in Hemoglobins Is Ubiquitous In Vitro, but Limited by Reduction In Vivo.* PloS one, 2008. **3**(4): p. e2039.
34. Poole, R.K., et al., *Nitric oxide, nitrite, and Fnr regulation of hmp (flavohemoglobin) gene expression in Escherichia coli K-12.* J Bacteriol, 1996. **178**(18): p. 5487-92.
35. Gardner, P.R., et al., *Nitric oxide dioxygenase: an enzymic function for flavohemoglobin.* Proc Natl Acad Sci U S A, 1998. **95**(18): p. 10378-83.
36. Gardner, A.M., et al., *Steady-state and transient kinetics of Escherichia coli nitric-oxide dioxygenase (flavohemoglobin). The B10 tyrosine hydroxyl is essential for dioxygen binding and catalysis.* The Journal of biological chemistry, 2000. **275**(17): p. 12581-9.

37. Gardner, P.R., *Nitric oxide dioxygenase function and mechanism of flavohemoglobin, hemoglobin, myoglobin and their associated reductases.* J Inorg Biochem, 2005. **99**(1): p. 247-66.
38. Bonamore, A. and A. Boffi, *Flavohemoglobin: structure and reactivity.* IUBMB Life, 2008. **60**(1): p. 19-28.
39. Sainz, M., et al., *Plant hemoglobins may be maintained in functional form by reduced flavins in the nuclei, and confer differential tolerance to nitro-oxidative stress.* The Plant Journal, 2013: p. n/a-n/a.
40. Igamberdiev, A.U., N.V. Bykova, and R.D. Hill, *Nitric oxide scavenging by barley hemoglobin is facilitated by a monodehydroascorbate reductase-mediated ascorbate reduction of methemoglobin.* Planta, 2006. **223**(5): p. 1033-40.

Abbreviations

Cgb: cytoglobin

Hb: hemoglobin

hxHb: hexacoordinated hemoglobin

Mb: myoglobin

MDHAR: monodehydroascorbate reductase

metHb: hemoglobin with its heme iron in ferric oxidation state

Ngb: neuroglobin

NOD: nitric oxide dioxygenation

nsHb1: nonsymbiotic hemoglobin class 1

oxyHb: hemoglobin with its heme binding oxygen molecule

SynHb: *Synechocystis* hemoglobin

Figures and Legends

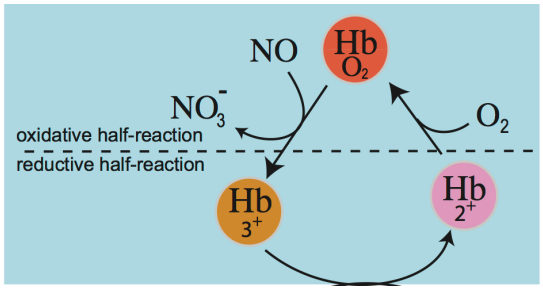

Figure 1-1. The nitric oxide dioxygenase (NOD) reaction. Oxy hemoglobins (Hb) will react with NO to make nitrate and ferric Hb. After the ferric Hb is reduced back to ferrous state (in the case of flavohemoglobin, using NADH), it will bind oxygen (if present) to start the reaction again.

CHAPTER 2

NITRIC OXIDE IN PLANTS:

THE ROLES OF ASCORBATE AND HEMOGLOBIN

A research paper in published in PLoS ONE, December 2013

Xiaoguang Wang[1], Mark Hargrove[2]

Abstract

Ascorbic acid and hemoglobins have been linked to nitric oxide metabolism in plants. It has been hypothesized that ascorbic acid directly reduces plant hemoglobin in support of NO scavenging, producing nitrate and monodehydroascorbate. In this scenario, monodehydroascorbate reductase uses NADH to reduce monodehydroascorbate back to ascorbate to sustain the cycle. To test this hypothesis, rates of rice nonsymbiotic hemoglobin reduction by ascorbate were measured directly, in the presence and absence of purified rice monodehyroascorbate reductase and NADH. Solution NO scavenging was also measured methodically in the presence and absence of rice nonsymbiotic hemoglobin and monodehydroascorbate reductase, under hypoxic and normoxic conditions, in an effort to gauge the likelihood of these proteins affecting NO metabolism in plant tissues. Our results indicate that ascorbic acid slowly reduces rice nonsymbiotic hemoglobin at a rate identical to myoglobin reduction. The product of the reaction is monodehydroascorbate, which can be efficiently reduced back to ascorbate in the

[1] Contributed in bench works, experimental design and writing.
[2] Contributed in experimental design and writing. To whom correspondence should be addressed.

presence of monodehydroascorbate reductase and NADH. However, our NO scavenging results suggest that the direct reduction of plant hemoglobin by ascorbic acid is unlikely to serve as a significant factor in NO metabolism, even in the presence of monodehydroascorbate reductase.

Finally, the possibility that the direct reaction of nitrite/nitrous acid and ascorbic acid produces NO was measured at various pH values mimicking hypoxic plant cells. Our results suggest that this reaction is a likely source of NO as the plant cell pH drops below 7, and as nitrite concentrations rise to mM levels during hypoxia.

Introduction

Ascorbic acid (AA) is an abundant and multifaceted biomolecule found in most living organisms [1-3]. The L-stereoisomer known as "vitamin C" is a cofactor for enzymatic reactions in animals that are important in collagen synthesis and wound repair. Additionally, humans normally maintain AA concentrations in the blood near 70 μM for the purpose of general antioxidant activity. These properties stem from the facile redox chemistry linking AA, monodehydroascorbic acid (MDHA), and dehydroascorbic acid (DHA) (Figure 2-1A).

The antioxidant role of AA in plants is evident from the relatively high concentrations found in many tissues [4]. On average, the AA concentration in *Arabidopsis* cells is 5.6 mM [5], and it is found in many sub-cellular organelles including mitochondria, peroxisomes, vacuoles, cytosol, the cell wall, and chloroplasts, where concentrations can reach 50 mM [4, 6-10]. Such high concentrations in metabolically active areas indicate an important role for AA in the defense against damage by reactive

oxygen species (ROS). AA is also important for mitigating damage by ROS produced in hypoxic and anoxic roots, which plants experience in a variety of soil conditions [11, 12].

The AA-glutathione cycle in plants. Plants contain a relatively robust mechanism for exploiting the antioxidant properties of AA, known as the AA-glutathione cycle [13, 14] (Figure 2-1C). In this cycle, AA reduces hydrogen peroxide (via AA peroxidase [15], APX), superoxide, and hydroxyl radical, each a product of excess reducing power in the cell. In these reactions, AA is initially oxidized to MDHA [16, 17], but DHA eventually results from spontaneous disproportionation of MDHA to AA and DHA [18]. The purpose of the cycle is that MDHA and DHA are much less reactive than superoxide, hydroxyl radical, and hydrogen peroxide, and the cell is granted time to dissipate chemical energy through less damaging mechanisms. The AA-glutathione cycle is completed by reduction of MDHA and DHA back to AA. Reduction of DHA is driven by reduced glutathione via the enzyme DHA-reductase (DHAR: EC 1.8.5.1), and reduction of MDHA is coupled to NAD(P)H oxidation by the enzyme MDHA-reductase (MDHAR: EC 1.6.5.4).

Nitric Oxide. Another free radical ROS produced in plants and animals is nitric oxide (NO), which has diverse and important signaling functions and is often produced during hypoxia [19, 20]. NO and AA have even longer histories in the food sciences, where nitrate, nitrite, and AA are used in curing batter to give cured meat its characteristic deep red color [21, 22]. The cause of the color is NO, which binds

hemoglobin and myoglobin and mimics the color of fresh meat. The source of NO in this reaction is the direct reduction of nitrous acid (protonated nitrite) by AA.

The origins of NO in hypoxic plant cells are not completely clear [23], but it is evident that significant NO concentrations are produced in these environments [20, 24]. The cytoplasmic pH of hypoxic plant cells can drop to pH 6.5 or lower [25, 26], while at the same time nitrite can rise to mM concentrations [23, 27] in the presence of similar levels of AA. These conditions are well-suited for NO formation from nitrite as a result of direct reduction by AA. However, this possibility has not yet been addressed directly in the context of plant physiology.

Hemoglobins and NO scavenging. Bacteria and some yeast have a specific mechanism for scavenging NO called the NO dioxygenase (NOD) reaction (Figure 2-1B), in which NO is oxidized to nitrate via an oxygen-dependent reaction catalyzed by the enzyme flavohemoglobin [28, 29]. Flavohemoglobin contains a heme domain that binds oxygen, and a reductase domain that can reduce the heme using electrons from NAD(P)H. Oxy-flavohemoglobin reacts rapidly with NO, forming nitrate and ferric hemoglobin. The reductase domain then reduces the heme, which binds oxygen to complete the cycle (Figure 2-1B).

No such specific mechanism for NO scavenging has yet been affirmed in plants or animals, but it has been hypothesized that nonsymbiotic plant hemoglobins (nsHbs) might participate in this function. This hypothesis is based largely on the ability of oxy-nsHb to carryout the oxidative half-reaction with NO (Figure 2-1B; [30]), and indirectly on increased nsHb expression in several species in response to nitrate, nitrite, and nitric

oxide [31, 32], in NO scavenging ability in several plant species over-expressing nsHb [33-35], decreases in the levels of NO-sensitive enzymes in plants with down-regulated nsHb [36], and increases in NO emission from plants with down-regulated nsHb [24]. However, none of this work characterizes the reductive half of the NOD reaction, consisting of the one electron reduction of ferric nsHb (Figure 2-1B).

nsHb reduction is considered to be the rate limiting step for NO scavenging using the NOD mechanism [37]. Several mechanisms of nsHb reduction have been proposed including specific reductases, free flavins [38], or ascorbic acid [39]. The latter mechanism proposes that AA, with help from MDHAR, might serve as the reducing agent for ferric nsHb in the reductive NOD half-reaction (Figure 2-1B). In this scenario, AA directly reduces ferric nsHb, forming MDHA. MDHAR then uses NAD(P)H to reduce MHDA back to AA, thus coupling the reducing power of NAD(P)H to nsHb reduction in support of NOD function. There are some questions remaining whose answers would provide an important test of the hypothesis. 1) How fast is nsHb reduced by AA? The crux of this hypothesis rests on the ability of AA to reduce nsHb in an efficient manner, yet this reaction has not been measured directly. 2) How does MDHAR affect nsHb reduction by AA? 3) Does the AA/MDHAR system improve nsHb-mediated NO scavenging compared to the AA cycle alone? Finally, a very basic question regarding AA and NO must be answered in order to clarify the origins of NO: 4) Can AA directly reduce nitrite to form measurable NO levels under conditions mimicking hypoxic plant cells?

The experiments presented here address these questions by measuring the kinetics and products of AA reduction of rice nsHb with and without a purified MDHAR, and by

directly measuring NO scavenging by each component of this system in controlled *in vitro* systems. Also measured is the direct production of NO by AA and nitrite as a function of pH, in an effort to gauge the likelihood of this reaction serving as an origin of NO in hypoxic plant cells.

Materials and Methods

Protein Production. *Oryza sativa* (rice) class 1 nonsymbiotic hemoglobin (nsHb) expression and purification was performed as described previously [40]. The cDNA sequence for rice cytosolic monodehydroascorbate reductase (MDHAR) was obtained from GenBank (D85764.1), and used to design PCR primers (Table 2-1). Single stranded *Oryza sativa* cDNA was produced by RT-PCR (Superscript III reverse transcriptase, Invitrogen, #18080-093) from total rice mRNA (a gift from Dr. Reuben Peters, Department of BBMB, Iowa State University), and oligo dT as a primer. Double stranded MDHAR cDNA was then amplified by PCR using the single stranded cDNA as a template, RCMD F and RCMD R as primers (Table 2-1). PCR primers RCMD NheI F and RCMD HindIII R were used to add NheI (5') and HindIII (3') restriction sites flanking MDHAR cDNA by another round of PCR. MDHAR cDNA was then cloned into pET-28a (Novagen, #69864-3) between the NheI and HindIII sites.

His-tagged MDHAR protein was expressed [16, 41] and transformed into *E. coli* BL21(DE3)-RIPL cells (Stratagene, #230280). The cells were grown in LB medium at 37^{o}C until the OD_{600nm} reached 0.6, then expression was induced with 0.5mM IPTG and the temperature lowered to 25°C for 3 hours. The cells were lysed, and the enzyme purified by Ni-NTA chromatography (Qiagen, #30210). Purified enzyme (determined as

a single band by SDS-PAGE) was dialyzed against 50mM phosphate buffer (pH=8.0) and concentrated with an Amicon Ultra-15 Centrifugal Filter Unit (Millipore, #UFC901008). MDHAR concentration was estimated based on its flavin absorbance using the extinction coefficient of 11.3 mM^{-1} cm^{-1} at 450 nm [42].

E. coli Ferredoxin-NADP reductase (FNR) (GenBank: AAA23805.1) was expressed from a pET-28a vector (Novagen, #69864-3). FNR was purified and quantified using the procedure described above for MDHAR.

MDHAR assays. MDHAR enzyme activity was measured by monitoring the decrease in NADH absorbance at 340 nm [16]. A Varian Cary 50 Bio UV/Visible Spectrophotometer with Cary WinUV Kinetics software (Agilent Technologies) was used for data collection. The total reaction volume was 1 ml, containing 50 mM phosphate buffer, pH 8.0. (This pH was chosen for our MDHAR experiments to be consistent with previous work leading to this hypothesis [39].) 0.2 mM NADH was first added into a cuvette with 1 ml phosphate buffer, followed by AA from a freshly prepared stock to generate 3 mM AA in the cuvette, and 0.125 U/ml ascorbate oxidase (AO) (Sigma-Aldrich, # A0157). 1.22 μM (or 0.024 μM) MDHAR were added to start the reaction. All data were plotted and analyzed using IGOR PRO software.

Rice nsHb reduction assays. Rice nsHb reduction assays were carried out by monitoring the increase in absorbance at 575 nm in air, or 415 nm in CO saturated buffer, using methods described previously [37]. CO-saturated buffer was prepared by bubbling CO for 20 minutes into 50 mM phosphate buffer pH 8.0 contained in a 20 ml glass

syringe. All assays were conducted in a cuvette with 1ml of 50 mM phosphate buffer, pH 8.0. For the reactions with high AA concentration (3, 6, 12 mM), 5 μM nsHb was added. For reduction experiments with excess nsHb, AA concentration was 2 μM and nsHb concentration was 10 μM. When NADH and MDHAR were involved, final concentrations were 0.2 mM and 0.73 μM respectively.

EPR measurements of monodehydroascorbate. EPR spectra were collected with a Bruker ESP 300 spectrometer in Dr. Yeon-Kyun Shin's laboratory (Department of Biochemistry, Iowa State University). All spectra were collected at room temperature with the same instrument settings: modulation frequency, 100 kHz; modulation amplitude, 0.71 G [43]; time constant, 1310.72 ms; sweep time, 41.94 s; center field, 3298 G; sweep width, 7 G. All EPR samples were prepared by premixing reagents with 50 mM phosphate buffer (pH 8.0) to a total volume of 10 μl. Concentration of reagents (when involved) were: AA, 3 mM; NADH, 0.2 mM; MDHAR, 0.73 μM; AO, 0.0125 U/μl. Fresh AA was prepared right before experiment, while equilibrated AA was prepared and set at room temperature for 72 hours before experiment. All samples were 6 μl in round capillaries (Vitrotubes, #CV6084).

NO scavenging and production experiments. Solution NO concentrations were measured with an ISO-NO MARK II Nitric Oxide Meter and Duo-18 recording system with Duo-18 software (WPI), which has been described previously [37]. A saturated NO solution (2 mM NO) was prepared by bubbling 50 mM phosphate buffer (pH 8.0) with ultra high purity N_2 gas for 20 minutes, followed by bubbling with ultra high purity NO

for 10 minutes. The NO was sparged through 5M NaOH on its way into the phosphate buffer. To prepare the sample, 1.95 ml of 50 mM phosphate buffer (pH 8.0) was first added into an electrode chamber, which was then sparged with ultra high purity N_2 for 5 minutes for conditions simulating hypoxia. A FOXY-R oxygen electrode and OOISensors software (Ocean Optics, Inc.) were used to measure the oxygen concentrations during the hypoxic experiments. The oxygen electrode was calibrated with two points; 1M sodium dithionite solution (in 50mM phosphate buffer, pH 8.0) was used as 0 μM oxygen, and 50mM phosphate buffer (pH 8.0) bubbled with air for 10 minutes was used as 262 μM oxygen. Based on this calibration, our "hypoxic" conditions are 0.1 μM in oxygen.

To begin the NO scavenging experiments, reagents were added into the chamber for a premix to establish a baseline, and then a final concentration of 50 μM NO (50 μl of the saturated NO solution) was added to start the reaction. Reagents were (when used in the experiment): 3 mM AA, 3 mM DHA, 0.2 mM NADH, 5 μM rice nsHb, 0.73 μM MDHAR, 0.73 μM FNR, and 0.125 U/reaction ascorbate oxidase. Time course data were graphed with IGOR PRO software. Experiments measuring NO production from nitrite at various pH values were conducted by addition of 3mM AA into 2 ml of 10 mM or 200 mM sodium nitrite (in the hypoxic NO electrode chamber) made in 50 mM phosphate buffer of varying pH. Sodium nitrite solutions in all experiments were first verified for pH and bubbled with ultra high purity N_2 for 5 minutes.

Statistical analysis and figure production. The spectra presented in Figure 2-2A and 2-2B are one example out of four independent replicates. Likewise, the time courses

shown in Figure 2-5 and 2-6 are examples of at least four independent replicates, analysis of which led to the values in Table 2-2. All the other curves in Figure 2-2, 2-3, 2-4, 2-5 and 2-6 represent the average of at least three independent replicates. In Table 2-2, the numbers are the average of at least four independent replicates. The absolute variance across the individual observations for each value in Table 2-2 was within 10 % of the average. All data were plotted and analyzed using IGOR PRO software, and figures were produced in Adobe Illustrator.

Results

Rice nsHb is reduced directly by AA and DHA. A reaction key to the NOD function for AA and nsHb is reduction of nsHb by AA. Previous investigations of AA, MDHAR, and nsHb interactions inferred reduction of the Hb from measurements of NO scavenging by root extracts and partially purified nsHb fractions, and NADH consumption by a purified by MDHAR [39]. Neither set of experiments, however, directly measured nsHb reduction by AA.

Results of the reaction of AA with rice nsHb are presented in Figure 2-2. The starting (ferric) and final (oxy-ferrous) spectra are labeled, and demonstrate an isosbestic transition between the two states. Figure 2-2C are time courses for rice nsHb reduction at different AA concentrations, showing an increase in rate at higher AA concentrations expected for a bimolecular reaction. Rate constants for these time courses, and for those associated with rice nsHb reduction by DHA are shown in Figure 2-2D as function of AA concentration. Also included in Figure 2-2D are rate constants for the reduction of horse heart Mb, which were measured to gauge the specificity of the reaction for rice nsHb. In

all cases, the rate constants are linearly dependent on AA and DHA concentrations, and fits yield bimolecular rate constants of 0.01 $mM^{-1}min^{-1}$ for nsHb and Mb, and 0.003 $mM^{-1}min^{-1}$ for reduction of nsHb by DHA.

Reduction of a ferric Hb to the ferrous oxidation state requires one electron. If the reduction is coupled to AA oxidation, the initial product is expected to be the MDHA radical. As most of the experiments in this article involve redox reactions with AA, it is prudent to characterize the chemical state of AA in our solutions, and document product formation. For MDHA, this is accomplished by measuring the room temperature EPR signal associated with the MDHA radical [43]. When 3mM AA is freshly dissolved, the solution initially contains MDHA on the order of 10 nM [43] (Figure 2-3A). The MDHA signal decays slowly (over hours) to an "equilibrated" value of ~ 1 nM, which is stable indefinitely. Addition of ferric rice nsHb to equilibrated AA results in an increase in the MDHA EPR signal (Figure 2-3B). Thus, as expected for a one-electron Hb reduction by AA, it results in the production of MDHA.

The role of MDHAR in nsHb reduction by AA. To test the effects of MDHAR on AA-mediated nsHb reduction, an MDHAR from rice was expressed using recombinant methods and purified to a single band as measured by SDS-PAGE. Rice MDHAR had the expected molecular mass of 46.6 kD, and purified from bacteria with a visible absorption spectrum characteristic of a flavoprotein (Figure 2-4A). Two experiments confirmed that our purified rice MDHAR contained the expected MDHA reductase activity. In the first, addition of MDHAR to a 3mM solution of fresh AA (in the presence of NADH) completely removed the EPR signal associated with MDHA

(Figure 2-4B). EPR was also used to confirm that AAOx produces MDHA from AA in our reaction conditions, so that we could be confident of substrate production for the reactions in Figure 2-4C). In the second experiment, MDHAR oxidized NADH only in the presence of MDHA (produced from AA and AAOx), and at rates proportional to MDHAR concentration (Figure 2-4C). Thus, our purified rice MDHAR has the expected ability to couple MDHA reduction to NADH oxidation.

Two experiments were also used to measure the effects of MDHAR on nsHb reduction by AA. In the first (Figure 2-4D), time courses for nsHb (5 μM) reduction were measured in the presence of excess AA (3 to 12 mM), with and without MHDAR and NADH. MDHAR alone (without AA or NADH) did not reduce nsHb at all, whereas NADH alone (or with MDHAR) reduced nsHb very slowly. In the presence of AA, reduction was accelerated to the levels observed in Figure 2-2C, but were not affected at all by the inclusion of MDHAR and NADH. These reduction rate constants are plotted along with those by AA alone in Figure 2-2D, and their linear fit yields a bimolecular rate constant of 0.01 $mM^{-1}min^{-1}$, identical to that by AA alone.

The second experiment tested nsHb reduction when AA concentration (2μM) is lower than nsHb (10 μM). Under these conditions one might expect that the benefit of MDHAR/NADH would become evident, as the AA must be cycled back from MDHA to complete the reaction. Figure 2-4E demonstrates a measurable effect of MDHAR, but the time courses for reduction are very slow (as expected from this AA concentration).

nsHb-driven NO scavenging; the effects of AA and MDHAR. The effects of AA, MDHAR, and nsHb on NO scavenging in solution were tested using an NO-specific

electrode. In each experiment, the test conditions were equilibrated to establish a stable baseline, and NO scavenging was initiated by the addition of 50 μM NO to the reaction cell. NO is only intermediately stable, as it reacts with itself and other molecules in solution, especially oxygen, over period of several minutes [44, 45]. Time courses for NO removal are complex and do not obey simple linear or exponential decay patterns. Thus, we have chosen the time it takes for 80% of the NO signal to decay (t_{NO}, Table 2) as our objective measure for the purpose of comparing different experimental conditions.

To establish a baseline for NO decay time courses, Figure 2-5A demonstrates NO removal in buffered solutions with and without 3 mM AA or 3 mM DHA. The time courses within the yellow circle are in hypoxic conditions (0.1 μM oxygen), while those outside the circle are equilibrated in air. In the presence of buffer alone, NO removal is faster in air (t_{NO} = 2.5 minutes, Table 2-2) due to reactions with oxygen in comparison to hypoxic conditions (t_{NO} = 16 minutes). AA has no effect in air, but actually slows hypoxic NO loss, whereas DHA speeds up NO removal under both conditions. This latter observation is not surprising as it is established that DHA and MDHA scavenge NO [46, 47]. The slowing of NO loss in hypoxia is probably due to reduction of nitrite (formed from NO oxidation during the experiment) by AA, which has been characterized in many systems [48-50] and is discussed in more detail below.

The experiments in Figure 2-5B were designed to test the effects of MDHAR/NADH and AAOx on NO scavenging. As described above, reactions with these enzymes were measured in air and under hypoxic conditions (in the yellow circle). These enzymes had few individual effects on NO scavenging. Under hypoxic conditions, the important variable was the presence or absence of AA. If AA is present under

hypoxic conditions, NO removal is slightly slower. In air, AA has little effect, and only AAOx (in the presence of AA) had a clear effect on the time course for NO removal; it generated a scavenging time course resembling that for DHA (Figure 2-5A), which differs from the others by a slightly faster t_{NO}, and also by the more-rapid removal of the final 20% of NO. We suspect that this is due to production of MDHA by AAOx as supported by the data in Figure 2-4B, showing that addition of NO removed the EPR signal associated with MDHA. There are also previous reports of direct scavenging of NO by MDHA [46, 51].

To test the effect of nsHb on NO scavenging in the conditions above, 5 μM ferric rice nsHb was included in reaction mixtures containing AA with and without MDHAR/NADH (Figure 2-5C). The lower concentration of nsHb compared to NO requires continued nsHb reduction to achieve complete NO scavenging. As a control for NO scavenging under these circumstances, time courses for scavenging by nsHb and ferredoxin reductase (Fdr)/NADH (a system characterized previously for rice nsHb [37, 52]) were also measured (dashed lines). The incorporation of rice nsHb into these various AA-containing conditions had little effect on t_{NO} values (Table 2-2). As was the case for the reactions in Figure 2-5B, the only parameter that generally affected NO removal was the hypoxic presence of AA (which slowed NO removal slightly).

The more subtle effects of NO scavenging in air are clearer in the expanded comparison of the aerobic reactions (Figure 2-5D). Compared to AA alone, the addition of nsHb has no effect (thin black lines). Addition of AAOx (which produces MDHA and DHA) or DHA slightly decreases t_{NO} (red lines), and increase the speed of complete (100%) return to baseline compared to AA alone. MDHAR actually increases t_{NO}

slightly, probably because it prevents formation of MDHA/DHA, which are better NO scavengers than AA [46, 47]. The presence of nsHb along with MDHAR has no effect on scavenging.

Production of NO by AA and nitrite. The experiments above have tested the role of AA in mediating NO scavenging by nsHb. But AA could have other roles in NO metabolism. As nitrite concentrations rise, and pH drops, conditions inside hypoxic plant cells favor NO production by the direct reduction of nitrous acid by AA [21, 48]. Our final experiment investigating the role of AA in NO metabolism was designed to test whether such conditions could yield measurable NO concentrations *in vitro*. Figure 2-6 demonstrates results from reactions in which AA was added to solutions of nitrite buffered at pH values ranging from 6 to 7, under hypoxic conditions. In each experiment (unless otherwise labeled), 10 mM nitrite solutions were equilibrated with the NO electrode at the desired pH, and then AA (to make the reaction 1 mM AA) was added (or not, as indicated) at time 0. Nitrite alone produces no NO emission at these pH values (Figure 2-6A). However, as pH is lowered to 6.75, measurable (~5 μM) NO is produced from the 10 mM nitrite samples over a thirty-minute period. As pH is lowered to 6.5, 6.25, and 6, NO emission increases accordingly to values approaching 50 μM over this time period. NO is not detected at pH 7 from 10 mM nitrite, but when nitrite is increased to a very high (100 mM) concentration, NO is released rapidly, reaching a maximum near 60 μM after 20 minutes (Figure 2-6B).

To test the role of nsHb under these conditions, 5 μM rice nsHb was included in the incubation mixture of separate reactions at pH 6 and pH 6.5. The amount of NO

produced in these reactions (compared to the respective ones lacking nsHb) was decreased by about 5 μM, as would be expected by stoichiometric NO binding to the nsHb. As nsHb concentration in cells is thought to be low (< 1 μM), direct binding of NO would have little effect on NO concentrations.

Discussion

NO metabolism in plants has been linked to functions in signaling, toxicity during hypoxia, and even minor manipulations of the mechanisms of production and scavenging are believed to have potentially important affects on downstream biochemistry [20, 53]. The results presented here are an important test of the hypothesis that the ascorbate cycle mediates nsHb scavenging of NO during hypoxia, and provides a plausible explanation for NO production during hypoxia based only on increased nitrite concentrations, lowered pH, and the presence of AA. The discussion below integrates our results into three subjects of current interest in plant physiology. The first addresses interactions between AA and nsHbs in the context of NO scavenging; the second concerns interactions between AA and nitrite in hypoxic tissues, and the third the physiological role of nsHbs.

The role of AA and MDHAR in nsHb-mediated NO scavenging. The AA/MDHAR hypothesis for NO scavenging states that nsHb uses the NOD reaction to scavenge NO (Figure 2-1B) [39]. The mechanism for the oxidative half of the reaction is not in question, as ferrous nsHbs readily bind oxygen [54], and oxy-nsHb rapidly reacts with NO to form nitrate [30]. The work presented here addresses the unique hypothesis

for the reductive half of the NOD reaction, which suggests that AA directly reduces nsHb, and that MHDAR facilitates this activity by reducing the product, MDHA, back to AA using the reduction power of NAD(P)H. Our results suggest that AA could contribute to slow nsHb reduction, but they do not lend support to a contributing role for MDHAR. Nor do they suggest that AA stimulates NO scavenging by nsHbs under hypoxic or normoxic conditions.

Most of our experiments were carried out starting with a reduced ascorbate pool (in the form of AA rather than MDHA or DHA), which mimics hypoxic cells [11]. It is possible that MDHA would have a larger effect on nsHb reduction if the ascorbate pool were oxidized (such as upon re-aeration of hypoxic plant tissue), because it could shift the pool back toward AA, which has a higher rate of reduction of nsHb than DHA (Figure 2-2). However, without an efficient reductase for nsHb, the direct reaction of NO with DHA would serve as a better NO scavenger than the nsHb/AA system. Thus, our results do not support a role for NO scavenging by nsHb using a NOD-based mechanism.

Interactions between nitrite and AA; a potential source of NO in hypoxic plant cells. The sources of NO in plant cells are not entirely clear, and there are several hypothesized mechanisms of NO production [23, 53]: 1) reduction of nitrite by nitrate reductase; 2) a plasma-membrane bound nitrite:NO reductase; 3) hypoxic mitochondria; 4) anaerobic xanthine oxidase; and 5) nsHb reduction of nitrite [55-57]. Only for reactions 1) and 5) have purified plant proteins been shown to produce NO in the laboratory.

Nitrate reductase produces NO by acting on nitrite rather than nitrate [58, 59]. This occurs when nitrite concentrations rise, such as when nitrite reductase is inhibited at lowered pH during hypoxia [58, 60, 61]. Ferrous nsHb produces NO by reducing nitrite under anaerobic conditions. *In vitro*, the resulting NO binds tightly to the remaining ferrous nsHb and rapidly inhibits further nitrite reduction [55], but low levels of NO release have been measured from this system [56].

Production of NO in plants from the direct reaction of AA and nitrite has been considered [59], but was discounted because of the low levels of nitrous acid (with a pKa of 3.4) that would be present at neutral pH. Our results affirm that NO production from AA and nitrite is directly proportional to nitrous acid concentrations. Thus, at pH values of 7, 6.75, 6.5, 6.25, and 6.0, and a starting nitrite concentration of 10 mM, one would expect nitrous acid concentrations of 2, 4, 8, 14, and 25 μM, respectively; these values are close to those observed for each experiment (Figure 2-6). Therefore, assuming AA is not limiting, one can estimate NO production from the nitrite concentration and pH. For example, at pH 6.5 and a nitrite concentration of 5 mM (as might be found in hypoxic plant roots), one would expect the production of 4 μM NO. Thus, even though the pKa for nitrous acid is relatively low, the nitrite concentrations present in hypoxic roots are sufficient for the production of significant levels of NO, especially as the pH drops below 7.

How do these results impact our hypothesis for nsHb function? The preponderance of data supports a function for nsHbs related to NO metabolism and hypoxia. The two clearest possibilities are NO scavenging using the NOD mechanism,

and NO production from nitrite. The direct chemical evidence in support of NOD function for nsHbs is not strong. These properties are not unique to nsHbs, are in fact common to most hemoglobins [37], and thus do not provide a stringent test for the potential of NOD as a specific physiological function.

Direct chemical evidence in support of NO production is stronger, as nsHbs are much better nitrite reductases than other hemoglobins [55, 56]. However, this story is incomplete, as it is not clear what happens to NO after it is produced. Some options are 1) it simply binds the remaining ferrous nsHb and prevents further reaction, 2) NO is somehow released, contributing to the NO pool in the hypoxic cell, or 3) the NO is further reduced in a dissimilatory manner in support of hypoxic respiration. Option 3) would result in net NO scavenging, as it proposes that whatever NO is produced by the nsHb is used in subsequent reactions.

A recent investigation of nsHbs demonstrated NO production and release by *Arabidopsis* leaves in wild type, nsHb knock-down, and nsHb over-expressing plant lines [24]. Only very low levels of NO was observed in an environment above 1% oxygen for any of the lines, but as oxygen levels were lowered below 1%, the knock-down line lost NO at elevated levels compared to the wild type and over-expressing lines. The most NO was released under total anoxia (0% oxygen) in the knock-down line, but all lines released significant amounts of NO under that condition. These data are important because they reveal NO production and release on a large scale during hypoxia even for wild-type plants, and show that nsHbs are involved. They were interpreted in support of NOD function by nsHbs because the nsHb knock-down line released the most NO during hypoxia and anoxia.

If nsHb were simply using the NOD mechanism to scavenge NO, the anoxic conditions should have shown no difference between plant lines, as none would be capable of NO scavenging in the absence of oxygen. Alternatively, these data could be interpreted as nsHb removal of NO using a dissimilatory reductive mechanism in which electrons are shuttled to nitrite, NO, and potentially hydroxylamine, to make ammonia (this is one possibility for Option 3 above). Dissimilatory reduction of NO could benefit the plant by consuming more respiratory and/or glycolytic electrons than would NO oxidation using NOD, and it would not require the consumption of oxygen, which could be put to better use in mitochondrial respiration. In support of this hypothesis is the fact that ferrous nsHb is a very effective hydroxylamine reductase, which forms ammonia under anaerobic conditions [62]. However, for nsHbs to serve as dissimilatory reductases would require mechanisms for producing hydroxylamine and over-coming NO-inhibition of ferrous nsHb, as well as a mechanism for reduction of ferric nsHb. Thus, further biochemical experiments with nsHbs and inorganic nitrogen species, and assays for hypoxic nitrogen utilization in plants lacking nsHbs will be critical for testing this hypothesis.

References

1. Smirnoff, N., *The Function and Metabolism of Ascorbic Acid in Plants.* Annals of botany, 1996. **78**: p. 661-669.
2. Smirnoff, N. and G.L. Wheeler, *Ascorbic acid in plants: biosynthesis and function.* Crit Rev Biochem Mol Biol, 2000. **35**(4): p. 291-314.
3. Smirnoff, N., *Ascorbic acid: metabolism and functions of a multi-facetted molecule.* Curr Opin Plant Biol, 2000. **3**(3): p. 229-35.
4. Foyer, C.H., *Ascorbic acid*, in *Antioxidants in higher plants*, R.G. Alscher and J.L. Hess, Editors. 1993, CRC Press. p. 31-58.
5. Zechmann, B., M. Stumpe, and F. Mauch, *Immunocytochemical determination of the subcellular distribution of ascorbate in plants.* Planta, 2011. **233**(1): p. 1-12.

6. Anderson, J.W., C. Foyer, and D.A. Walker, *Light-dependent reduction of dehydroascorbate and uptake of exogenous ascorbate by spinach chloroplasts.* Planta, 1983. **158**(5): p. 442-450.
7. Jimenez, A., et al., *Evidence for the Presence of the Ascorbate-Glutathione Cycle in Mitochondria and Peroxisomes of Pea Leaves.* Plant physiology, 1997. **114**(1): p. 275-284.
8. Jimenez, A., et al., *Role of the ascorbate-glutathione cycle of mitochondria and peroxisomes in the senescence of pea leaves.* Plant physiology, 1998. **118**(4): p. 1327-35.
9. Rautenkranz, A., et al., *Transport of Ascorbic and Dehydroascorbic Acids across Protoplast and Vacuole Membranes Isolated from Barley (Hordeum vulgare L. cv Gerbel) Leaves.* Plant physiology, 1994. **106**(1): p. 187-193.
10. Takahama, U., *Oxidation of vacuolar and apoplastic phenolic substrates by peroxidase: Physiological significance of the oxidation reactions.* Phytochemistry Reviews, 2004. **3**(1-2): p. 207-219.
11. Biemelt, S., U. Keetman, and G. Albrecht, *Re-Aeration following Hypoxia or Anoxia Leads to Activation of the Antioxidative Defense System in Roots of Wheat Seedlings.* Plant Physiol, 1998. **116**(2): p. 651-8.
12. Inglett, P., K. Reddy, and R. Corstanje, *Anaerobic soils*, in *Encylopedia of Soils in the Environment*, D. Hillel, Editor. 2005, Elsevier. p. 72-78.
13. Foyer, C. and B. Halliwell, *The presence of glutathione and glutathione reductase in chloroplasts: A proposed role in ascorbic acid metabolism.* Planta, 1976. **133**(1): p. 21-25.
14. Groden, D. and E. Beck, *H2O2 destruction by ascorbate-dependent systems from chloroplasts.* Biochimica et biophysica acta, 1979. **546**(3): p. 426-35.
15. Kelly, G.J. and E. Latzko, *Soluble ascorbate peroxidase: detection in plants and use in vitamim C estimation.* Die Naturwissenschaften, 1979. **66**(12): p. 617-619.
16. Drew, D.P., et al., *Heterologous expression of cDNAs encoding monodehydroascorbate reductases from the moss, Physcomitrella patens and characterization of the expressed enzymes.* Planta, 2007. **225**(4): p. 945-54.
17. Hossain, M.A., Y. Nakano, and K. Asada, *Monodehydroascorbate Reductase in Spinach Chloroplasts and Its Participation in Regeneration of Ascorbate for Scavenging Hydrogen Peroxide.* Plant and Cell Physiology, 1984. **25**(3): p. 385-395.
18. Hossain, M.A. and K. Asada, *Monodehydroascorbate reductase from cucumber is a flavin adenine dinucleotide enzyme.* Journal of Biological Chemistry, 1985. **260**(24): p. 12920-6.
19. Gentiloni Silveri, N., et al., *Nitric oxide. A general review about the different roles of this innocent radical.* Minerva Med, 2001. **92**(3): p. 167-71.
20. Mur, L.A., et al., *Nitric oxide in plants: an assessment of the current state of knowledge.* AoB Plants, 2013. **5**: p. pls052.
21. Hollenbeck, C. and R. Monahan. *Application of Ascorbic Acid in Meat Curing*. in *Proceedings of the Fifth Research Conference Sponsored by the Council on Research of the American Meat Institute at the University of Chicago*. 1953. Chicago, Ill.

22. Honikel, K.O., *The use and control of nitrate and nitrite for the processing of meat products.* Meat Science, 2008. **78**(1-2): p. 68-76.
23. Gupta, K.J., et al., *On the origins of nitric oxide.* Trends in plant science, 2011. **16**(3): p. 160-8.
24. Hebelstrup, K.H., et al., *Haemoglobin modulates NO emission and hyponasty under hypoxia-related stress in Arabidopsis thaliana.* J Exp Bot, 2012. **63**(15): p. 5581-91.
25. Roberts, J.K., F.H. Andrade, and I.C. Anderson, *Further Evidence that Cytoplasmic Acidosis Is a Determinant of Flooding Intolerance in Plants.* Plant Physiol, 1985. **77**(2): p. 492-4.
26. Roberts, J.K., et al., *Cytoplasmic acidosis as a determinant of flooding intolerance in plants.* Proc Natl Acad Sci U S A, 1984. **81**(19): p. 6029-33.
27. Ferrari, T.E. and J.E. Varner, *Intact tissue assay for nitrite reductase in barley aleurone layers.* Plant Physiol, 1971. **47**(6): p. 790-4.
28. Gardner, P.R., *Nitric oxide dioxygenase function and mechanism of flavohemoglobin, hemoglobin, myoglobin and their associated reductases.* J Inorg Biochem, 2005. **99**(1): p. 247-66.
29. Gardner, P.R., et al., *Nitric oxide dioxygenase: an enzymic function for flavohemoglobin.* Proc Natl Acad Sci U S A, 1998. **95**(18): p. 10378-83.
30. Perazzolli, M., et al., *Arabidopsis nonsymbiotic hemoglobin AHb1 modulates nitric oxide bioactivity.* Plant Cell, 2004. **16**(10): p. 2785-94.
31. Ohwaki, Y., et al., *Induction of class-1 non-symbiotic hemoglobin genes by nitrate, nitrite and nitric oxide in cultured rice cells.* Plant Cell Physiol, 2005. **46**(2): p. 324-31.
32. Bustos-Sanmamed, P., et al., *Regulation of nonsymbiotic and truncated hemoglobin genes of Lotus japonicus in plant organs and in response to nitric oxide and hormones.* New Phytol, 2011. **189**(3): p. 765-76.
33. Dordas, C., et al., *Expression of a stress-induced hemoglobin affects NO levels produced by alfalfa root cultures under hypoxic stress.* Plant J, 2003. **35**(6): p. 763-70.
34. Seregelyes, C., et al., *NO-degradation by alfalfa class 1 hemoglobin (Mhb1): a possible link to PR-1a gene expression in Mhb1-overproducing tobacco plants.* FEBS Lett, 2004. **571**(1-3): p. 61-6.
35. Igamberdiev, A.U., et al., *NADH-dependent metabolism of nitric oxide in alfalfa root cultures expressing barley hemoglobin.* Planta, 2004. **219**(1): p. 95-102.
36. Igamberdiev, A.U., et al., *Class-1 hemoglobin and antioxidant metabolism in alfalfa roots.* Planta, 2006. **223**(5): p. 1041-6.
37. Smagghe, B.J., J.T. Trent, 3rd, and M.S. Hargrove, *NO dioxygenase activity in hemoglobins is ubiquitous in vitro, but limited by reduction in vivo.* PLoS One, 2008. **3**(4): p. e2039.
38. Sainz, M., et al., *Plant hemoglobins can be maintained in functional form by reduced flavins in the nuclei and confer differential tolerance to nitro-oxidative stress.* Plant J, 2013.
39. Igamberdiev, A.U., N.V. Bykova, and R.D. Hill, *Nitric oxide scavenging by barley hemoglobin is facilitated by a monodehydroascorbate reductase-mediated ascorbate reduction of methemoglobin.* Planta, 2006. **223**(5): p. 1033-40.

40. Hargrove, M.S., et al., *Crystal structure of a nonsymbiotic plant hemoglobin.* Structure, 2000. **8**(9): p. 1005-14.
41. Chih-Yu Huang, L.W., Rong-Huay Juang, Dey-Chyi Sheu, and Chi-Tsai Lin, *Monodehydroascorbate reductase cDNA from sweet potato: expression and kinetic studies.* Botanical Studies, 2010. **51**(1): p. 37-44.
42. Aliverti, A., B. Curti, and M.A. Vanoni, *Identifying and quantitating FAD and FMN in simple and in iron-sulfur-containing flavoproteins.* Methods in molecular biology, 1999. **131**: p. 9-23.
43. Buettner, G.R. and B.A. Jurkiewicz, *Ascorbate free radical as a marker of oxidative stress: An EPR study.* Free Radical Biology and Medicine, 1993. **14**(1): p. 49-55.
44. Ford, P.C., D.A. Wink, and D.M. Stanbury, *Autoxidation kinetics of aqueous nitric oxide.* FEBS Lett, 1993. **326**(1-3): p. 1-3.
45. Lewis, R.S. and W.M. Deen, *Kinetics of the reaction of nitric oxide with oxygen in aqueous solutions.* Chem Res Toxicol, 1994. **7**(4): p. 568-74.
46. Kurz, C.R., et al., *Rapid scavenging of peroxynitrous acid by monohydroascorbate.* Free Radic Biol Med, 2003. **35**(12): p. 1529-37.
47. Kytzia, A., et al., *On the mechanism of the ascorbic acid-induced release of nitric oxide from N-nitrosated tryptophan derivatives: scavenging of NO by ascorbyl radicals.* Chemistry, 2006. **12**(34): p. 8786-97.
48. Carlsson, S., et al., *Effects of pH, nitrite, and ascorbic acid on nonenzymatic nitric oxide generation and bacterial growth in urine.* Nitric Oxide, 2001. **5**(6): p. 580-6.
49. Lundberg, J.O., et al., *Intragastric nitric oxide production in humans: measurements in expelled air.* Gut, 1994. **35**(11): p. 1543-6.
50. McKnight, G.M., et al., *Chemical synthesis of nitric oxide in the stomach from dietary nitrate in humans.* Gut, 1997. **40**(2): p. 211-4.
51. Blokhina, O. and K.V. Fagerstedt, *Reactive oxygen species and nitric oxide in plant mitochondria: origin and redundant regulatory systems.* Physiol Plant, 2010. **138**(4): p. 447-62.
52. Kundu, S., et al., *Direct measurement of equilibrium constants for high-affinity hemoglobins.* Biophys J, 2003. **84**(6): p. 3931-40.
53. Planchet, E. and W.M. Kaiser, *Nitric oxide production in plants: facts and fictions.* Plant Signal Behav, 2006. **1**(2): p. 46-51.
54. Smagghe, B.J., et al., *Review: correlations between oxygen affinity and sequence classifications of plant hemoglobins.* Biopolymers, 2009. **91**(12): p. 1083-96.
55. Sturms, R., A.A. DiSpirito, and M.S. Hargrove, *Plant and cyanobacterial hemoglobins reduce nitrite to nitric oxide under anoxic conditions.* Biochemistry, 2011. **50**(19): p. 3873-8.
56. Tiso, M., et al., *Nitrite reductase activity of nonsymbiotic hemoglobins from Arabidopsis thaliana.* Biochemistry, 2012. **51**(26): p. 5285-92.
57. Rasmusson, A.G., K.L. Soole, and T.E. Elthon, *Alternative NAD(P)H dehydrogenases of plant mitochondria.* Annu Rev Plant Biol, 2004. **55**: p. 23-39.
58. Yamasaki, H. and Y. Sakihama, *Simultaneous production of nitric oxide and peroxynitrite by plant nitrate reductase: in vitro evidence for the NR-dependent formation of active nitrogen species.* Febs Letters, 2000. **468**(1): p. 89-92.

59. Yamasaki, H., Y. Sakihama, and S. Takahashi, *An alternative pathway for nitric oxide production in plants: new features of an old enzyme.* Trends Plant Sci, 1999. **4**(4): p. 128-129.
60. Kaiser, W.M., et al., *Modulation of nitrate reductase: some new insights, an unusual case and a potentially important side reaction.* Journal of Experimental Botany, 2002. **53**(370): p. 875-882.
61. Rockel, P., et al., *Regulation of nitric oxide (NO) production by plant nitrate reductase in vivo and in vitro.* Journal of Experimental Botany, 2002. **53**(366): p. 103-110.
62. Sturms, R., et al., *Hydroxylamine reduction to ammonium by plant and cyanobacterial hemoglobins.* Biochemistry, 2011. **50**(50): p. 10829-35.

Tables

Table 2-1. Cloning primers.

Primer Name	Sequence
RCMD F	5’-ATGGCGTCGGAGAAGCACTTC-3’
RCMD R	5’-TCATATTTTGCTGGCGAACTGGAGG-3’
RCMD NheI F	5’ACAACAACACGCTAGCATGGCGTCGGAGAAGCACTTC-3’
RCMD HindIII R	5’ACAACAACACAAGCTTTCATATTTTGCTGGCGAACTGGAGG-3’
EcoRV Fdx F	5’-ACAACAACACGATATCATGGCTGATTGGGTAACAGGC AAAG-3’
BamHI Fdx R	5’ACAACAACACGGATCCGGAGCTCGAATTCTTACCAGTA ATGCTCC-3’

Table 2-2. NO scavenging reactions. The time (in minutes) at which 80% of signal associated with 50 μM NO has been depleted (t_{NO}) is listed at various reaction conditions.

Reactions with Asc, DHA, MDHAR, and Asc Oxidase.

	Buffer	Asc	DHA	NADH	NADH Asc	MDHAR NADH Asc	AscOx Asc
Air	2.5	2.4	1.6	2.0	2.7	3.2	1.9
Hypoxia	16	>30	4	19	>30	>30	>30

Reactions involving nsHb1.

	nsHb1	nsHb1 Asc	nsHb1 NADH	nsHb1 Asc NADH	nsHb1 Asc NADH MDHAR	nsHb1 FdxR NADH
Air	2.9	2.4	2.7	2.4	3.0	1.1
Hypoxia	27	36	16	26	29	10

Figures and Legends

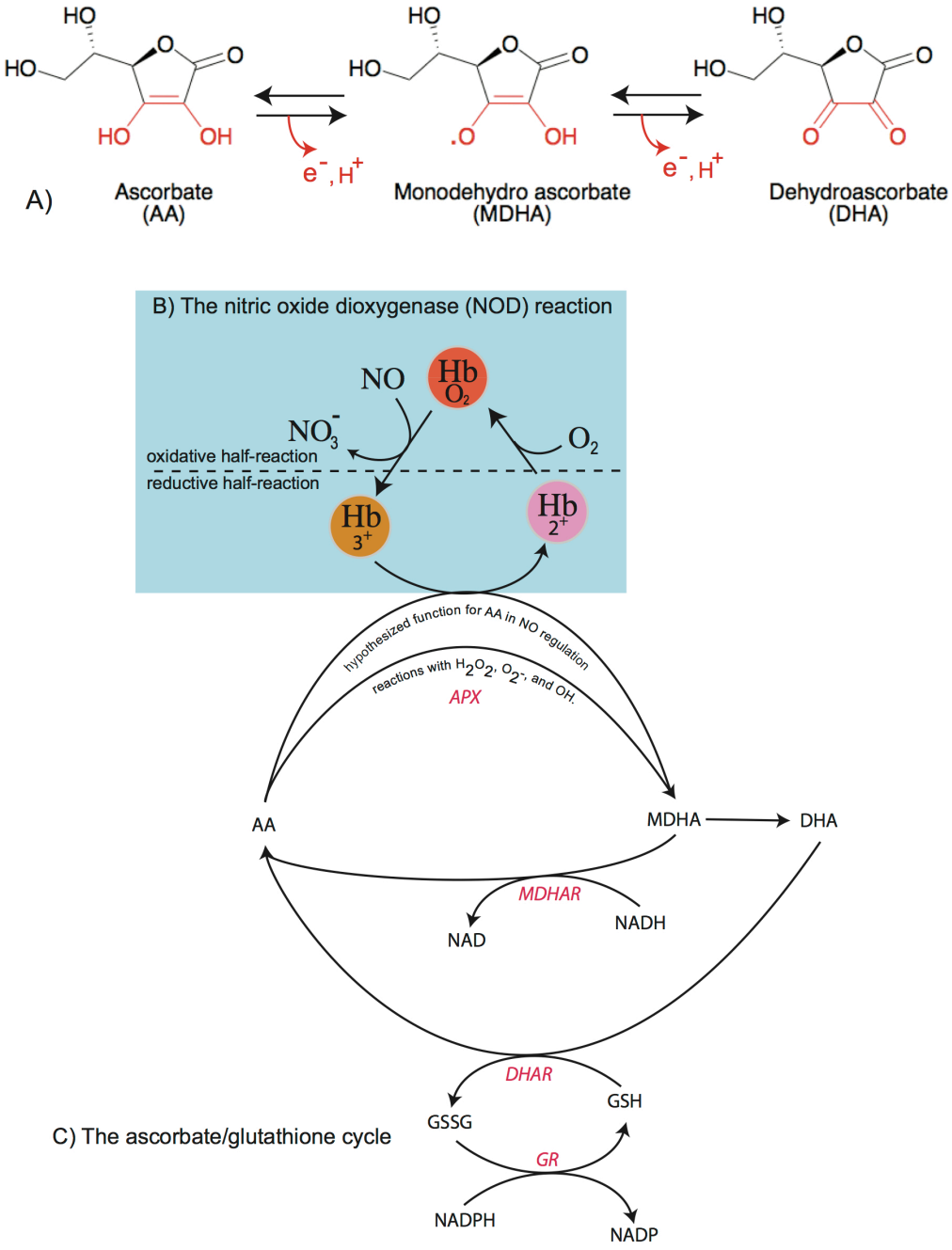

Figure 2-1. Pertinent chemical reactions of AA, hemoglobin, and NO. A) Ascorbic acid (AA) can lose an electron to become monodehydroascorbate (MDHA) radical, which can lose an electron to become dehydroascorbate (DHA). B) The nitric oxide dioxygenase (NOD) reaction; oxy hemoglobins (Hb) will react with NO to make nitrate and ferric Hb. If the ferric Hb is reduced (in this case by AA), it will bind oxygen (if present) to start the reaction again. C) The AA/glutathione cycle in plants is associated with scavenging of peroxide, superoxide, and hydroxyl radical, and is hypothesized to reduce nsHbs in support of NOD.

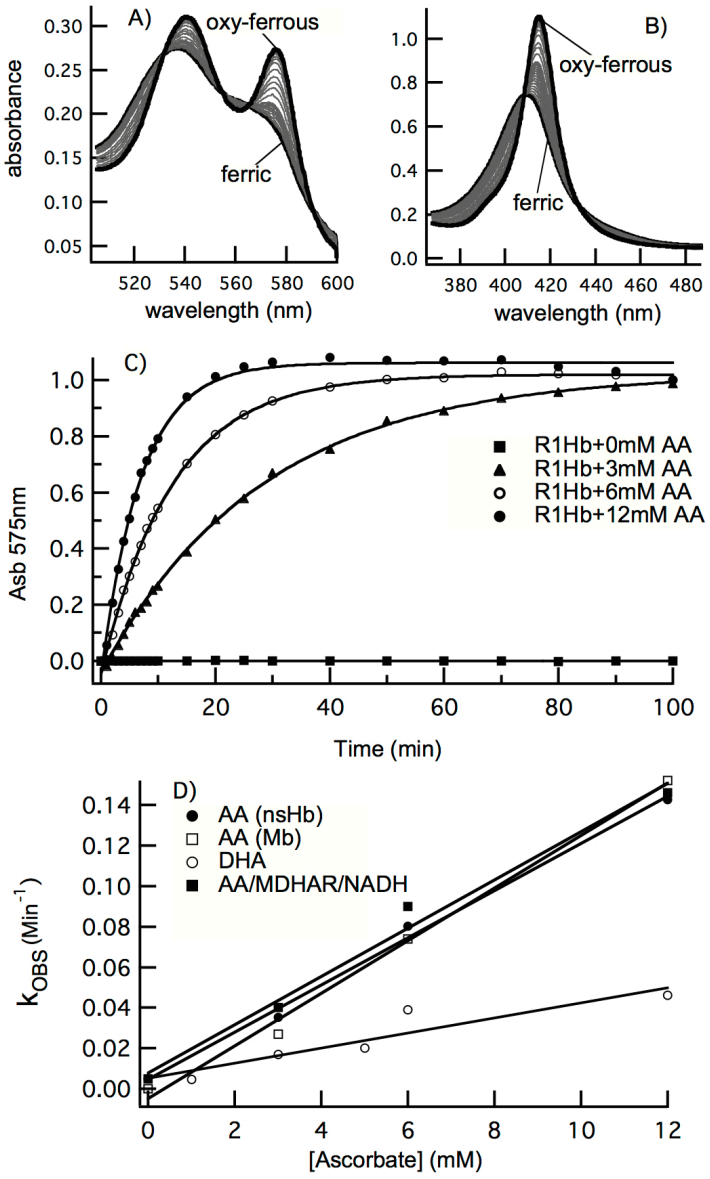

Figure 2-2. nsHb reduction by AA, DHA, and MDHAR. A) ferric rice nsHb (5 μM) was mixed with 3 mM AA in air-saturated buffer. The absorbance changes in the visible and B) Soret regions are associated with nsHb reduction and oxygen binding. C) Time courses for nsHb reduction by various concentrations of AA. D) The rate constants for AA reduction of nsHb and Mb (5 μM) are plotted as a function of AA concentration, which have slopes equal to the bimolecular rate constants for reduction of nsHb.

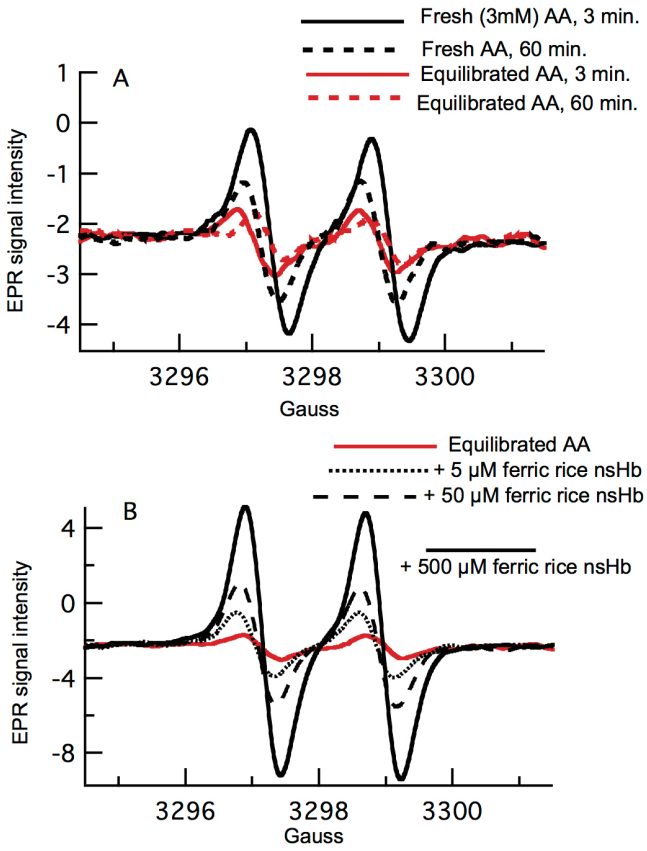

Figure 2-3. EPR measurements of MDHA radical in solutions of AA (A), and produced from AA reduction of nsHb (B). A) Freshly dissolved 3 mM AA solutions contain MDHA, which decays to a lower equilibrium level over several hours. B) Addition of ferric nsHb to AA increases the EPR signal associated with MDHA.

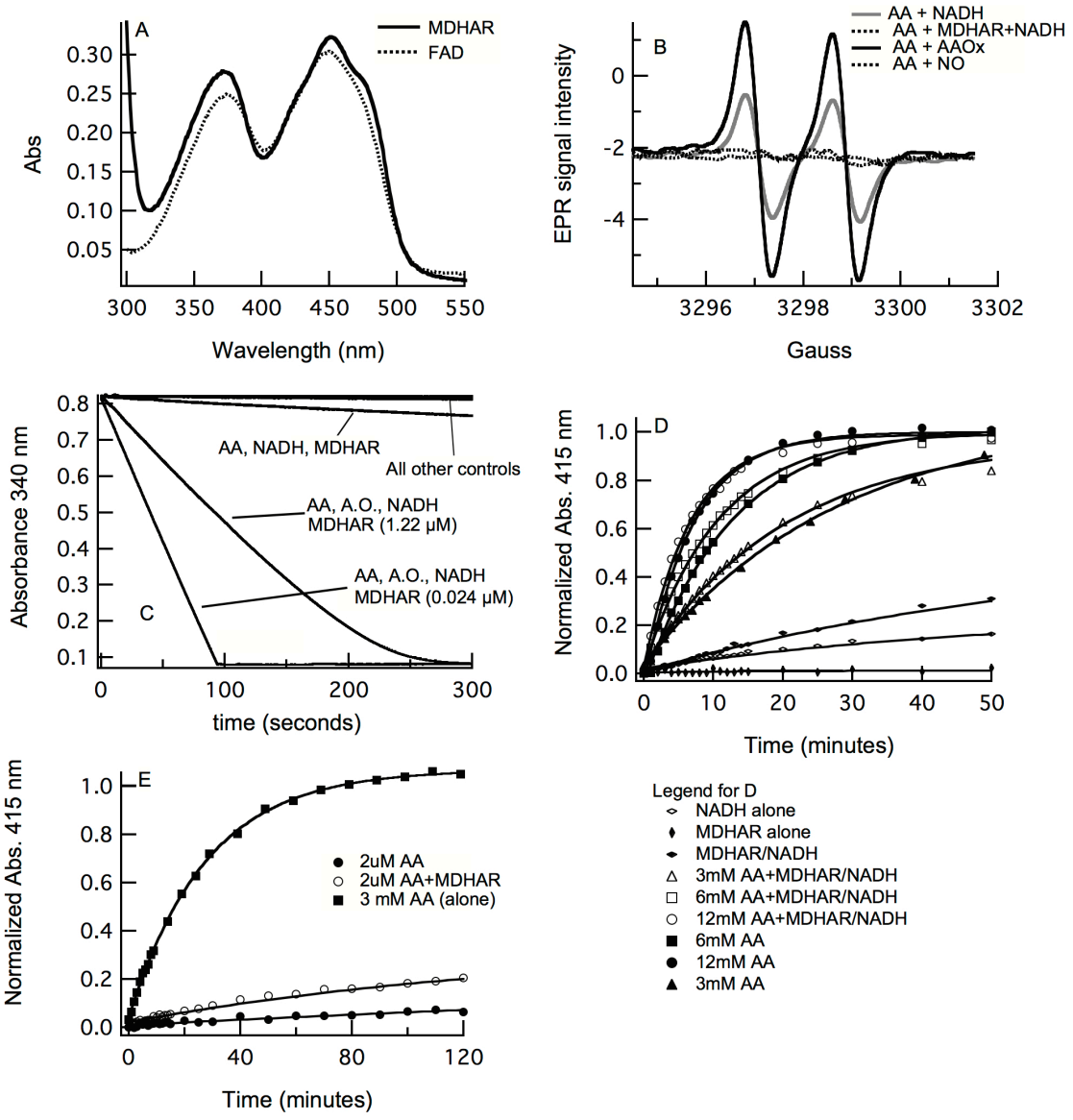

Figure 2-4. The effect of MDHAR on AA reduction of nsHb. A) Recombinant rice MDHAR was purified and quantified based on its flavin absorbance spectrum. B) The EPR signal associated with MDHA was used to demonstrate the activity of AAOx (which increases the MDHA signal in the presence of AA), and MDHAR (which decreases MDHA in the presence of NADH). These data also show that NO reacts directly with MDHA. C) MDHAR oxidizes NADH in the presence of MDHA (produced from AA and AAOx, as in (B)). D) Time courses for nsHb reduction by AA in the absence and present of MDHAR and NADH are nearly identical. E) When nsHb concentration is greater than AA, reduction is very slow, and slightly faster in the presence of MDHAR and NADH.

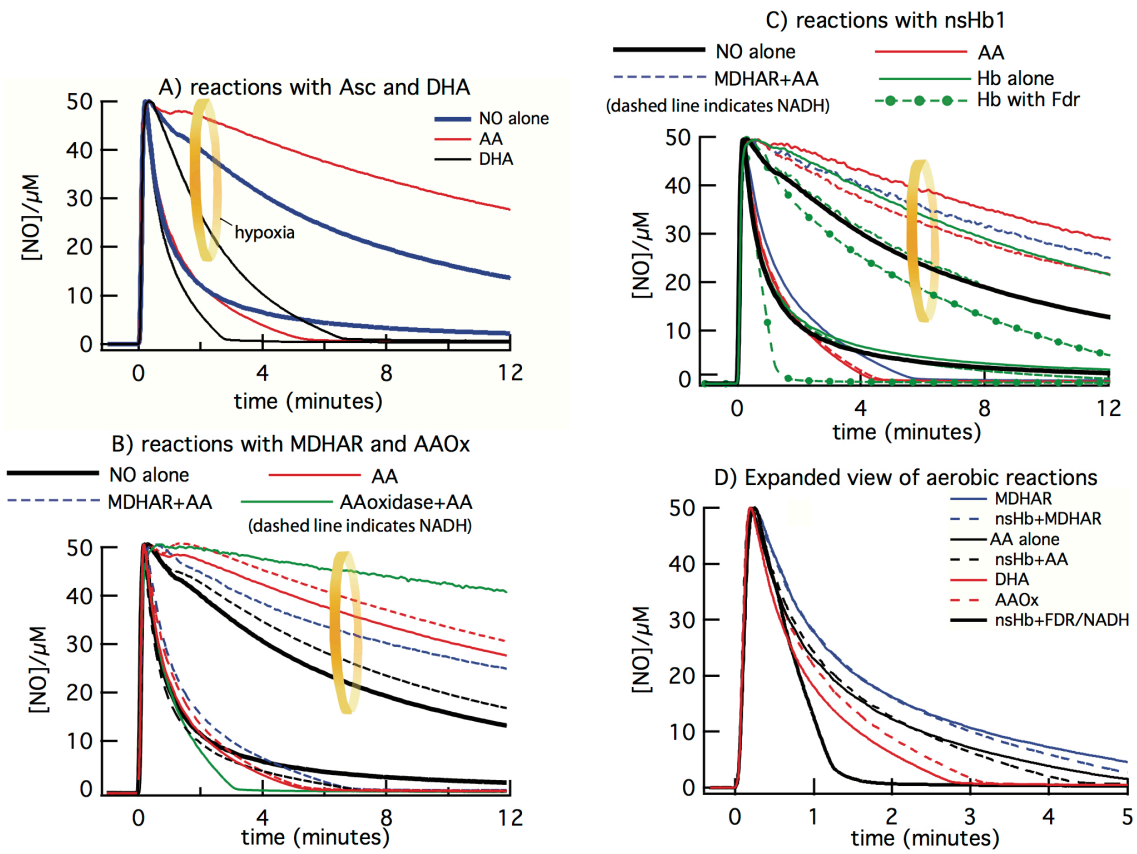

Figure 2-5. NO scavenging by AA, nsHb, and MDHAR. A) NO scavenging by buffer, AA, and DHA are compared under aerobic and hypoxic (0.1 μM [O_2], inside the yellow circle) conditions. B) NO scavenging with MDHAR and AAOx under aerobic and hypoxic (inside the yellow circle) conditions. The curves for NO alone are black, and the presence of AA (red), MDAHR and AA (blue), and AAOx (green) are indicated by color. A dashed line indicates the presence of NADH (0.2 mM) in that reaction condition. C) NO scavenging by nsHb, with and without MDHAR are compared to that facilitated with reduction of nsHb by ferredoxin reductase (Fdr, green dashed line with filled circles, indicating Fdr and NADH are present along with nsHb). D) An expanded view of aerobic NO scavenging demonstrates the subtle effects of AA and DHA.

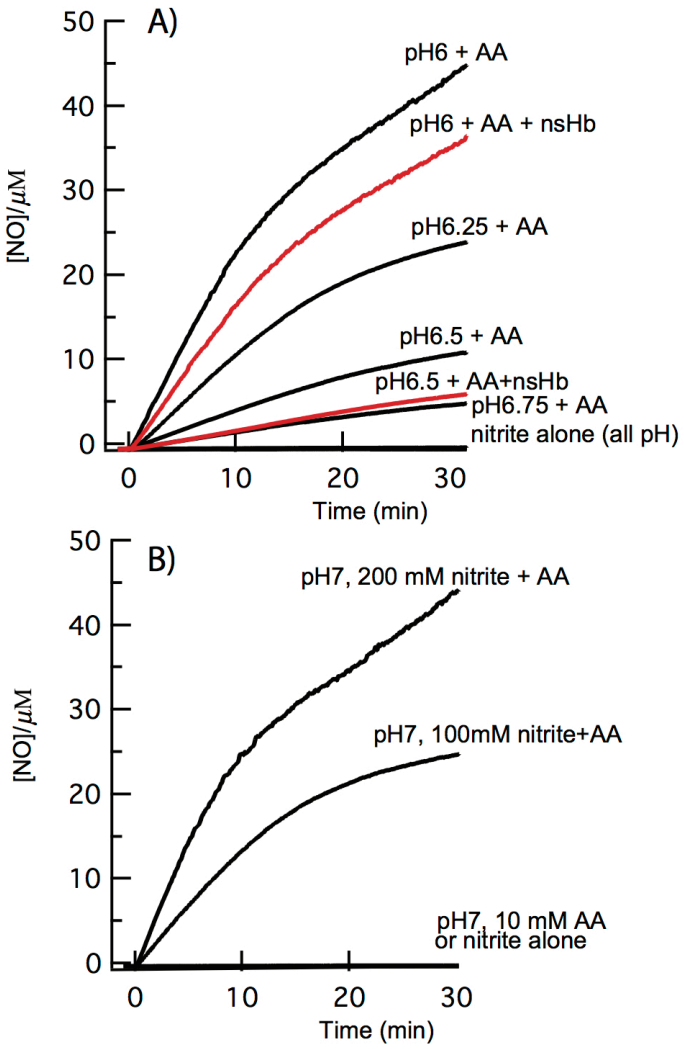

Figure 2-6. Production of NO from nitrite and AA. NO production from solutions of nitrite (10 mM unless otherwise indicated) were stimulated by addition of AA at pH values ranging from 6 to 7. A) NO production is measurable at pH 6.75 and increases with decreasing pH. When 5 μM nsHb is included (red traces) there is a decrease in the level NO proportional to the Hb concentration. B) The amount of NO produced is directly related to nitrite concentration, as is evident from the high levels produced even at pH 7 when nitrite concentration is very high.

CHAPTER 3

GROWTH PHENOTYPES OF *E. COLI* NITRITE REDCUTASE MUTANTS REVEAL A ROLE FOR NIR NITRIE ASSIMILATION DURING ANAEROBIC NITRATE RESPIRATION

A research paper in preparation by

Xiaoguang Wang[1234], Denis Tamiev[12], Alan DiSpirito[2], Gregory Phillips[2], Mark Hargrove[24]

Introduction

Nitrate assimilation is the limiting factor in plants growth and productivity. Under stressful conditions such as hypoxia and anoxia, often caused by flooding and waterlogged soil, nitrite and NO can accumulate to toxic levels [1, 2]. More importantly, ammonium production is correspondingly decreased. This limits the amount of nitrogen incorporation into the organics and lowers yield. However, there is evidence that plants can benefit from nitrate under hypoxic and anoxic conditions [3]. This is possibly mediated by plant nonsymbiotic hemoglobins (nsHbs), as supported by for two observations: 1) plant nsHbs are up-regulated by nitrite, nitrate and hypoxia [4]; 2) plant nsHbs are efficient nitrite and hydroxylamine reductases compared to other hemoglobins [5, 6]. However the biochemical mechanisms are still unclear. Understanding such

[1] Contributed in bench works.
[2] Contributed in experimental design.
[3] Contributed in writing.
[4] Contributed in editing and proof reading.

mechanisms are very important for us to improve plant nitrate assimilation under hypoxic and anoxic pressures.

Previous study has shown that the reaction between ferrous nsHb and nitrite progresses to 50% ferric nsHb and 50% NO-bound ferrous nsHb [6]. Once the ferrous nsHb binds to NO, nitrite reduction stops. So every time this reaction happens, 50% of nsHb is lost, which means there is no way *in vitro* that nsHbs alone can accomplish reduction of nitrite all the way to ammonium. However the fact that nsHbs can catalyze the nitrite to NO and hydroxylamine to ammonium reactions very efficiently [5, 6] suggests the nsHbs might able to mediate the nitrite to ammonium reaction *in vivo* through an alternative mechanism or with the help of additional cofactors(s). To find the possible cofactors(s), we need a model system to screen for plant nsHb-mediated nitrite reductase activity. *E.coli* is potentially a good model system for our case, because 1) it carries out the nitrite to ammonium reduction by two nitrite reductases, 2) both nitrite reductase knockouts are available from CGSC and 3) easy DNA transformation for the actual screen. But to make *E.coli* a real model system for us, we must first find the growth phenotypes of the two nitrite reductase mutants.

The efforts to unveil the nature of nitrite reduction systems in *E.coli* trace back to 1950s. There were four lines followed by researchers. The first line started in 1956. Atkinson and McNall [7] reported an *E. coli* mutant strain Bn that can grow under aerobic condition with nitrate or nitrite as sole nitrogen source (glucose as carbon source), whose parental strain B cannot. They monitored nitrite disappearance during growth of Bn in nitrite medium, which suggests a nitrite reductase activity in this mutant. In 1961, Lazzarirn and Atkinson [8] purified a NADH-dependent nitrite reductase from *E.coli* Bn.

With ^{15}N labeled nitrite, they showed that this nitrite reductase reduces nitrite directly to ammonia. They concluded that hydroxylamine was an intermediate because the enzyme also reduced hydroxylamine as a substrate. In the same enzyme preparation, they also found two other activities: a sulfite reductase and a cytochrome *c* reductase. These two activities later on became the second and third lines for *E.coli* nitrite reduction studies. Zarowny and Sanwal [9] also reported the NADH-dependent reductase activity from *E.coli* K12 in the same year. However they could not identify the product, except they know it is not ammonia but some gas products. So the enzyme in strain K12 is different from the one in Bn found by Lazzarini and Atkinson. In their discussion, for the first time, they hypothesized that *E.coli* anaerobic nitrite respiration and assimilation are mediated by two separated pathways.

The second line was presesnted by Kemp and Atkinson [10] in 1963. They characterized an NADPH-dependent nitrite reductase, which reduces nitrite to ammonia. However this enzyme was also found to be a NADPH-dependent sulfite reductase. The fact that cycteine is a repressor of this enzyme, and that it was absent in sulfite deficient strains, made them suggest that this enzyme works exclusively as sulfite reductase *in vivo*. This was also the end of the second line of research. The third line started also in 1963 but by Fujita and Sato [11]. They purified the soluble cytochrome c_{552} from *E.coli* grown anaerobically in their nitrate respiration studies. Then they reported a series of comprehensive studies of this new cytochrome c_{552} in 1966 [12-15]. Cytochrome c_{552} was only detected in cells grown anaerobically with nitrate in semi-synthetic medium. It is soluble, reducible by NADH and NADPH and it has a very low reduction potential and high autoxidizability [12]. It is localized in the periplasm [14] and most importantly, it

efficiently reduces nitrite to ammonia at the expense of 3 NADH [13]. So at that time they thought cytochrome c_{552} was involved in NADH-dependent nitrite reduction. Up to then, the first three lines had all been started, the NADPH-dependent nitrite reductase line had already ended, the NADH-dependent and cytochrome c_{552} lines were thought to be the same pathway.

As the *E.coli* NADH-dependent nitrite reductase and cytochrome c_{552} kept drawing research attention, Cole, Ward and Coleman reported some related work in the late 1960s. They found that both NADH-dependent nitrite reductase activity and cytochrome c_{552} synthesis were not only completely inhibited by oxygen, but also is strongly inhibited by nitrate [16, 17]. Also they were able to separate cytochrome c_{552} from *E. coli* lysate without affecting the NADH-dependent nitrite reductase activity [18], suggesting that there are two nitrite reductases in *E. coli*. In 1973, Cole and Ward [19] found a nitrite reductase mutant, *nirA*, which simultaneously lost most of NADH-dependent nitrite reductase activity and production of cytochrome c_{552}. So again, they suggested cyt c_{522} was involved in NADH-dependent nitrite reduction. But they did not rule out the possibility that the *nirA* gene product was a super regulator of both. Later on, mutant strains *nirR* and *fnr* found by other groups also showed the same phenotype [20, 21]. With more genetic work, *nirA*, *nirR* and *fnr* all seemed to be the same gene, which regulates nitrite reductase, nitrate reductase, fumarate reductase and cytochrome c_{552} biosynthesis [22, 23].

In the late 1970s, the fourth line of research was started by Abou-Jaoude *et al.* [24] when they reported the role of format in nitrite reduction. They found that 25% of the overall nitrite reduction (using glucose as electron donor) by unbroken *E. coli* cells is

contributed by formate as an electron donor. The formate-dependent nitrite reductase is simultaneously induced with cytochrome c_{552} biosynthesis. And all formate-nitrite reductase mutants also lacked cytochrome c_{552} biosynthesis. So they proposed a link between the formate-nitrite reductase and cytochrome c_{552} [25].

Coleman and Cole continued to follow the NADH-dependent nitrite reductase line by purifying it from *E.coli* [26]. It was separated from cytochrome c_{552} with increased specific activity. So they concluded that cytochrome c_{552} is not an integral part of NADH-dependent nitrite reductase. Three NADH molecules were used by one nitrite ion and they did not find any reaction intermediates between nitrite and ammonia. So the product was assumed to be ammonia. In 1980, Cole [27] reported a *nirB* mutant that is lacked NADH-dependent nitrite reductase activity, but still synthesized cytochrome c_{552}, suggesting they belong to two different pathways. However, Liu *et al*. co-purified a NADH oxidase when purifying cytochrome c_{552}. They proved that a high nitrite reduction activity is shown from cytochrome c_{552} by using NADH as electron donor when the co-purified NADH oxidase and FAD are also included. This again put the role of cytochrome c_{552} in NADH-dependent nitrite reduction to a question.

In 1982, breakthrough work was done by Pope and Cole [28] to clearly demonstrate two independent nitrite reduction pathways in *E. coli*. In this work, they generated *E. coli* mutants in which either formate-dependent nitrite reductase or NADH-dependent nitrite reductase was independently non-functional. Only the formate dependent one could generate a membrane potential. Page and Cole [29] verified the two independent pathways in 1990. They started calling the formate-dependent nitrite reductase “Nrf”, and the NADH-dependent nitrite reductase “Nir”. Nrf is repressed but

Nir is induced by nitrate. So they proposed that the role of Nrf is to reduce nitrite for energy when the favorable electron acceptor is not available, and that the role of Nir is to detoxify the cytoplasmic nitrite generated by the respiratory nitrate reductase (contributing the majority (80%) of the total nitrite reduction activity anaerobically in rich medium supplied with glucose and nitrite). In early 1990s, genetics components of the *nir* and *nrf* operons were respectively identified [30, 31] and finally the cytochrome c_{552} was identified as the terminal reductase in the Nrf pathway encoded by the structural gene *nrfA* [32]. The structural gene of Nir pathway is *nirB* [30, 33]. Expression of both enzymes are strictly inhibited by oxygen.

Up to middle 1990s, genetic components and the biochemical nature of the two nitrite reductase pathways were clear. The main question was then what are their physiological roles. A lot of later studies tried to answer this question by looking at the genetic regulation of the two operons. They found that both operons are positively regulated by Fnr, which is only expressed under anaerobic conditions [30, 31]. The *nir* operon is activated by both nitrate and nitrite [34]. The *nrf* operon is also activated nitrite but is only activated by very low concentration (~1 mM), and is strongly inhibited by nitrate [35]. So it was proposed that the role of the Nrf pathway was to help *E. coli* survive nitrogen limited environments. To test this, a growth phenotype of the *nrfA* mutant in medium with nitrate or nitrite as a sole nitrogen source is essential. However, such work has never been reported. For the *nirB* mutant, there is also no reported growth phenotype. Further more, the Cole group always concluded that the role of Nir is dissimilatory nitrite detoxification [29, 30, 36, 37], in order to protect E.coli from nitrite in the cytoplasm produced by the nitrate reductase. All of such conclusions trace back to

one of their work in 1978 [38]. In that work, when *E. coli* was grown in synthetic medium with excess nitrite as sole nitrogen source, excess ammonium was produced and secreted into the medium. They also saw accumulation of acetate. Their logic was that since NADH was not used to reduce acetate to ethanol, it must have been used for nitrite reduction, and so the ammonium accumulation was attributed to NADH-dependent nitrite reductase activity. But the real source of electron donor for nitrite reduction and ammonium production in those experiments has never been tested. So more work needs to be done to understand the physiological role of Nir.

The present work is to find the growth phenotypes of the two *E. coli* nitrite reductase mutants, *nrfA* and *nirB*, to test Nir's function as a dissimilatory nitrite detoxifier, and to find out whether Nir has other roles during nitrate respiration.

Materials and Methods

Strains and growth conditions. All three strains are purchased from *E. coli* Genetic Stock Center (CGSC) at Yale University. The source of these strains is the Keio Collection. The wild type strain is BW25113. Both *nrfA* (JW4031-1) and *nirB* (JW3328-1) mutants are single knockouts of wild type created by replacing target gene with a *kanamycin* marker. So all three strains share the genetic background of BW25113, but wild type is kanamycin sensitive and the two mutants are kanamycin resistant. All minimal medium used for *E.coli* growths contained Evans base (contains no carbon or nitrogen), pH 7.0. Carbon sources (20 mM glucose or 0.5% v/v glycerol) and nitrogen sources (sodium nitrate, sodium nitrite and/or ammonium chloride) were added separately as needed. Evans base is revised from the Evans medium recipe from Dr.

Robert Poole by leaving out all the carbon and nitrogen sources. Evans base is composed of 40 mM K2HPO$_4$, 10 mM NaH$_2$PO$_4$, 10 mM KCl, 1.25 mM MgCl$_2$, 2 mM Na$_2$SO$_4$, 0.38g/l nitrilotriacetic acid, 0.02 mM CaCl$_2$, 5ml/l trace elements solution, 3 µg/l Na$_2$SeO$_3$.5H$_2$O. The composition of trace elements solution is 8 ml/l HCl (37%), 0.412 g/l ZnO, 5.4 g/l FeCl$_3$.6H$_2$O, 2g/l MnCl$_2$.4H$_2$O, 0.172g/l CuCl$_2$.2H$_2$O, 0.476 g/l CoCl$_2$.6H$_2$O, 0.064 g/l H$_3$BO$_3$, 0.004 mg/l Na$_2$MoO$_4$.2H$_2$O. 30 ml anaerobic flask cultures were grown in 50 ml flasks on a 15-position stir plate in 37ºC warm room, purging with 95% N_2 and 5% CO_2 mixture gas. 30 ml aerobic flask cultures were grown in a regular 37ºC water bath shaker, with foam stoppers and no purging. All 4L batch culture experiments were done in a 14 L New Brunswick BioFlo fermenter. Temperature was 37ºC, pH was controlled at 7.0, and 95% N_2 and 5% CO_2 mixture gas was purged all time to keep culture anaerobic. For all anaerobic flask growth experiment, starter cultures of wild type (except in complementation experiment) and *nrfA* mutant were conditioned as follow: 1) 5 ml LB cultures were prepared over night; 2) cells were washed and resuspended in Evans base to inoculate Evans medium with 20 mM glucose and 20 mM sodium nitrate; 3) after culturing for 24 hours, cultures were used to re-inoculate the same glucose/nitrate medium; 4) after another 24 hours, cultures (conditioned) were used to inoculate experimental growths. Starter cultures for *nirB* cells and all fermenters were grown in LB over night then washed and resuspended in Evans base before inoculation (non-conditioned).

Nitrite quantification. After cell cultures were sampled, cells were separated from the medium by centrifugation. Media Nitrite concentration were quantified by the Griess

assay. The protocol followed was the "Griess Reagent System Technical Bulletin" from Promega. Reagents used were 10 g/l sulfinalmide (in 5% v/v phosphoric acid) and 1 g/l NED.

NMR. ^{15}N labeled chemicals, $Na^{15}NO_3$ and $Na^{5}NO_2$ were purchased from Sigma, and $^{15}NH_4Cl$ was from Cambridge Isotopes. After cell cultures were sampled, media was separated from cells by centrifugation (and filtering when large volumes were needed). Clean media (with 10% v/v D_2O) was used for 1D ^{15}N NMR with a Bruker Avance III 600 Spectrometer. For 1D ^{15}N NMR samples from 30 ml flask cultures, media was not concentrated; for those from batch culture experiments, media was concentrated 200 times by lyophilization. Cell pellets were lysed by lysozyme and DNAse in 50 mM citrate buffer (pH 2.0). 10% v/v D_2O was added to lysis supernatants and used for ^{15}N-HMQC experiments with a Bruker Avance 700 Spectrometer. For 30 ml flask cultures, cells combined from three flasks (90 ml) were used to prepare 1 ml ^{15}N-HMQC samples. For batch culture experiments, cells from 200 ml cultures were used for 1 ml ^{15}N-HMQC samples.

Cloning. Colony PCR using wild type *E.coli* (BW25113) as template was used to amplify the *nir* operon region (-406 to -1 up stream of *nirB* gene) and *nirB* gene. Primers used for the *nir* operon were *pnir*_F and *pnir*_R, and for the *nirB* gene were *nirB*_F and *nirB*_R. Using the colony PCR product as template, a second PCR with restriction site containing primers was done for both DNA fragments. Primers used in the second PCR for *nir* operon were EcoRI_*pnir*_F and NdeI_*pnir*_R, for *nirB* gene were NdeI_*nirB*_F

and HindIII_*nirB*_R. All primer sequences are shown in Table 3-2. Platinum® Pfx DNA Polymerase (catalog number: 11708-039) from Life Technologies was used for all PCR reactions. FastDigest restriction enzymes, EcoRI, NdeI and HindIII were purchased from Thermo Scientific. Rapid DNA Ligation Kit (#K1422) was purchased from Thermo Scientific for DNA ligation. Both plasmids generated by cloning, pNXW and pNXW-*nirB*, were verified by DNA sequencing in DNA Facility of Iowa State University.

Results

Growth phenotype of E.coli nrfA knockout strain (nrfA). Previous studies on the *E. coli* Nrf pathway provided knowledge about genetic components and regulation of the *nrf* operon [34, 35], expression and biochemical functions of Nrf proteins [16, 17, 31], and structure of the functional Nrf nitrite reductase, NrfA [39]. These earlier studies suggest that cells lacking Nrf should be deficient of anaerobic nitrite respiration. However, there is still lack of a growth phenotype when the functional gene *nrfA* is knocked out.

The first effort to look for a *nrfA* growth phenotype was done in 50 ml flasks filled with 30 ml medium, continuously purged with 95% N_2 and 5% CO_2 to create anaerobic conditions. Figure 3-1 shows the cell growth density after 24 hours of culturing. 20 mM glucose (Glu) was used as sole carbon source for all conditions. Neither wild type (wt) nor *nrfA* mutant was able to grow under the condition "Glu", which is a negative control that only has glucose as carbon but not any nitrogen sources. However, with either 20 mM sodium nitrate (Glu+Nitrate) or 5 mM sodium nitrite (Glu+Nitrite), both wt and *nrfA* mutant grew to similar extents. The "Glu+Nitrate" experiment was then

repeated under aerobic conditions (Glu+Nitrate (air)), and the results were negative to both wt and *nrfA* mutant, confirming our anaerobic growth system was working. So these data show no nitrate or nitrite utilization deficient phenotype for the *nrfA* mutant.

Similar growth experiments were done by switching glucose to glycerol, a non-fermentable carbon source, aiming to induce the dissimilatory Nrf in wild type, so that it benefits more from nitrate or nitrite than the *nrfA* mutant (Table 3-1). Neither strain was able to grow in glycerol plus ammonium (Trial 9), confirming glycerol is not fermentable under our experiment conditions. Both strains can grow with co-appearance of ammonium and nitrate (Trial 10) but not with ammonium and nitrite (Trail 11), meaning they can both utilize nitrate as an electron accepter for respiration but not nitrite. Also, the two strains were able to grow with nitrate or nitrite as a single nitrogen source together with glucose (Trial 3 and 5) but not with glycerol (Trail 7 and 8). These data suggest that both wild type and *nrfA* mutant 1) can reduce nitrate and nitrite to ammonium for assimilatory purpose; 2) can reduce nitrate to nitrite for dissimilatory purpose; 3) cannot reduce nitrite for dissimilatory purpose. The hypothesis based on these data is that Nrf was not induced in wild type cells under those growth conditions in Figure 3-1 and Table 3-1.

To see if wild type and the *nrfA* mutant grow differently in the middle of the 24-hour growth, growth curves were collected in medium with 20 mM glucose and 20 mM sodium nitrate (20 mM ammonium chloride was used instead as positive control, Figure 3-2). Black curves represent time courses for cell density. After sampling for OD measurements, media was separated for nitrite measurement. Red curves represent corresponding nitrite concentration time courses. However, not only the wild type (black

circle) was growing the same extent as the *nrfA* mutant (black bowtie), they also shared nitrite accumulation time courses and total final nitrite concentration (~18 mM) in the medium (red circle and red bowtie). Since 18 mM nitrate was converted to nitrite, less than 2 mM nitrate must have been reduced to ammonium for assimilation. But there is still no evidence of nitrite dissimilation by wild type cells. To find an *nrfA* deficient phenotype, the key is to find a condition under which the Nrf is actively induced so that the wild type can benefit from it.

Expression of Nrf was reported to be sensitive to nitrate concentration [35]. To find the nitrate condition at which wild type benefits from Nrf expression, we tested the growth of wild type and *nrfA* mutant in a gradient of nitrate concentrations. Results are shown in Figure 3-3. Medium used in these experiments were 20 mM glucose plus 0.5, 1, 5, 10, 20, 300 or 500 mM sodium nitrate. Main graph shows data from 0.5 to 20 mM nitrate, sub graph shows data for 300 and 500 mM nitrate. Cell densities after 24 hours culturing are in black, medium nitrite concentrations in the same cell density samples are in red. Circles represent wild type and triangles represent *nrfA* mutant. The most interesting data were at 10 mM nitrate. With 10 mM nitrate, wild type grew to an OD of 1.1 and used up all the nitrite converted from nitrate, while the *nrfA* mutant only grew to 0.6 and had left over ~ 4 mM nitrite in the medium. This suggests that the wild type can benefit from dissimilating the 4 mM nitrite through Nrf but the *nrfA* mutant cannot. This is our first *nrfA* mutant phenotype.

To find a clear growth phenotype for the *nrfA* mutant, we did a sequential batch culture experiment in which cells were grown in three stages with three different media at each stage (Figure 3-4). In the fermenter, pH was controlled at 7.0, culturing temperature

was 37ºC, agitation was at 400 rpm, mixture gas of 95% N_2 + 5% CO_2 was purged during whole experiment (to create a anaerobic environment). In Figure 3-4, black curves represent time courses of cell density and red curves represent time courses of nitrite concentration in the growth medium. Wild type (black and red circle) is shown on the top and *nrfA* mutant (black and red triangle) is shown on the bottom of the main graph. Sub graphs are spectra of whole cell samples without (dash line) and with (solid line) dithionite, taken by an OLIS CLARiTY spectrometer. At Stage 1 with 20 mM glucose and 5 mM sodium nitrate, both wild type and *nrfA* mutant showed a growth lag phase of 30 hours, during which nitrite concentration in medium slowly built up to ~ 5 mM. Then there was a log phase of 6 hours, after which both strains reached to an OD of ~ 1.0, and medium nitrite concentrations came back to 0. Although the two strains were similar in both growth and nitrite time courses at Stage 1, wild type did show a spectrum of cytochrome c_{552} coded by the *nrfA* gene (Figure 3-4a), represented by an absorbance peak at 552 nm after reduced by dithionite [19], while the *nrfA* mutant did not (Figure 3-4d). At 36 hours, the culture from Stage 1 was drained. Stage 2 was started by refilling medium with glycerol and 5 mM sodium nitrate. The purpose of this stage was to induce Nrf by switching to a non-fermentable carbon source. At Stage 2, wild type showed a 30-hour lag phase (38 to 68 hour), during which nitrite was building up in the medium to ~ 5 mM. Then the cells started a log phase of 18 hours (68 to 86 hour), used up the nitrite and stopped growing (86 to 92 hour). The *nrfA* mutant, on the other hand, did not show any obvious lag or log phases. Instead of waiting until all nitrate became nitrite, *nrfA* mutant took off growing right at the beginning of the stage, and reached to stationary after 30 hours (38 to 68 hour). Also, the medium nitrite maximum of *nrfA* mutant showed up 18

hours earlier (at 44 hour) than the wild type (at 62 hour). Again, wild type showed a cytochrome c_{552} spectrum (Figure 3-4b) but the *nrfA* mutant did not (Figure 3-4e). Stage 2 culture was drained at 92 hour and the fermenter was filled with minimal medium containing 0.5% v/v glycerol but no nitrogen source (finished at 93 hour). Cells with the no nitrogen medium were incubated for an hour (93 to 94 hour) to get rid of any left over nitrogen from previous stage. At 94 hour, 0.2 mM sodium nitrite was fed into the fermenter to start Stage 3. The nitrite feeding amount and frequency was determined by the utilization speed of the wild type cells. The nitrite feeds were: 0.2 mM at 100.1, 104.1, 108.1 and 110.1 hour, 0.4 mM at 112.1 and 115.1 hour, 0.8 mM at 117.1, 121.1, 123.1, 125.1, 126.6, 127.6 and 128.6 hour, 1 mM at 129.6, 130.6, 131.6, 132.6 and 133.6 hour (^{15}N labeled sodium nitrite), 10 mM (actual value for wild type is 9.98 mM, for *nrfA* mutant is 12.11 mM) at 134.6 hour. The fed nitrite concentration before 133.6 hour was estimated by volume of 1M sodium nitrite stock added and total fermenter volume (assuming volume changes due to small sample withdraws were negligible). After ^{15}N labeled nitrite was fed at 133.6, large volume (100-200 ml) samples were taken, hence it was not accurate to estimate the nitrite concentration. So right after the "10 mM" feed at 134.6 hour, a sample was taken to assay for nitrite concentration. This is why the "10 mM" feed gave wild type and *nrfA* mutant difference nitrite concentration increases. By feeding nitrite, the wild type cells were able to utilize nitrite faster and faster, and the cell OD increased correspondingly to 1.6. The *nrfA* mutant, however, did not grow at all and all the fed nitrite was accumulated in the medium. This is a very clear growth deficient phenotype for the *nrfA* mutant. Also the spectrum of wild type cells (Figure 3-4c) showed 5 to 10 fold as much cytochrome c_{552} expression in Stage 3 as in the first two stages.

Right after (at 133.6 hour) and 1 hour after (at 134.5 hour) 1 mM ^{15}N labeled nitrite was added, samples were taken and the medium portions were used for 1D ^{15}N-NMR. The results clearly show that within an hour, all labeled nitrite (610 ppm) was reduced to ammonium (21 ppm) and secreted back to the medium by wild type (Figure 3-5A and B), but not by *nrfA* mutant (Figure 3-5C and D). This confirms the dissimilatory nitrite reduction activity of Nrf in the wild type, and defines the growth conditions necessary to observe the phenotype.

Growth phenotype of E .coli nirB knockout strain (nirB). The *nirB* mutant is a single knock out of the *nirB* gene in the *nir* operon, which codes for the big subunit of NADH-dependent nitrite reductase [30]. It has a very clear growth deficient phenotype in minimal medium with glucose plus nitrate or nitrite. In Figure 3-1, under both conditions "Glu+Nitrate" and "Glu+Nitrite", the *nirB* mutant did not grow. Only when ammonium is added to the medium (Figure 3-1 "Glu+Ammonium", Figure 3-6 Stage 1) or when Nrf is induced (Figure 3-6 Stage 2) will the *nirB* mutant grow. In the growth curve experiment, there was also no growth of *nirB* mutant in glucose and nitrate (Figure 3-2 black diamond), and no nitrite was converted from nitrate (Figure 3-2 red diamond).

Can Nrf replace Nir? Under conditions when Nir is not available, could *E. coli* utilize the ammonium produced by Nrf for nitrogen assimilation? To answer this question, we did a sequential batch culture experiment with the *nirB* mutant (Figure 3-6). Cell density time courses are in black and media nitrite time course are in red. Sub graph a) and b) are whole-cell spectra taken by OLIS CLARiTY spectrometer for samples from

the end of the two stages. Since this mutant cannot grow in glucose plus nitrate (this phenotype will be described in detail later), which was used in Stage 1 of wild type and *nrfA* mutant sequential batch cultures, 0.5% v/v glycerol plus 5 mM sodium nitrate and 2 mM ammonium chloride was used instead (Figre 3-6, Stage 1). The purpose was to give the *nirB* mutant readily available ammonium for assimilation to cover its deficiency, so it can grow and induce Nrf.

As expected, the *nirB* mutant was able to grow in Stage 1 (to OD 0.5), converted all 5 mM nitrate to nitrite then utilized all the nitrite within 24 hours. Also, whole cell samples from Stage 1 did show cytochrome c_{552} expression (Figure 3-6a). At 24 hours, the Stage 1 culture was drained and the fermenter was refilled with media containing 0.5% v/v glycerol but no nitrogen. Cells were cultured in such medium for an hour (from 25 to 26 hour) to eliminate possible nitrogen sources from Stage 1. At 26 hours, the fermenter was fed with 0.2 mM sodium nitrite to start Stage 2. The same nitrite feeding strategy was used as in Stage 3 of the wild type and *nrfA* mutant sequential batch culture growths. The nitrite feedings were: 0.2 mM at 26 and 30.1 hour, 0.4 mM at 32.1, 36.1 and 40.1 hour, 0.8 mM at 42.1 and 46.1 hour, 1 mM at 48.1, 52.1, 54.1, 56.1, 57.1, 58.6, 59.6, 60.6, 61.6, 62.6 and 63.6 (^{15}N labeled) hour, 10 mM at 64.6 hour (actual value is 10.61 mM, see explanation in wild type and *nrfA* mutant sequential batch cultures paragraph). In this stage, the *nirB* mutant was utilizing the nitrite to grow, similarly to the wild type (Figure 3-4 Stage 3), and there was cytochrome c_{552} expression (Figure 3-6b). To track the destiny of nitrite, 1 mM ^{15}N labeled sodium nitrite was fed to the fermenter at 63.6 hour. Right after (at 63.6 hour), about an hour after (at 64.5 hour) and 11.5 hours after (at 75 hour) addition of labeled nitrite, culture samples were collected. The cell-free

media from these samples was used in 1D ^{15}N-NMR experiments for inorganic nitrogen detection, and the cell lysis supernatants were used in ^{15}N-HMQC experiments for organic nitrogen detection. These NMR results are shown in Figure 3-7. Right after adding labeled nitrite, it showed up in the medium (610 ppm, Figure 3-7A), and no labeled organic nitrogen was in the cell (Figure 3-7D). An hour later, all labeled nitrite was reduced to ammonium (21 ppm, Figure 3-7B), but still there was no labeled organic nitrogen was in the cell (Figure 3-7E). About 10 hours later, the amount of labeled ammonium in the medium reduced (Figure 3-7C), and labeled organic nitrogen appeared in cells (Figure 3-7F). These NMR data show that the ammonium produced by Nrf was first secreted to medium and then taken back up by the *nirB* cells for assimilation. So Nrf as a dissimilatory nitrite reductase can also play a role in nitrite assimilation if Nir is not available.

Evidence of that Nir is not a dissimilatory nitrite reductase. *E.coli* Nir was reported to be a dissimilatory nitrite reductase [38], with its proposed role being to detoxify the cytoplasmic nitrite generated by the dissimilatory nitrate reductase (NR) [36, 37, 40]. If this is true, when wild type *E.coli* is grown anaerobically with excess nitrate as the sole nitrogen source (that is, Nrf is not expressed [35]), we would expect to see ammonium accumulation in the medium due to the dissimilatory detoxification function of Nir. However, our data in Figure 3-8 demonstrate otherwise. In Figure 3-8, A) and C) are 1D ^{15}N-NMR controls with fresh medium composed of minimal medium base plus 20 and 300 mM ^{15}N labeled sodium nitrate respectively. In these controls, we only see labeled nitrate with a chemical shift of 376 ppm. 24-hour wild type anaerobic flask

cultures with labeled nitrate (no non-labeled nitrogen was added) were harvested and medium portions were used for ^{15}N-NMR experiments. Figure 3-8B shows results from wild type growths in glucose plus 20 mM (low) labeled nitrate. In this case, all nitrate was converted to nitrite (610 ppm), and no ammonium (21 ppm) appeared in the medium as expected (because nitrate was not in excess and there was no need to detoxify). The same experiment was done in 300 mM labeled nitrate (Figure 3-8D). This time we see excess nitrate, similar amounts of nitrite (as in 20 mM nitrate experiment), but still no ammonium accumulation in the medium. Then we switched from glucose to glycerol plus 300 mM nitrate (Figure3-8E), to force the cells to dissimilate nitrate and produce more nitrite for the cells to detoxify. However, we still did not see any ammonium in the medium. These data suggest that *E.coli* Nir is not a dissimilatory nitrite detoxifier.

Role of Nir during E.coli nitrate respiration. It has been suggested that *E. coli* has no need to reduce nitrate for assimilatory purposes, as it would always has access to ammonium and organic nitrogen compounds in the gut. If so, and Nir does not detoxify nitrite or contribute directly to nitrite respiration, what is its role? This question led us to hypothesize that Nir might be responsible for nitrogen assimilation during nitrate and nitrite respiration. If this was the case, wild type cells would have a competitive advantage over *nirB* cells during growth on nitrate in the presence of ammonium.

To test this hypothesis, a competition sequential batch culture experiment was used to see if wild type has any anaerobic growth advantage over the *nirB* mutant when nitrate is in the medium (Figure 3-9). Similar amount of wild type and *nirB* starter cultures were washed with minimal medium and mixed together as an inoculant for the

fermenter. Six 16-hour cycles were carried out. After each cycle, cultures were sampled, drained and refilled to start the next one. Medium in all cycles had 20 mM glucose as sole carbon source. In the first three cycles (Cycles 1 to 3), only 2 mM ammonium was used as the source of nitrogen. In the last three cycles (Cycles 4 to 6), both 2 mM ammonium and 20 mM nitrate were added. Cell samples taken at the end of each cycle were plated on LB agar plates with no antibiotics. These plates were used as master plates to replica plate on LB plates with (kanamycin) and without antibiotics. The number of colonies was counted on both types of plates, with the difference between the two representing wild type census (kanamycin sensitive, Kan^S) and the number of colonies on kanamycin plates reporting the *nirB* mutant population (kanamycin resistant, Kan^R). Figure 3-9 shows the colony number ratios of wild type to *nirB* mutant. When there is no nitrate in the medium in Cycle 1, 2 and 3, the ratios of wild type to *nirB* mutant are about 1:1, which are close to the inoculant. But when nitrate is added to the medium, the ratios wild type to *nirB* mutant increased to 5 in Cycle 4 and Cycle 5, then increased to larger than 6 in Cycle 6. These data show that wild type cells have a growth advantage in nitrate medium because of Nir.

Complementation of the nirB mutant. To complement *nirB* mutant, a parental plasmid pNXW (Figure 3-10), was first assembled by replacing the *hmp* promoter (between EcoRI and NdeI) in pANX plasmid to the *nir* promoter located at -406 to -1 base pairs up stream of the *nirB* gene [30] in wild type. Then the *nirB* gene from wild type was sub-cloned in this parental plasmid between NdeI and HindIII sites, resulting plasmid pNXW-*nirB*. pNXW (negative control) and pNXW-*nirB* were transformed into

nirB mutant respectively to test for complementation in medium with 20 mM glucose and 5 mM sodium nitrate. After grown in such medium for 24 hours, OD at 600 nm was taken and plotted as Figure 3-11. As shown in this figure, wild type (wt) was able to grow as a positive control. The *nirB* mutant itself and when transformed with pNXW plasmid, as negative controls, were not able to grow. When pNXW-*nirB* was transformed into the *nirB* mutant, the growth was recovered, representing a successful complementation.

Discussion

Phenotypes of nrfA and nirB mutants. In the present study, we have found growth phenotypes for both *nrfA* and *nirB* mutants. The *nrfA* mutant grows similarly to wild type in glucose plus nitrate media, while the *nirB* mutant was unable to grow at all in the same medium (Figure 1 and 2). The reason why the *nrfA* mutant was growing in glucose and nitrate is because it can potentially ferment glucose and respire on the conversion of nitrate to nitrite to make ATP, and there was no need for nitrite respiration under these conditions. To find the phenotype for the *nrfA* mutant, we had to remove the option for fermentation by using glycerol as the carbon source, and force nitrite respiration by providing on this source of nitrogen. In the sequential batch culture experiment for the *nrfA* mutant (Figure 3-4), we were able to achieve this goal in three stages. These data indicate that Nrf only works under continuously low nitrite conditions. Even though it was very difficult to find this clear *nrfA* mutant phenotype and no such phenotype has been demonstrated in the literature, it is consistent with previous studies that *E. coli nrfA* only expresses under anaerobic conditions [11, 12, 30, 31] and it is only induced by low nitrite concentration (~1 mM) [35]. The *nirB* mutant's no-growth

phenotype in glucose and nitrate demonstrates that Nir is essential for assimilation of nitrite (produced by nitrate reductase) for cell growth when there is no available ammonium. This is also expected from previous work by Cole *et al.* [26, 41].

Can Nrf replace Nir for nitrite assimilation? *E. coli* Nrf can respire on nitrite and produce ammonium which can be used for assimilatory purposes. Thus, Nrf can serve both dissimilatory and assimilatory roles. When Nrf was induced under continuously low nitrite conditions, the cells were able to re-uptake the ammonium secreted after Nrf nitrite reduction and then assimilate, as demonstrated by 1D ^{15}N-NMR and ^{15}N-HMQC experiments (Figure 3-7). But since we know that it is located in the periplasm [14] and it produces ammonium as a final product [12], none of these data are too surprising.

Is E.coli Nir a dissimilatory nitrite detoxifier? If so, one would expect ammonium accumulation in the medium when wild type cells are grown in glucose and nitrate, a condition at which we know that Nrf is not active (and not producing ammonium). But our data show that there is no ammonium accumulation in the medium in growth on low (20 mM) or high (300 mM) nitrate concentrations (Figure 3-8). So Nir's role is not for dissimilatory nitrite detoxification. This results contrasts with conclusions of previous studies. All literatures in which the dissimilatory detoxification role of Nir is mentioned can be traced back to Cole's work in 1978 [38]. He found that when *E. coli* was grown with nitrite as the sole nitrogen source, most of nitrite was reduced to ammonium and accumulated in the medium. Meanwhile, because acetate also accumulated instead of ethanol, he concluded that the NADH which would have been

consumed in ethanol fermentation must have been used for nitrite reduction by the NADH-dependent nitrite reductase or Nir. However, none of these conclusions have been tested by experiments. According to our results, when nitrite is used as the sole nitrogen source, the ammonium accumulated in the medium is made by Nrf but not Nir. As a matter of fact, the *nrfA* mutant, which only has Nir, cannot even grow in medium with glycerol and nitrite (Figure 3-4 Stage 3). This means Nir cannot use nitrite for respiration or dissimilation, otherwise it would grow under such conditions. On the other hand, the *nirB* mutant, which only has Nrf, can grow in glycerol and nitrite (Figure 3-6 Stage 2), and more importantly accumulate ammonium in the medium (Figure 3-7). So the ammonium accumulation Cole had seen in 1978 is due to the Nrf but not Nir, and thus we conclude that Nir is not a dissimilatory nitrite detoxifier.

What is *E.coli* Nir's role during nitrate respiration? To answer this question, we first tried to find out whether Nir plays any role during nitrate respiration. In a competition sequential batch culture experiment (Figure 3-9), we found that when nitrate is supplied in the medium, wild type cells have a growth advantage over *nirB* mutant cells. This suggests that Nir does play some role in nitrate respiration. We hypothesize that Nir functions to assimilate the nitrite generated from nitrate respiration. To test this hypothesis, we need evidence of organic nitrogen incorporation through Nir with the same growth condition as in the competition sequential batch culture, which is glucose plus nitrate and ammonium. In other words, if our hypothesis is right, we will expect to see the nitrite converted from nitrate being assimilated by Nir and incorporated into organics, even when ammonium is supplied.

The nirB mutant is a good candidate screen for plant hemoglobin cofactors in nitrite reduction. We found a clear growth phenotype of the *nirB* mutant and successfully complemented the phenotype by transforming a plasmid containing wild type *nirB* gene (pNXW-*nirB*). This makes the *nirB* mutant a very good candidate to screen against some plant root cDNA libraries for plant hemoglobin cofactors in nitrite reduction. With a positive complementation by *nirB* gene, the *nirB* mutant is ready to test nitrite reductase activities of other gene of interests *in vivo*, such as rice *nsHb1*, spinach *nir* (nitrite reductase gene) and so on.

References

1. Ferrari, T.E. and J.E. Varner, *Intact tissue assay for nitrite reductase in barley aleurone layers.* Plant Physiol, 1971. **47**(6): p. 790-4.
2. Botrel, A. and W.M. Kaiser, *Nitrate reductase activation state in barley roots in relation to the energy and carbohydrate status.* Planta, 1997. **201**(4): p. 496-501.
3. Igamberdiev, A.U. and R.D. Hill, *Nitrate, NO and haemoglobin in plant adaptation to hypoxia: an alternative to classic fermentation pathways.* Journal of Experimental Botany, 2004. **55**(408): p. 2473-2482.
4. Ohwaki, Y., et al., *Induction of class-1 non-symbiotic hemoglobin genes by nitrate, nitrite and nitric oxide in cultured rice cells.* Plant Cell Physiol, 2005. **46**(2): p. 324-31.
5. Sturms, R., et al., *Hydroxylamine reduction to ammonium by plant and cyanobacterial hemoglobins.* Biochemistry, 2011. **50**(50): p. 10829-35.
6. Sturms, R., A.A. DiSpirito, and M.S. Hargrove, *Plant and cyanobacterial hemoglobins reduce nitrite to nitric oxide under anoxic conditions.* Biochemistry, 2011. **50**(19): p. 3873-8.
7. Atkinson, D.E. and E.G. McNall, *Nitrate reduction. I. Growth of Escherichia coli with nitrate as sole source of nitrogen.* J Bacteriol, 1956. **72**(2): p. 226-9.
8. Lazzarini, R.A. and D.E. Atkinson, *A triphosphopyridine nucleotide-specific nitrite reductase from Escherichia coli.* J Biol Chem, 1961. **236**: p. 3330-5.
9. Zarowny, D.P. and B.D. Sanwal, *characterization of a nicotinamide adenine dinucleotide specific nitrite reductase from escherichia coli, strain k12.* Canadian Journal of Microbiology, 1963. **9**(4): p. 531-539.

10. Kemp, J.D., et al., *evidence for the identity of the nicotinamide adenine dinucleotide phosphate-specific sulfite and nitrite reductases of escherichia coli.* J Biol Chem, 1963. **238**: p. 3466-71.
11. Fujita, T. and R. Sato, *Soluble cytrochromes in Escherichia coli.* Biochimica et Biophysica Acta, 1963. **77**(0): p. 690-693.
12. Fujita, T., *Studies on soluble cytochromes in Enterobacteriaceae. I. Detection, purification, and properties of cytochrome c-552 in anaerobically grown cells.* J Biochem, 1966. **60**(2): p. 204-15.
13. Fujita, T. and R. Sato, *Studies on soluble cytochromes in Enterobacteriaceae. IV. Possible involvement of cytochrome c-552 in anaerobic nitrite metabolism.* J Biochem, 1966. **60**(6): p. 691-700.
14. Fujita, T. and R.Y.O. Sato, *Studies on Soluble Cytochromes in Enterobacteriaceae III. Localization of Cytochrome c-552 in the Surface Layer of Cells.* The Journal of Biochemistry, 1966. **60**(5): p. 568-577.
15. Fujita, T. and Y. Sato, *Studies on soluble cytochromes in Enterobacteriaceae. V. Nitrite-dependent gas evolution in cells containing cytochrome c-552.* J Biochem, 1967. **62**(2): p. 230-8.
16. Wimpenny, J.W. and J.A. Cole, *The regulation of metabolism in facultative bacteria. 3. The effect of nitrate.* Biochim Biophys Acta, 1967. **148**(1): p. 233-42.
17. Cole, J.A. and J.W. Wimpenny, *Metabolic pathways for nitrate reduction in Escherichia coli.* Biochim Biophys Acta, 1968. **162**(1): p. 39-48.
18. Cole, J.A., *Cytochrome c552 and nitrite reduction in Escherichia coli.* Biochim Biophys Acta, 1968. **162**(3): p. 356-68.
19. Cole, J.A. and F.B. Ward, *Nitrite reductase-deficient mutants of Escherichia coli K12.* J Gen Microbiol, 1973. **76**(1): p. 21-9.
20. Chippaux, M., et al., *A mutation leading to the total lack of nitrite reductase activity in Escherichia coli K 12.* Molecular and General Genetics MGG, 1978. **160**(2): p. 225-229.
21. Lambden, P.R. and J.R. Guest, *Mutants of Escherichia coli K12 Unable to use Fumarate as an Anaerobic Electron Acceptor.* Journal of General Microbiology, 1976. **97**(2): p. 145-160.
22. Abou-Jaoude, A., et al., *Nitrite reduction in Escherichia coli: genetic analysis of nir mutants.* Mol Gen Genet, 1978. **167**(1): p. 113-8.
23. Newman, B.M. and J.A. Cole, *The chromosomal location and pleiotropic effects of mutations of the nirA+ gene of Escherichia coli K12: the essential role of nirA+ in nitrite reduction and in other anaerobic redox reactions.* J Gen Microbiol, 1978. **106**(1): p. 1-12.
24. Abou-Jaoude, A., et al., *Formate : a new electron donor for nitrite reduction in Escherichia coli K12.* Biochem Biophys Res Commun, 1977. **78**(2): p. 579-83.
25. Abou-Jaoude, A., M.C. Pascal, and M. Chippaux, *Formate-nitrite reduction in Escherichia coli K12. 2. Identification of components involved in the electron transfer.* Eur J Biochem, 1979. **95**(2): p. 315-21.
26. Coleman, K.J., A. Cornish-Bowden, and J.A. Cole, *Purification and properties of nitrite reductase from Escherichia coli K12.* Biochem J, 1978. **175**(2): p. 483-93.

27. Cole, J.A., B.M. Newman, and P. White, *Biochemical and genetic characterization of nirB mutants of Escherichia coli K 12 pleiotropically defective in nitrite and sulphite reduction.* J Gen Microbiol, 1980. **120**(2): p. 475-83.
28. Cole, J.A., *Independent pathways for the anaerobic reduction of nitrite to ammonia by Escherichia coli.* Biochem Soc Trans, 1982. **10**(6): p. 476-8.
29. Page, L., L. Griffiths, and J.A. Cole, *Different physiological roles of two independent pathways for nitrite reduction to ammonia by enteric bacteria.* Arch Microbiol, 1990. **154**(4): p. 349-54.
30. Harborne, N.R., et al., *Transcriptional control, translation and function of the products of the five open reading frames of the Escherichia coli nir operon.* Mol Microbiol, 1992. **6**(19): p. 2805-13.
31. Hussain, H., et al., *A seven-gene operon essential for formate-dependent nitrite reduction to ammonia by enteric bacteria.* Mol Microbiol, 1994. **12**(1): p. 153-63.
32. Darwin, A., et al., *Regulation and sequence of the structural gene for cytochrome c552 from Escherichia coli: not a hexahaem but a 50 kDa tetrahaem nitrite reductase.* Mol Microbiol, 1993. **9**(6): p. 1255-65.
33. MacDonald, H., N.R. Pope, and J.A. Cole, *Isolation, characterization and complementation analysis of nirB mutants of Escherichia coli deficient only in NADH-dependent nitrite reductase activity.* J Gen Microbiol, 1985. **131**(10): p. 2771-82.
34. Tyson, K.L., J.A. Cole, and S.J. Busby, *Nitrite and nitrate regulation at the promoters of two Escherichia coli operons encoding nitrite reductase: identification of common target heptamers for both NarP- and NarL-dependent regulation.* Mol Microbiol, 1994. **13**(6): p. 1045-55.
35. Wang, H. and R.P. Gunsalus, *The nrfA and nirB nitrite reductase operons in Escherichia coli are expressed differently in response to nitrate than to nitrite.* Journal of bacteriology, 2000. **182**(20): p. 5813-22.
36. Cole, J., *Nitrate reduction to ammonia by enteric bacteria: redundancy, or a strategy for survival during oxygen starvation?* FEMS Microbiol Lett, 1996. **136**(1): p. 1-11.
37. Potter, L., et al., *Survival of bacteria during oxygen limitation.* Int J Food Microbiol, 2000. **55**(1-3): p. 11-8.
38. Cole, J.A., *The rapid accumulation of large quantities of ammonia during nitrite reduction by Escherichia coli.* FEMS Microbiology Letters, 1978. **4**(6): p. 327-329.
39. Bamford, V.A., et al., *Structure and spectroscopy of the periplasmic cytochrome c nitrite reductase from Escherichia coli.* Biochemistry, 2002. **41**(9): p. 2921-31.
40. Page, L., L. Griffiths, and J.A. Cole, *Different physiological roles of two independent pathways for nitrite reduction to ammonia by enteric bacteria.* Archives of microbiology, 1990. **154**(4): p. 349-54.
41. Cole, J.A., et al., *Nitrite and ammonia assimilation by anaerobic continuous cultures of Escherichia coli.* J Gen Microbiol, 1974. **85**(1): p. 11-22.

Tables

Table 3-1. *E.coli* growth trails.

Trial	Carbon/Energy		Nitrogen			*E.coli* Strain Growth		
	Glucose	**Glycerol**	**Ammonium**	**Nitrate**	**Nitrite**	**wt**	***nrfA***	***nirB***
1	+					-	-	-
2	+		+			+	+	+
3	+			+		+	+	-
4*	+			+		-	-	-
5	+				+	+	+	-
6		+				-	-	-
7		+		+		-	-	-
8		+			+	-	-	-
9		+	+			-	-	-
10		+	+	+		+	+	+
11		+	+		+	-	-	-

***** indicates trials at aerobic conditions; all other trails are under anaerobic conditions. Concentrations: glucose 20 mM, glycerol 5% v/v, ammonium chloride 20 mM, sodium nitrate 20 mM, sodium nitrite 5 mM. “wt” is short for “wild type”.

Table 3-2. PCR primers for cloning.

Primers	Sequence
*pnir*_F	5'-GGTTACCGGCCCGATCGTTG-3'
*pnir*_R	5'-TTTTGCCTCGATTTCTTTTCTATTACCGCCTAC-3'
EcoRI_*pnir*_F	5'-ACAACAACACGAATTCGGTTACCGGCCCGATCGTTG-3'
NdeI_*pnir*_R	5'-ACAACAACACCATATGTTTTGCCTCGATTTCTTTTCTAT TACCGCCTAC-3'
*nirB*_F	5'-ATGAGCAAAGTCAGACTCGCAATTATCGG-3'
*nirB*_R	5'-TCATGCGTTGTCCTCCACCAG-3'
NdeI_*nirB*_F	5'-ACAACAACACCATATGATGAGCAAAGTCAGACTCGCA ATTATCGG-3'
HindIII_*nirB*_R	5'-ACAACAACACAAGCTTTCATGCGTTGTCCTCCACCAG-3'

Figures and Legends

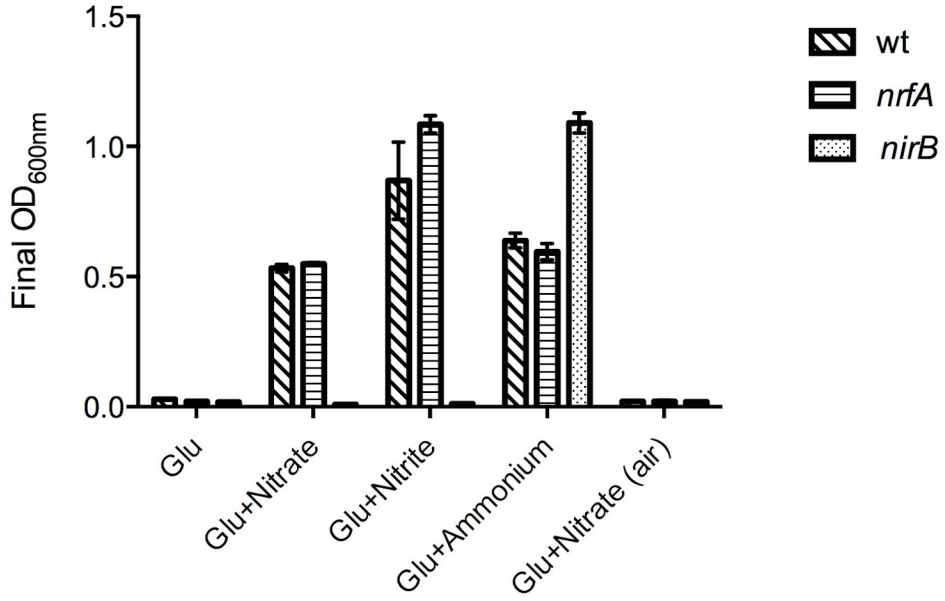

Figure 3-1. Growth of *E.coli* strains in glucose minimal medium with different nitrogen sources. Conditioned wild type (wt) and *nrfA* mutant strains were used as inoculants, while *nirB* mutant inoculants were non-conditioned since it is not able to grow in medium with glucose and nitrate. All medium conditions contained 20 mM glucose as the sole carbon source, plus 20 mM sodium nitrate, 5 mM sodium nitrite, or 20 mM ammonium chloride as the sole nitrogen source. The condition Glu (short for "glucose") is a negative control without any nitrogen sources. All experiments were done anaerobically except for condition "Glu+Nitrate (air)" was done aerobically. Final OD readings at 600 nm were taken 24 hours after inoculation.

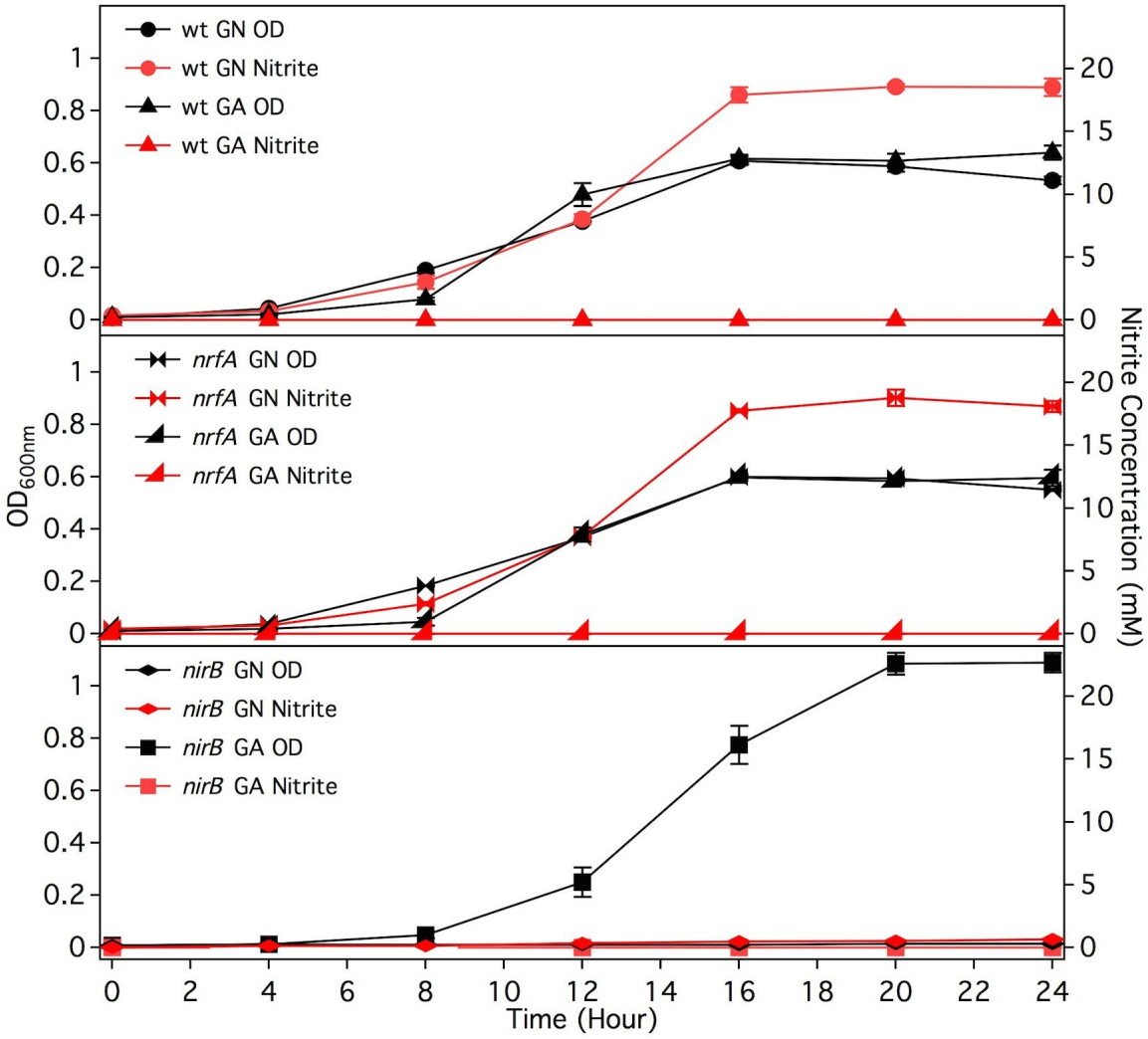

Figure 3-2. Growth curves with nitrate or ammonium as sole nitrogen source. Both wild type (wt) and *nrfA* mutant strain were conditioned; *nirB* mutant strain was non-conditioned. Medium conditions used were Evans medium base with 20 mM glucose plus 20 mM sodium nitrate (GN) or plus 20 mM ammonium chloride (GA). All growth curves (curves in black) were done anaerobically with 24 hours duration and 4 hours sampling intervals. Cell samples were centrifuged and medium supernatants were used for quantifying nitrite concentration by Griess assay (curves in red). Legends are shown on the graph.

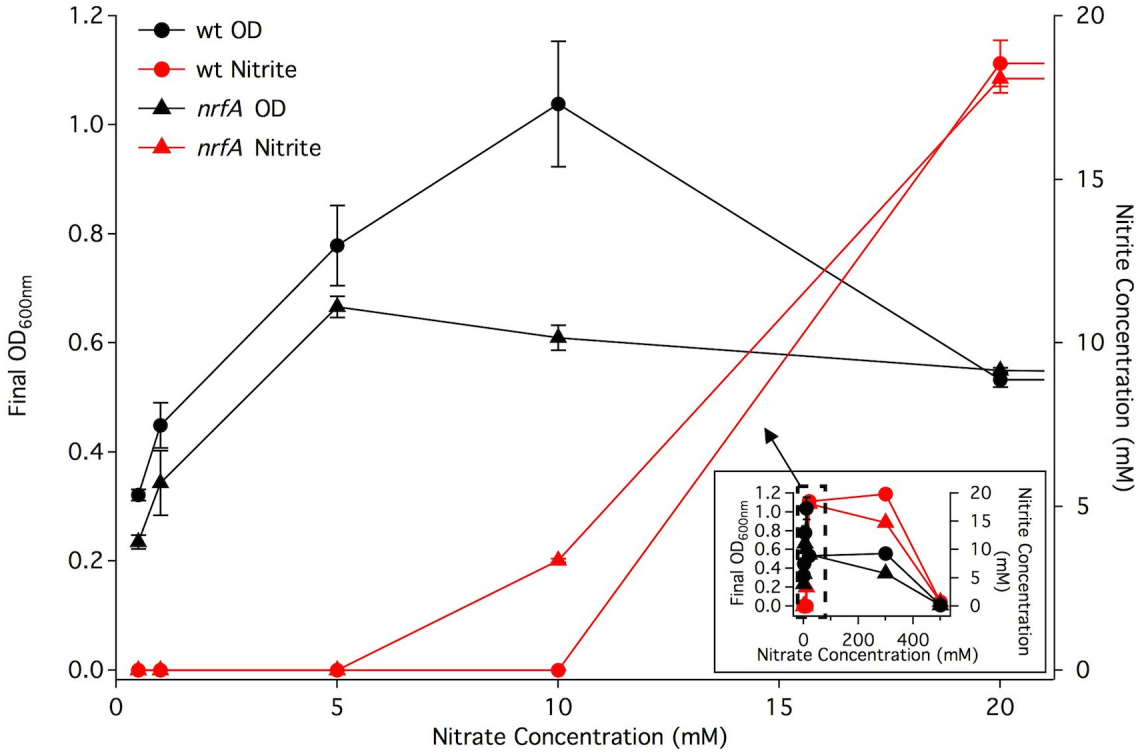

Figure 3-3. Growth of wild type (wt) and *nrfA* mutant strain with gradient of nitrate concentrations. Both wt and *nrfA* mutant strain were conditioned. 20 mM glucose was used as the sole carbon source in all conditions. The gradient of sodium nitrate concentrations was 0.5, 1, 5, 10, 20, 300 and 500 mM. Cells were cultured for 24 hours anaerobically, after which OD at 600 nm and nitrite concentration in medium were measured. Data from 0.5 mM to 20 mM nitrate are shown as main graph, while 20 to 500 mM are shown in sub graph. Legends are shown on the graph.

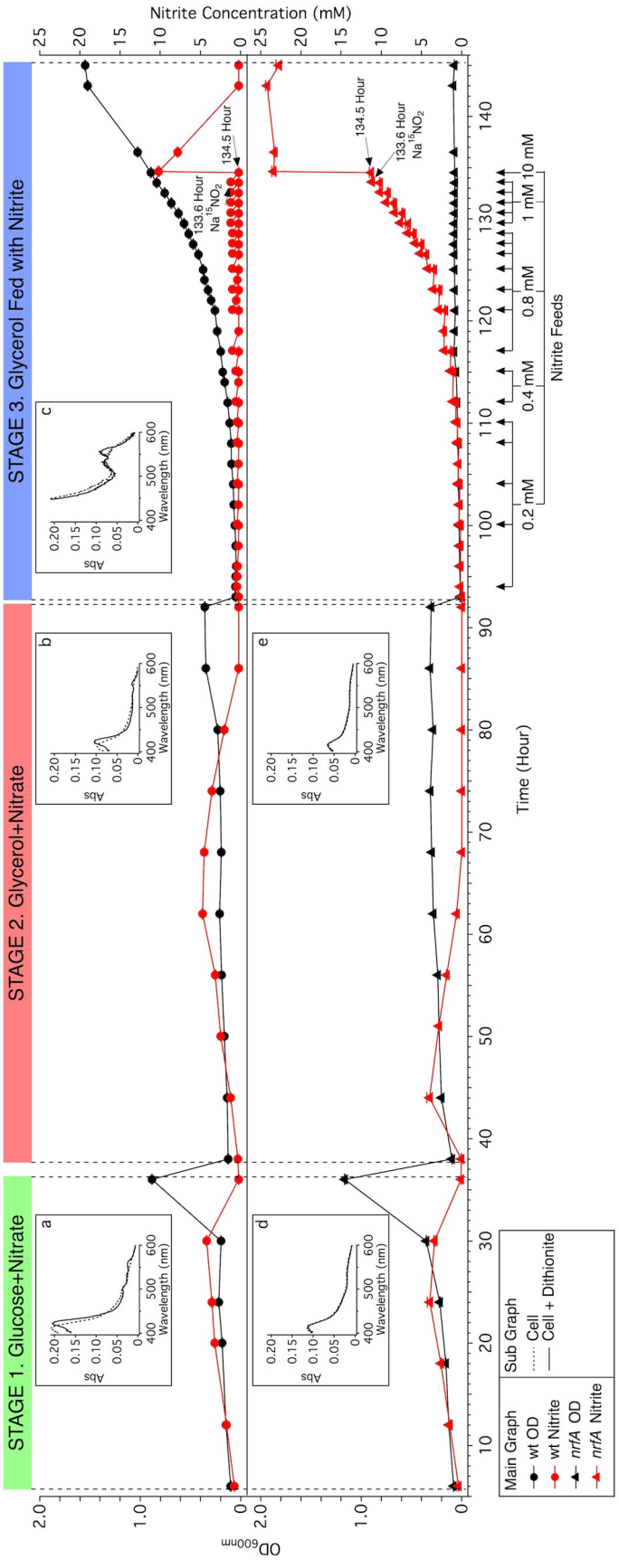

Figure 3- 4. Sequential batch culture of wild type (wt) and *nrfA* mutant strains. Sequential batch culture for each strain were carried out as three stages with different sole carbon and nitrogen sources. Medium in Stage 1 contained 20 mM glucose and 5 mM sodium nitrate, in Stage 2 contained 0.5% v/v glycerol and 5 mM sodium nitrate, and in Stage 3 contained 0.5% v/v glycerol and certain amount of sodium nitrite was fed at certain time points (nitrite feeds are indicated by arrows below the "Time" axis). After each stage, the culture was drained to minimum amount and refilled with new medium to start next stage. Small samples (~5 ml) were collected during sequential batch culture to monitor cell OD and nitrite concentration in growth medium. In the main graph, black points represent the cell OD at 600 nm (unit on left axis); red points are nitrite concentrations (unit on right axis). At 133.6 hour (Stage 3, tagged in main graph), 1mM ^{15}N labeled sodium nitrite ($Na^{15}NO_2$) was added to the fermenter. Right after (at 133.6 hour) and about 1 hour after (at 134.5 hour) adding labeled nitrite, 100 ml sample was saved respectively for 1D ^{15}N-NMR (see **Figure 3-5** for results). After whole cells were drained from each stage (~3.5 to 4 liters), they were concentrated 10 times and spectrums were taken by an OLIS CLARiTY spectrometer. The spectrums are shown as sub graphs. a) and d) are wt and *nrfA* mutant at 36 hour (end of Stage 1). b) and e) are wt and *nrfA* mutant at 92 hour (end of Stage 2). c) is wt at 145 hour (end of Stage 3). Dash line represent whole cell only and solid line represent whole cell mixed with dithionite.

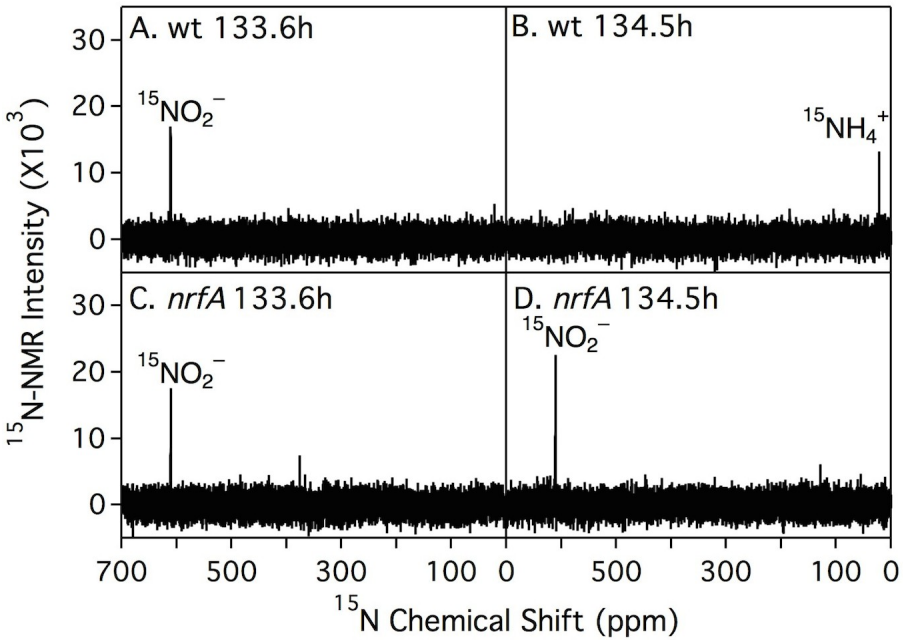

Figure 3-5. 1D ^{15}N-NMR for wild type (wt) and *nrfA* mutant sequential batch culture (Figure 3-4). See Figure 3-4 caption for sampling strategy and see Materials and Methods for sample preparation. Legends are shown on the graph. Chemical shift of $^{15}NO_2^-$ was 610 ppm and that of $^{15}NH_4^+$ was 21 ppm.

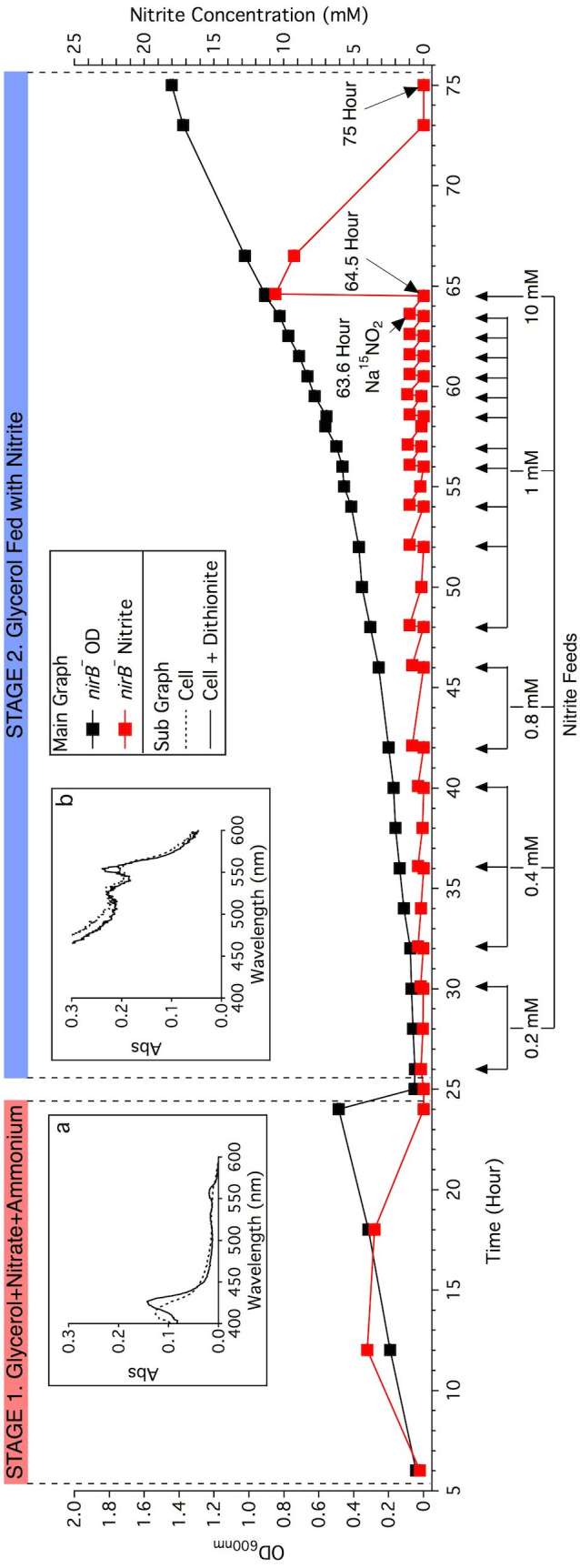

Figure 3-6. Sequential batch culture of *nirB* mutant strain. The *nirB* mutant sequential batch culture included two stages. Medium of Stage 1 contained 0.5% v/v glycerol, 5 mM sodium nitrate and 2 mM ammonium chloride. Medium of Stage 2 contained 0.5% v/v glycerol and certain amount of sodium nitrite was fed at certain time points (nitrite feeds are indicated by arrows below the "Time" axis). No other carbon or nitrogen sources were added to the minimal medium. After Stage 1, cell culture were drained to minimum amount and refilled with new medium to start Stage 2. Sampling strategy were the same as wt and *nrfA* (Figure 3-4). Black curve represents OD (unit on left axis) and red curve represents nitrite concentration (unit on right axis). At 63.6 hour, 1 mM ^{15}N labeled sodium nitrite ($Na^{15}NO_2$) was added to the fermenter. 100 ml cell samples were collected right after adding labeled (63.6 hour), about an hour later (64.5 hour) and about 11.5 hours later (75 hour) respectively. The cells in the three samples were separated from the medium (see Materials and Methods for details). Medium samples were used in 1D ^{15}N-NMR for inorganic nitrogen detection; while cells samples were used in ^{15}N-HMQC for organically incorporated nitrogen. See Figure 3-7 for NMR results. At the end of both stages, drained whole cells (3.5-4 from each stage) were concentrated 10 times and spectrums were taken using an OLIS CLARiTY spectrometer. Spectrums are shown as sub graphs. a) is from sample at 24 hour (end of Stage 1) and b) is from sample at 75 hour (end of Stage 2). Legends are shown on the graph.

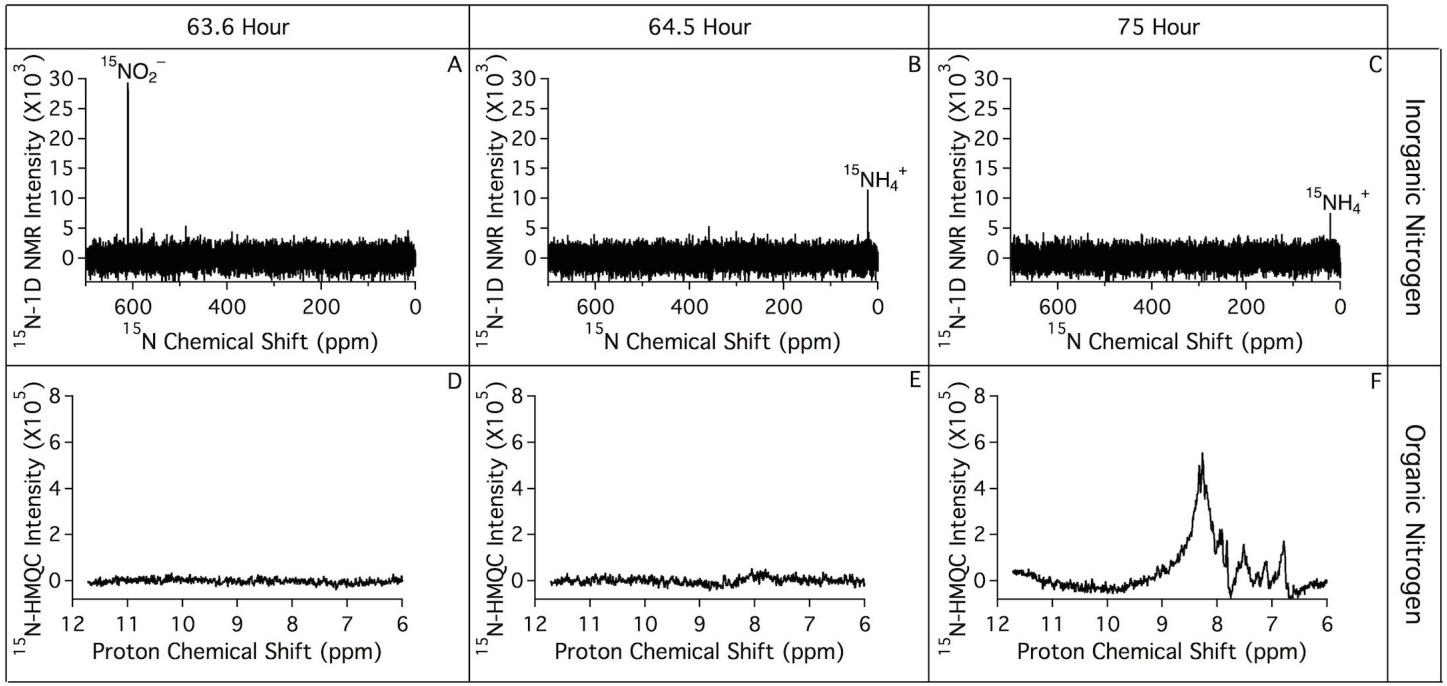

Figure 3-7. 1D ^{15}N-NMR and ^{15}N-HMQC for *nirB* sequential batch culture (Figure 3-6). See Figure 3-6 caption for sampling strategy and see Materials and Methods for sample preparation. A-C are 1D ^{15}N-NMR for inorganic nitrogen; D-F are ^{15}N-HMQC for organic nitrogen. A and D were 63.6 hour sample, B and E 64.5 hour, C and F 75h. Chemical shift of $^{15}NO_2^-$ was 610 ppm and that of $^{15}NH_4^+$ was 21 ppm.

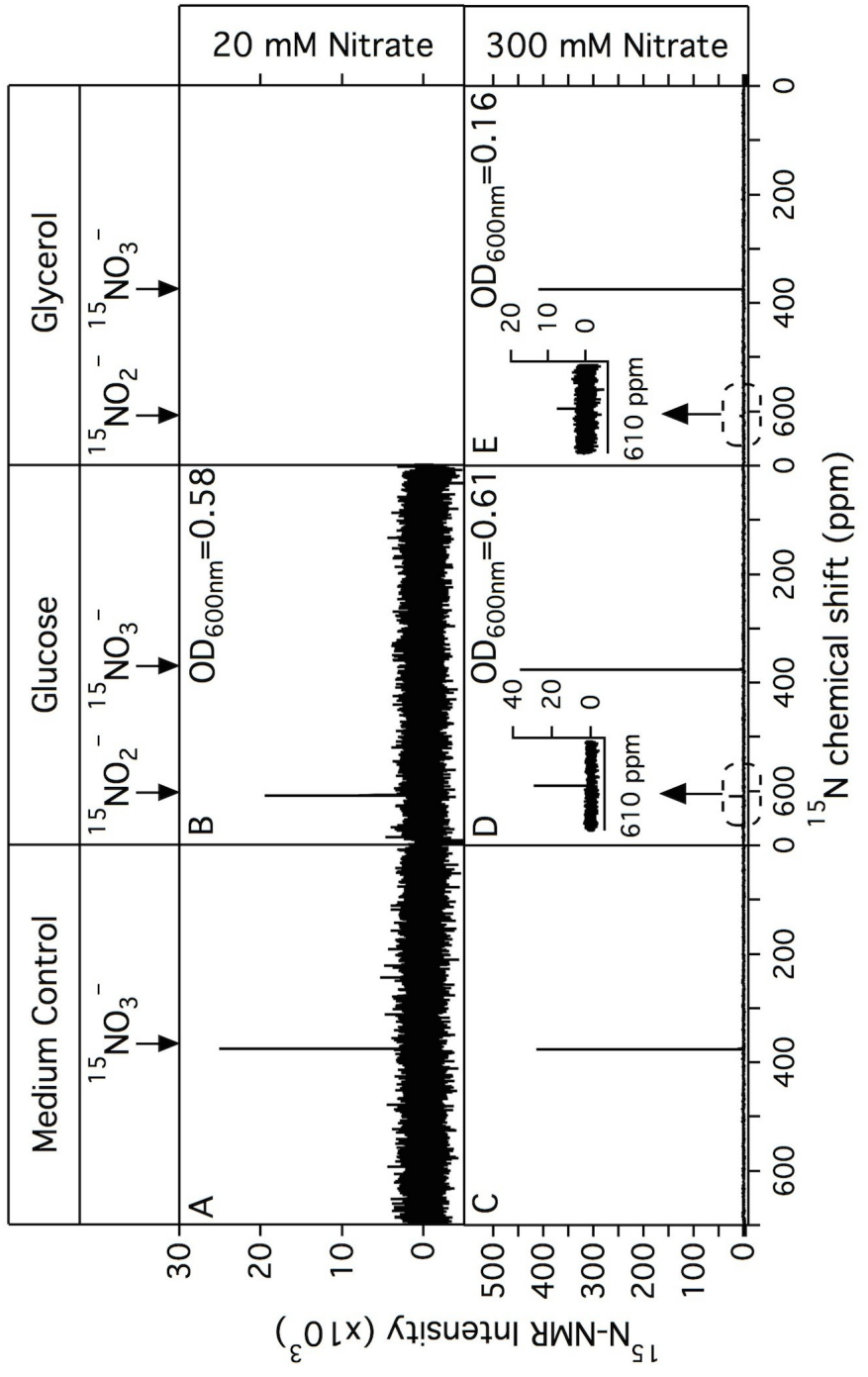

Figure 3-8. 1D ^{15}N-NMR for wild type strain with glucose or glycerol plus nitrate. Medium Control (A and C) was medium sample with 20 or 300 mM sodium nitrate before inoculation. Experiment samples were medium of 24-hour anaerobic cultures from three growth conditions: 20 mM glucose plus 20 mM (B) or 300 mM (D) ^{15}N labeled sodium nitrate, and 0.5% v/v glycerol plus 300 mM ^{15}N labeled sodium nitrate (E). Chemical shift of $^{15}NO_2^-$ was 610 ppm and that of $^{15}NO_3^-$ was 376 ppm.

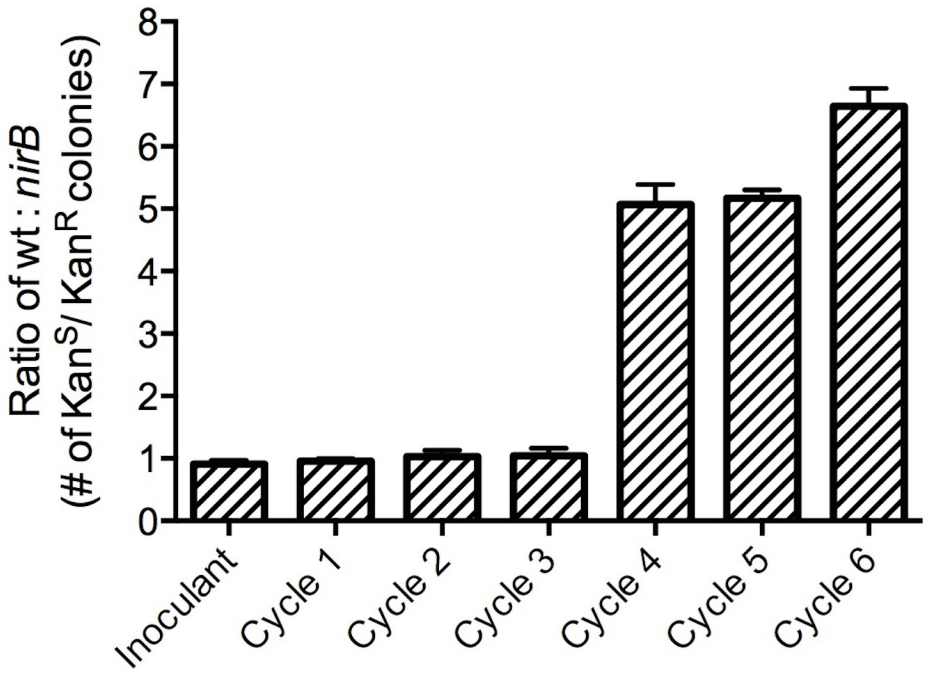

Figure 3-9. Competition between wild type (wt) and *nirB* mutant strains in sequential batch culture. Similar amount of wt and *nirB* mutant cells were first inoculated (labeled as "Inoculant") in 4 L of fresh medium to start Cycle 1. After culturing for 16 hours, the Cycle 1 culture was sampled, drained to minimum amount, refilled with fresh medium to start Cycle 2 and so on. First three cycles (Cycle 1 to 3) used medium with 20 mM glucose and 2 mM ammonium chloride. Last three cycles (Cycle 4 to 6) used same medium plus 20 mM sodium nitrate. Inoculant and samples after each cycle was diluted 50,000 times (same for inoculant) and plated on LB (no antibiotic) plates (this step happened right after sampling). These LB plates were then used as master plates for replica plating on LB (no antibiotic) and LB (kanamycin) plates. wt is kanamycin sensitive (Kan^S), represented by number of colonies on replica plates with no antibiotic minus that with kanamycin. *nirB* mutant is kanamycin resistant (Kan^R), represented by number of colonies on kanamycin replica plates. Data shown in the graph is the ratio of wt to *nirB* colonies.

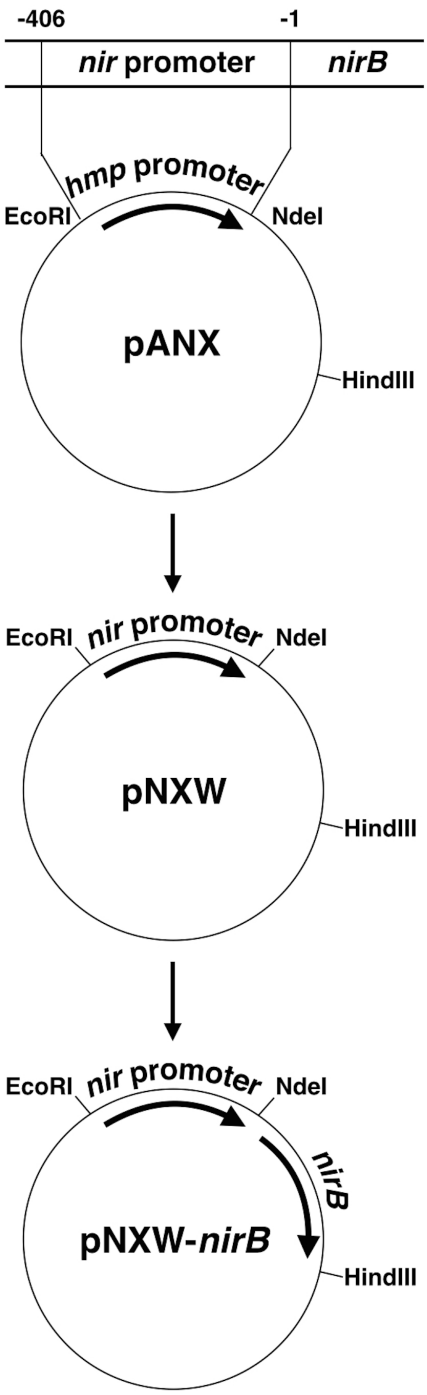

Figure 3-10. Cloning diagram for complementation of *nirB* mutant. The *nir* operon promoter region from wild type, located at -406 to -1 base pairs up stream of *nirB* gene, was sub-cloned into pANX plasmid to replace the *hmp* promoter between EcoRI and NdeI restriction sites. The result plasmid was named pNXW. Then the *nirB* gene from wild type was sub-cloned into the pNXW plasmid between NdeI and HindIII sites, resulting plasmid pNXW-*nirB*.

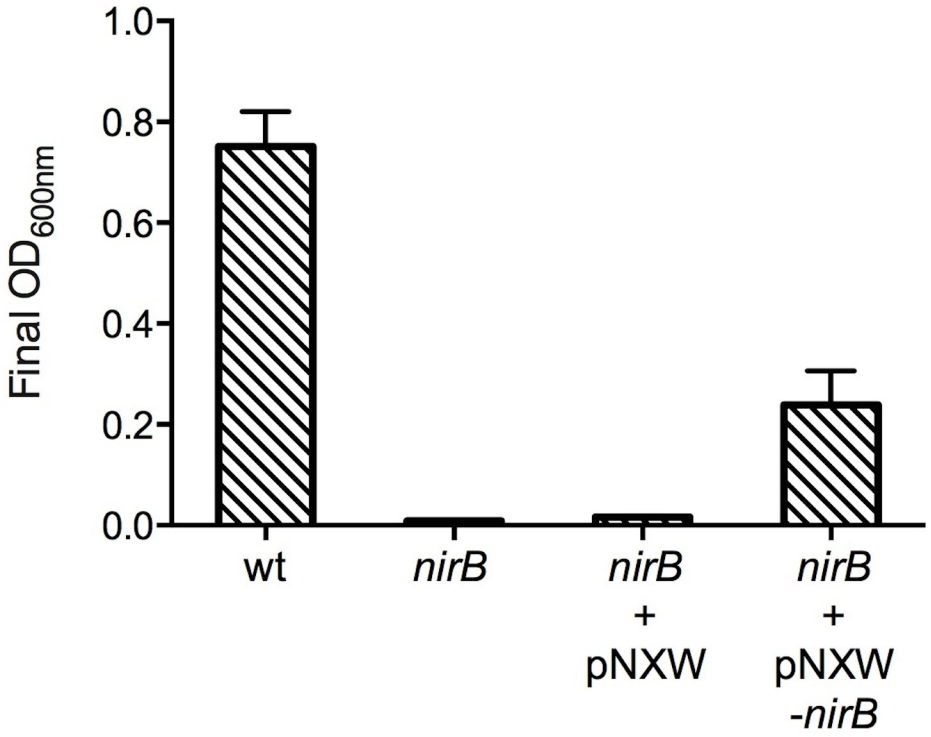

Figure 3-11. Complementation of *nirB* mutant. Wild type (wt), *nirB* mutant, *nirB* mutant transformed with pNXW empty plasmid (*nirB* + pNXW), *nirB* mutant transformed with pNXW plasmid carrying the *nirB* gene (*nirB* + pNXW-*nirB*) were cultured anaerobically in 30 ml flasks for 24 hours. Medium used for all cells were 20 mM glucose and 5 mM sodium nitrate. OD at 600 nm were taken for these 24-hour cultures and plotted. Left axis shows OD scale.

CHAPTER 4

STUDY OF S-NITROSOGLUTATHIONE REDUCTASE AS A POSSIBLE COFACTOR OF CLASS 1 NONSYMBIOTIC HEMOGLOBIN FOR PLANT HYPOXIC NITRITE REDUCTION

A research paper in preparation

Xiaoguang Wang[1234], Singh Navjot[12], Mark Hargrove[24]

Introduction

S-nitrosoglutathione reductase (GSNOR) was originally identified as glutathione-dependent formaldehyde dehydrogenase (GS-FDH, EC 1.2.1.1) or class III alcohol dehydrogenase (ADH III, EC 1.1.1.1) [1]. Recently, it was found to efficiently reduce s-nitrosoglutathione (GSNO) with NADH or NADPH as an electron donor [2-4], so it started to be called GSNOR. The *E. coli* GSNOR was reported to produce oxidized glutathione (GSSG) and ammonia as major products, in a GSH (reduced glutathione) dependent manner [3]. The human GSNOR was found to irreversibly produce glutathione sulfinamide ($GSONH_2$) and GSSG [5]. However, the products of plant GSNOR have not yet been systematically characterized.

In general, the role of plant GSNOR is proposed to control GSNO levels and protect cells against nitrosative stress [6, 7]. Plant GSNOR is highly expressed in root tips [8]. It is also found in plant roots, where the GSNO/GSH ratio is 1.5-2 fold as high as in

[1] Contributed in bench works.
[2] Contributed in experimental design.
[3] Contributed in writing.
[4] Contributed in editing and proof reading.

stem and leaf [9]. Considering nitrite and nitric oxide (NO) accumulation and pH decrease in plant roots under hypoxic or anoxic pressures, more GSNO is potentially produced under such conditions [10-12]. These conditions support a role for GSNOR in plant roots during hypoxia or anoxia.

Meanwhile, class 1 non-symbiotic plant hemoglobin (nsHb1) is also up-regulated in plant roots by hypoxia [13]. Previous studies have shown that ferrous nsHb1 can efficiently reduce nitrite to NO *in vitro* [14]. But right after NO is produced, it binds to the rest of ferrous nsHb1 and form an extremely tight $Hb^{(2+)}$:NO complex, presumably preventing further reactions by the hemoglobin. Although nsHb1 can also efficiently reduce hydroxylamine to ammonium [15], there is no evidence that it can reduce nitrogen past NO once it is bound to the ferrous Hb (Figure 4-1). However, it is possible that the ferrous $Hb^{(2+)}$:NO complex could be reduced by some other as-of-yet unidentified component of the anoxic plant root cell.

Since GSNOR and nsHb1 are both important for plant hypoxia, they are both induced in plant root and localized in the cytosol [8, 10-13, 16], the present work tested rice (*Oryza sativa* Japonica Group) GSNOR as a possible cofactor of rice nsHb1 for anaerobic nitrite reduction *in vitro*. Experiments were carried out based on two hypotheses (shown in Figure 4-1). Hypothesis 1 is that FDH can directly reduce the NO in the $Hb^{(2+)}$:NO complex (possibly through a HbS-NO intermediate) to release the ferrous nsHb, so that ferrous Hb can continue to reduce hydroxylamine to ammonium. Hypothesis 2 is that the GSNHOH reduced from GSNO by GSNOR is favored by ferrous nsHb rather than nitrite as a substrate, so the $Hb^{(2+)}$:NO production is avoided and ammonium can be produced. The results of this chapter present a test of this hypothesis

consisting of measuring a number of *in vitro* reactions of rice nsHb with rice GSNOR and inorganic nitrogen metabolites. We could find no significant interaction between nsHb and GSNOR, but present product analysis and enzyme kinetics constants for rice GSNOR reacting with GSNO.

Materials and Methods

GSNOR cloning, expression and purification. *Oryza sativa* Japonica Group total mRNA was kindly provided by Dr. Reuben Peters from Biochemistry Department of Iowa State University. Using the rice total mRNA as template, RT-PCR followed by regular PCR with done to amplify the *GSNOR* gene. The gene was sub-cloned into the pET28 expression vector between NdeI and HindIII restriction sites. The resulted pET28-*GSNOR* vector was transformed into *E. coli* BL21(DE3) competent cells (Promega). A single colony of transformed *E.coli* was used to make a 5 ml LB starter culture over night. 1 ml of starter culture was used to inoculate 1 L fresh LB medium. A total of two 1 L LB cultures were prepared. Cell cultures were first incubated at 37ºC until cell OD reached 0.6, and were then induced with 0.5 mM IPTG, and the temperature was lowered to 16ºC. After incubating at 16ºC for 8 hours, cell cultures were harvested by centrifugation, followed by lysing with a homogenizer. Soluble fraction of the cell lysate were passed through a Ni-NTA Agarose column (Qiagen). Using this method, GSNOR was purified to more than 95% purify.

GSNOR enzyme kinetics. All kinetics experiments were done aerobically with 100 mM phosphate buffer (pH 7.0). Concentration of GSNO and NADH were first mixed

in a 1 ml quartz cuvette, then 2 ug GSNOR was added to initiate the reaction. Kinetics traces were recorded at 340 nm for NADH oxidotion, which was used to calculate initial velocity. In reactions to measure the K_m of GSNO, NADH concentrations were constant at 100 μM, and GSNO was varied from 0 to 750 μM. In reactions to measure the K_m of NADH, GSNO was constant at 250 μM, and NADH was varied from 0 to 200 μM. Initial velocities were plotted against GSNO or NADH concentrations and fit to the Michaelis-Menten equation using Igor Pro software. Each reaction was repeated 3 times.

GSNOR product analysis. For LC/MS experiments, all samples were prepared in an anaerobic chamber in 100 mM phosphate buffer (pH 7.0). Concentrations for all standards including GSH, GSNO and GSSG was 1 mM. All standards were purchased from Sigma. For reaction mixtures, final concentration of reactants, when involved, were 1 mM GSNO, 1 mM NADH, 2 ug/ml GSNOR, 1 mM GSH. Reactions were first mixed and incubated at room temperature in the dark (to avoid GSNO degradation) for 1 hour before LC/MS. Agilent 6540 QTOF was used for accurate mass detection. All samples were run in positive ionization mode. For ^{15}N-NMR experiments, samples were prepared both aerobically and anaerobically. ^{15}N labeled GSNO was prepared in lab by mixing the equal volumes of 500 mM reduced-glutathione (GSH) and 500 mM ^{15}N-labeled sodium nitrite (pH adjusted to 3.0 by hydrochloric acid). After mixing, pH was adjusted to 7.4 and concentrations were measured by absorbance at 340 nm and extinction coefficient of 767 M^{-1} cm^{-1}. ^{15}N-NMR spectrums were collected with a Bruker Avance III 600 Spectrometer.

Assays to test GSNOR interactions with nsHb. Samples for all such assays are prepared in an anaerobic chamber in the dark in 100 mM phosphate buffer (pH 7.0). Then samples are loaded in an airtight quartz cuvette for measuring absorbance spectra outside of the chamber. Stock solutions were also prepared in the anaerobic chamber and stored in glass vials sealed with air tight crimped stoppers. Airtight Hamilton syringes were used to transfer stock solutions from vial to cuvette to avoid oxygen contamination. Ferrous rice nsHb1 and anaerobic NO solutions were prepared as previously described [17]. 1 M NADH stock solution was prepared for all assays, then diluted in cuvette to proper final concentration.

Results

Oryza sativa GSNOR enzyme kinetics. The *Oryza sativa* (Japonica Group) *GSNOR* gene was sub-cloned into a pET28 vector and over-expressed in *E. coli* BL21(DE3). After the soluble GSNOR was purified by Ni-NTA column, the GSNO reductase activity was verified by mixing the GSNOR with GSNO and NADH. As is shown in Figure 4-2, after 2 μg GSNOR was added to 1 ml mixture of 500 μM GSNO and 150 μM NADH in a cuvette, the NADH peak at 340 nm started to decay. In less than 16 minutes, the reaction was finished, demonstrating GSNO reductase activity of the purified GSNOR enzyme. Figure 4-3 shows the enzyme kinetics results. To measure K_m for GSNO, varying concentrations of GSNO (0 to 750 μM) were mixed with 100 μM NADH and 2 μg GSNOR in a 1 ml reaction. For each reaction, the NADH decay at 340 nm was used to calculate the initial reaction velocity $V_{0,}$ and plotted against GSNO concentration as Figure 4-3A. The K_m for GSNO is 43 ± 3 μM. To measure K_m for

NADH, varying concentrations of NADH (0 to 200 μM) were mixed with 250 μM GSNO and 2 μg GSNOR in a 1 ml reaction. The NADH decay at 340 nm was also used to calculate the $V_{0,}$ and plotted against NADH concentration as Figure 4-3B. The K_m for NADH is 9 ± 1 μM. All kinetics reactions were measured under aerobic condition.

Product analysis for GSNOR catalyzed GSNO reduction. LC/MS and ^{15}N-NMR were used to characterize the products of anaerobic GSNO reduction by rice GSNOR. The LC/MS data are shown in Figure 4-4 and 4-5. A C-18 HPLC column was used for separation, and isocratic elution was performed with 10% H_2O and 90% acetonitrile. Figure 4-4 shows that all three glutathione derivative standards are readily detectable by LC/MS, including reduced glutathione (GSH, Figure 4-4A), s-nitrosoglutathione (GSNO, Figure 4-4B) and oxidized glutathione (GSSG, Figure 4-4C). Mass/charge ratio (m/z) of both GSH and GSNO showed up as 1 proton charged, 308.09 for GSH (MW 307.08) and 337.08 for GSNO (MW 336.07). GSSG (MW 612.15) can be either 1 proton charged (m/z 613.16) or 2 protons charged (m/z 307.08). Figure 4-5 shows LC/MS results for reaction mixtures that were incubated anaerobically for 1 hour after mixing. Figure 4-5A is 1 mM GSNO and 1 mM NADH with out enzyme, as a negative control. We can see the GSNO peak at retention time of 5.9 minute and some GSSG at 5.7 minute as seen in the standard (Figure 4-4B). When 2 μg GSNOR was mixed with 1 mM GSNO and 1 mM NADH in a 1 ml mixture, there was a new broad peak with a retention time of 2.5 to 2.7 minutes (Figure 4-5B), representing the products after the GSNO reduction. In the product peak, there are two m/z values, one is 322.07 the other is 339.10. If both are 1 proton charged, the m/z 339.10 is GSNHOH (MW 338.09) or the rearranged $GSONH_2$,

which matches with the human GSNOR product reported previously [5]. The m/z 322.07 then should represent a compound with a molecular weight of 321, which is 1 mass less than $GSNH_2$ (MW 322.09). So with this data, we cannot identify the m/z 322.07. When 1 mM GSH was involved in the reaction (Figure 4-5C), the same 2.5 to 2.7 minute peak was shown with the same two m/z 322.07 and 339.10. In addition to these products, large amounts of GSSG are also present. However, when 1 mM GSNO and 1 mM GSH were mixed, there were also similar amounts of GSSG (Figure 4-5D). So GSH reacts with products from GSNO reduction, but does react with GSNO directly.

The NMR data are shown in Figure 4-6. For each reaction mixture, samples were prepared under both aerobic and anaerobic conditions. $GS^{15}NO$ was used for all reactions. 10 μg GSNOR was added when "+" is shown under the "GSNOR" column. 21 ppm represents ammonium. 80.7 and 80.1 ppm are possibly GSNHOH and $GSNH_2$, because these two products show up together, just like the m/z 322.07 and 339.10 in LC/MS. With 10 mM GSNO and 10 mM NADH, there were not any products (Figure 4-6 A and B). With 10 mM GSNO, 5 mM NADH and GSNOR, 80.7 and 80.1 ppm products and ammonium were produced (Figure 4-6 C and D). When NADH was increased to 10, 20 and 40 mM, all products were increased correspondingly under air condition (Figure 4-6 E, G and I). But under anaerobic condition, this increase was only obvious when NADH increased from 5 to 10 mM (Figure 4-6 D and F), not from 10 to 20 and 40 mM (Figure 4-6 H and J). Involvement of 10 or 20 mM GSH in the 10 mM GSNO, 10 mM NADH, and GSNOR reactions did not seem to change any product profiles in aerobic or anaerobic conditions (Figure 4-6 K, L, M and N). Involvement of 10 or 20 mM GSH in the 10 mM GSNO, 20 mM NADH, and GSNOR reactions in air

showed a decrease of all products (Figure 4-6 O and Q) compared to the absence of GSH. However, when 10 mM GSH was mixed with 10 mM GSNO, 20 mM NADH and GSNOR anaerobically (Figure 4-6P), all products showed an increase compared to the absence of GSH, while 20 mM GSH did not make any change in the product profile (Figure 4-6R).

A test of GSNOR as a possible cofactor for rice nsHb1 nitrite reduction. To test hypothesis 1 (Figure 4-1), ferrous rice nsHb1 (Hb^{2+}) was prepared anaerobically. Then it was loaded in an airtight cuvette to take a spectrum and verify the ferrous state of heme at 500 to 600 nm wavelength range (Figure 4-7A solid line). Then NO saturated buffer, NADH and GSNOR was added to the cuvette with airtight Hamilton syringes sequentially. Right after NO was added, the $Hb^{(2+)}$:NO complex was formed, as evident from a flat spectrum from 540 to 590 nm (Figure 4-7A dash line with small interval). When NADH and GSNOR were added, the $Hb^{(2+)}$:NO spectrum did not change (Figure 4-7A dash lines with middle and big interval), meanwhile the NADH was not consumed (Figure 4-7B dash lines with middle and big interval). After waiting for 30 min after everything was mixed, $Hb^{(2+)}$:NO was still there with NADH not consumed (Figure 4-7 A and B dash lines with small/big interval). So GSNOR cannot reduce the NO in $Hb^{(2+)}$:NO complex and release $Hb^{(2+)}$. Hypothesis 1 is thus rejected.

Figure 4-8 shows results for testing hypothesis 2. Ferrous rice nsHb1 ($Hb^{(2+)}$) was prepared in the anaerobic chamber. Meanwhile, the reactants to be mixed with $Hb^{(2+)}$were also prepared anaerobically. One reactant was 10 mM GSNO only, the other is a mixture of 10 mM GSNO, 10 mM NADH and 10 μg/ml GSNOR. Both reactants were incubated

for 1 hour anaerobically before sealed in glass vials and used for mixing with ferrous hemoglobin. Two mixing experiments were done. For both mixing experiments, 900 µl of Hb^{2+} was first loaded in an airtight cuvette, and absorbance spectrum was measured. Deoxy ferrous heme was observed, as expected (Figure 4-8A and B bold solid lines). Then in the first mixing experiment, 100 µl of 10 mM GSNO was added to Hb^{2+} to give a final concentration of 1 mM GSNO. Right after mixing, 0.5 minutes, 1 minute and 15 minutes after mixing, spectra were measured (Figure 4-8A, thin solid line, dash lines with big, middle and small intervals respectively). Within 1 minute, the Hb^{2+} was completely reacted with GSNO and showed a $Hb^{(2+)}$:NO complex spectrum that was stable for the next 15 minutes. However, when 100 µM of the GSNO, NADH and GSNOR mixture was added to Hb^{2+} in the second mixing experiment, nsHb1 remained in the ferrous state (Figure 4-8B, thin solid line, dash lines with big, middle and small intervals). From time courses of absorbance at 557 nm (Figure 4-8C), we can clearly see that ferrous nsHb1 was quickly reacted in first mixing experiment but not in the second. This means the products from GSNOR-catalyzed GSNO reduction do not react with ferrous nsHb1, and hence hypothesis 2 is also rejected.

Discussion

Although the rice and other plant glutathione-dependent formaldehyde dehydrogenases were well characterized [18-22], the s-nitrosoglutathione reductase (GSNOR) activity of this enzyme in plants has only been reported in the last decade [22]. Our steady-state kinetic measurements show that the rice GSNOR K_m for GSNO is 43 µM, and for NADH is 9 µM. The K_m for GSNO is similar to that reported for tomato

GSNOR (57 μM) [23]. The K_m for NADH, although in the same range as the tomato enzyme (58 μM) [23], is about 5 fold smaller. The glutathione-dependent formaldehyde dehydrogenases activity of our GSNOR was also verified.

Our product analysis with LC/MS shows two m/z values in the product, 322.07 and 339.10. Since we used the positive ionization mode for mass detection, and both GSNO and GSH standards were charged with 1 proton, the m/z 339.10 is determined as GSNHOH or $GSONH_2$, whose mass is 338.09. This product matches with the human GSNOR as reported previously [5]. According to the *E. coli* GSNOR product from a previous study [3], the m/z value of 322.07 is possibly $GSNH_2$. However the mass of $GSNH_2$ is 322.09, and if it is 1 proton charged, the m/z should be 323 instead of 322.07. So in this case, we cannot verify the identity of the m/z 322.07, and we cannot rule out the possibility that it is a fragment of the m/z 338.09. To further verify this, we will need more information about these two m/z by doing MS-MS or run the same MS experiment with negative ionization mode.

In the ^{15}N-NMR experiments, we identified ammonium as a product from the GSNOR catalyzed GSNO reduction. And the ammonium production is neither GSH dependent, nor anaerobic condition dependent. Together with ammonium, we also see another two chemical shifts at 80.7 and 80.1 ppm. These two peaks show up under the same circumstances as the two m/z in the MS, suggesting the two NMR chemical shifts and the two m/z from LC/MS are the same compounds. However, at this point we cannot tell if the two NMR chemical shifts are from one compound or two, since they always show up simultaneously. To further analyze the reaction products, we need purified GSNHOH and $GSNH_2$ compounds as ^{15}N-NMR standards.

We are interested in the plant GSNOR because we thought it might be a potential cofactor of the plant nonsymbiotic hemoglobin (nsHb) for hypoxic nitrite reduction. However after testing two possible hypotheses *in vitro*, the rice GSNOR is not working as a cofactor of rice nsHb1 to facilitate its anaerobic nitrite reductase activity. To be specific, the GSNOR does not help ferrous nsHb1 to either go beyond or avoid forming $Hb^{(2+)}$:NO complex, which is a dead end and stops nsHb1 from reducing nitrite all the way to ammonium.

Although our data do not support a connection between GSNOR and nsHb1, it does not necessarily mean the GSNOR is not important for plant to survive hypoxia and anoxia pressure. It is proposed that the plant GSNOR is to help plants to release the nitrosative stress [6, 7]. However, in plant root, usually facing such nitrosative stress caused by hypoxia and anoxia, have a lower GSNOR activity than in steam [23], even though the plant root has extremely high GSNOR expression [8]. Thus the role of GSNOR in plants remains a mystery, which needs future investigation. One interesting side note from this work is that the reaction of GSNO with plant Hbs is faster than it should be if it were limited by NO release from GS. Thus, there appears to be some mechanism stimulating NO transfer from GSNO to the Hb heme iron. Future work in the Hargrove lab will investigate this phenomenon across different Hbs and under different ligand and oxidation states.

References

1. Strittmatter, P. and E.G. Ball, *Formaldehyde dehydrogenase, a glutathionedependent enzyme system.* J Biol Chem, 1955. **213**(1): p. 445-61.

2. Jensen, D.E., G.K. Belka, and G.C. Du Bois, *S-Nitrosoglutathione is a substrate for rat alcohol dehydrogenase class III isoenzyme.* Biochem. J., 1998. **331**(2): p. 659-668.
3. Liu, L., et al., *A metabolic enzyme for S-nitrosothiol conserved from bacteria to humans.* Nature, 2001. **410**(6827): p. 490-494.
4. Sakamoto, A., M. Ueda, and H. Morikawa, *Arabidopsis glutathione-dependent formaldehyde dehydrogenase is an S-nitrosoglutathione reductase.* FEBS letters, 2002. **515**(1,Äì3): p. 20-24.
5. Hedberg, J.J., et al., *Reduction of S-nitrosoglutathione by human alcohol dehydrogenase 3 is an irreversible reaction as analysed by electrospray mass spectrometry.* Eur J Biochem, 2003. **270**(6): p. 1249-56.
6. Valderrama, R., et al., *Nitrosative stress in plants.* FEBS Lett, 2007. **581**(3): p. 453-61.
7. Leterrier, M., et al., *Function of S-nitrosoglutathione reductase (GSNOR) in plant development and under biotic/abiotic stress.* Plant Signal Behav, 2011. **6**(6): p. 789-93.
8. Xu, S., et al., *S-nitrosoglutathione reductases are low-copy number, cysteine-rich proteins in plants that control multiple developmental and defense responses in Arabidopsis.* Front Plant Sci, 2013. **4**: p. 430.
9. Airaki, M., et al., *Detection and quantification of S-nitrosoglutathione (GSNO) in pepper (Capsicum annuum L.) plant organs by LC-ES/MS.* Plant & cell physiology, 2011. **52**(11): p. 2006-15.
10. Ferrari, T.E. and J.E. Varner, *Intact tissue assay for nitrite reductase in barley aleurone layers.* Plant Physiol, 1971. **47**(6): p. 790-4.
11. Botrel, A. and W.M. Kaiser, *Nitrate reductase activation state in barley roots in relation to the energy and carbohydrate status.* Planta, 1997. **201**(4): p. 496-501.
12. Corpas, F.J., J.d.D. Alché, and J.B. Barroso, *Current overview of S-nitrosoglutathione (GSNO) in higher plants.* Frontiers in Plant Science, 2013. **4**.
13. Ohwaki, Y., et al., *Induction of class-1 non-symbiotic hemoglobin genes by nitrate, nitrite and nitric oxide in cultured rice cells.* Plant Cell Physiol, 2005. **46**(2): p. 324-31.
14. Sturms, R., A.A. DiSpirito, and M.S. Hargrove, *Plant and cyanobacterial hemoglobins reduce nitrite to nitric oxide under anoxic conditions.* Biochemistry, 2011. **50**(19): p. 3873-8.
15. Sturms, R., et al., *Hydroxylamine reduction to ammonium by plant and cyanobacterial hemoglobins.* Biochemistry, 2011. **50**(50): p. 10829-35.
16. Sainz, M., et al., *Plant hemoglobins may be maintained in functional form by reduced flavins in the nuclei, and confer differential tolerance to nitro-oxidative stress.* The Plant Journal, 2013: p. n/a-n/a.
17. Wang, X. and M.S. Hargrove, *Nitric oxide in plants: the roles of ascorbate and hemoglobin.* PLoS One, 2013. **8**(12): p. e82611.
18. Dolferus, R., et al., *Cloning of the Arabidopsis and rice formaldehyde dehydrogenase genes: implications for the origin of plant ADH enzymes.* Genetics, 1997. **146**(3): p. 1131-41.
19. Martinez, M.C., et al., *Arabidopsis formaldehyde dehydrogenase. Molecular properties of plant class III alcohol dehydrogenase provide further insights into*

the origins, structure and function of plant class p and liver class I alcohol dehydrogenases. Eur J Biochem, 1996. **241**(3): p. 849-57.

20. Shafqat, J., et al., *Pea formaldehyde-active class III alcohol dehydrogenase: common derivation of the plant and animal forms but not of the corresponding ethanol-active forms (classes I and P).* Proc Natl Acad Sci U S A, 1996. **93**(11): p. 5595-9.
21. Uotila, L. and M. Koivusalo, *Purification of formaldehyde and formate dehydrogenases from pea seeds by affinity chromatography and S-formylglutathione as the intermediate of formaldehyde metabolism.* Archives of Biochemistry and Biophysics, 1979. **196**(1): p. 33-45.
22. Wippermann, U., et al., *Maize glutathione-dependent formaldehyde dehydrogenase: protein sequence and catalytic properties.* Planta, 1999. **208**(1): p. 12-8.
23. Kubienova, L., et al., *Structural and functional characterization of a plant S-nitrosoglutathione reductase from Solanum lycopersicum.* Biochimie, 2013. **95**(4): p. 889-902.

Figures and Legends

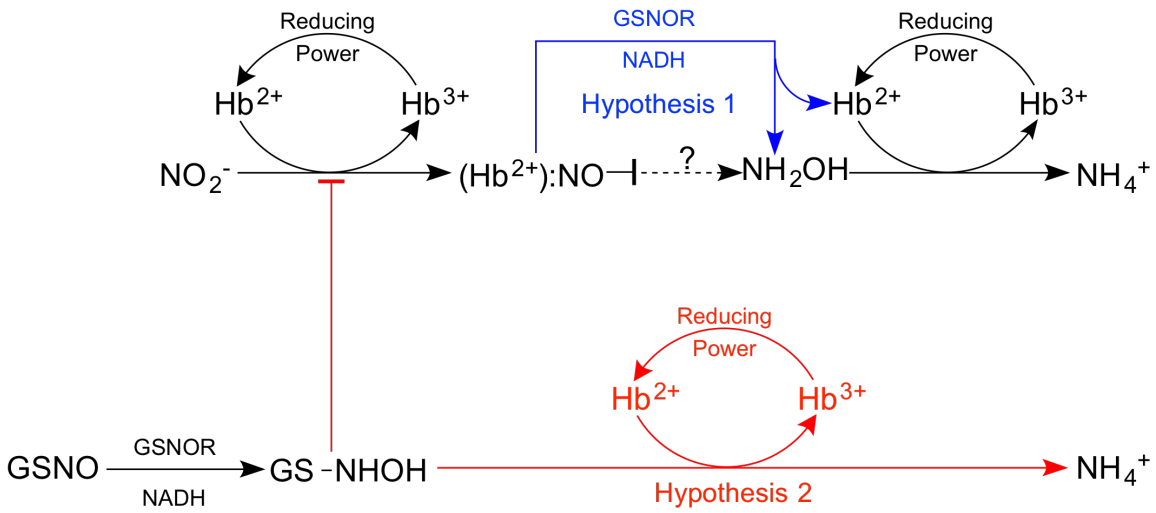

Figure 4-1. Two hypotheses for GSNOR being a cofactor of nsHb1 for anaerobic nitrite reduction. Hb^{2+} is ferrous rice class 1 nonsymbiotic hemoblogin (nsHb1), Hb^{3+} is ferric nsHb1. Hypothesis 1 (blue) is that GSNOR can directly react with $Hb^{(2+)}$:NO complex to reduce the NO and release Hb^{2+}, so the Hb^{2+} can continue to reduce hydroxylamine and produce ammonium. Hypothesis 2 is based on 1) the fact that ferrous nsHb1 can reduce hydroxylamine (rate constant 25 mM^{-1} s^{-1}, [15]) way faster than nitrite (rate constant 0.083 mM^{-1} s^{-1}, [14]); 2) the product GS-NHOH from GSNO reduction by GSNOR is similar to hydroxylamine, so it might be a potential substrate of Hb^{2+}. Hence we hypothesize that the GS-NHOH produced from GSNO reduction can compete with nitrite as a substrate of Hb^{2+}, protect the it from toxifying by the NO produced from nitrite reduction, and produce ammonium as final product.

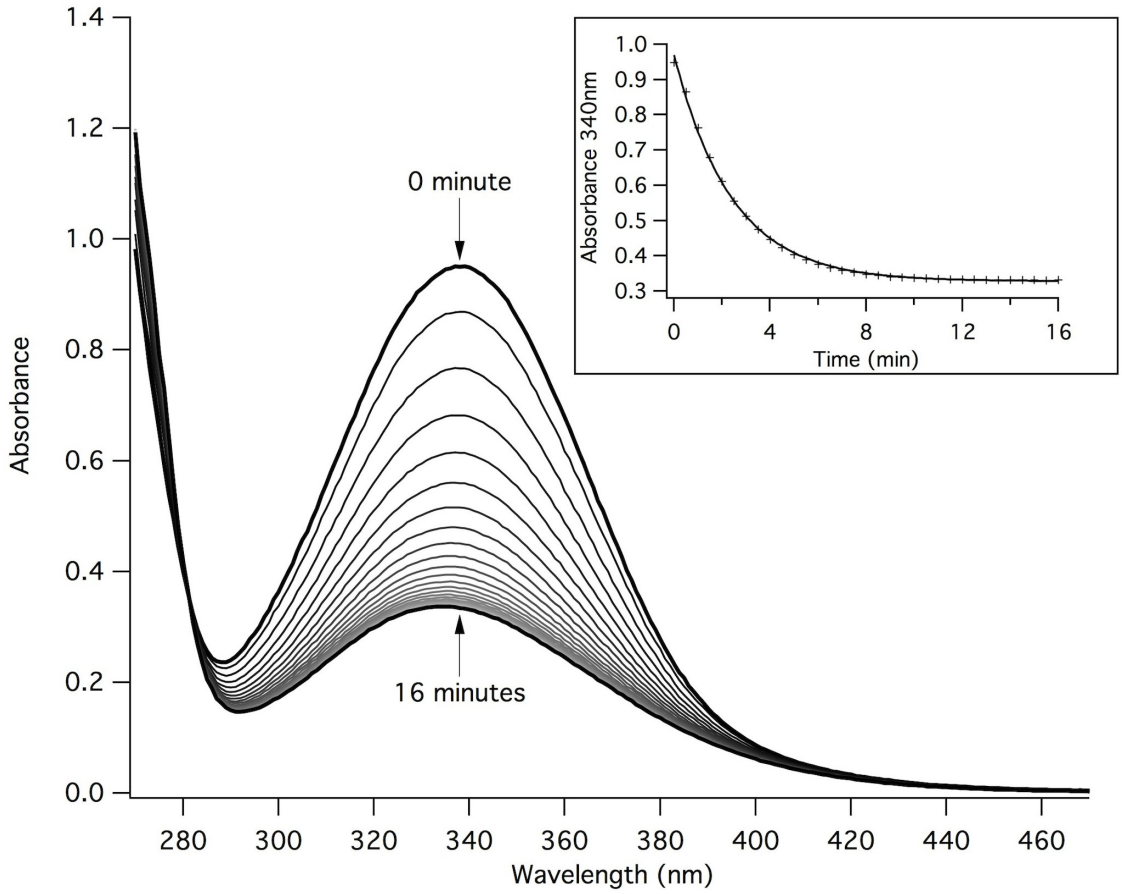

Figure 4-2. NADH dependent GSNO reduction by GSNOR. 500 μM GSNO and 150 μM NADH were mixed in 1 ml cuvette in air, 2 ug purified GSNOR was added to initiate the reaction. Scan kinetics was recorded and shown in main graph. The peak at 340 nm represents reduced NADH. NADH decay is shown from 0 to 16 minute. Time course for 340 nm reading is plotted in sub-graph on top right and fitted as an exponential curve.

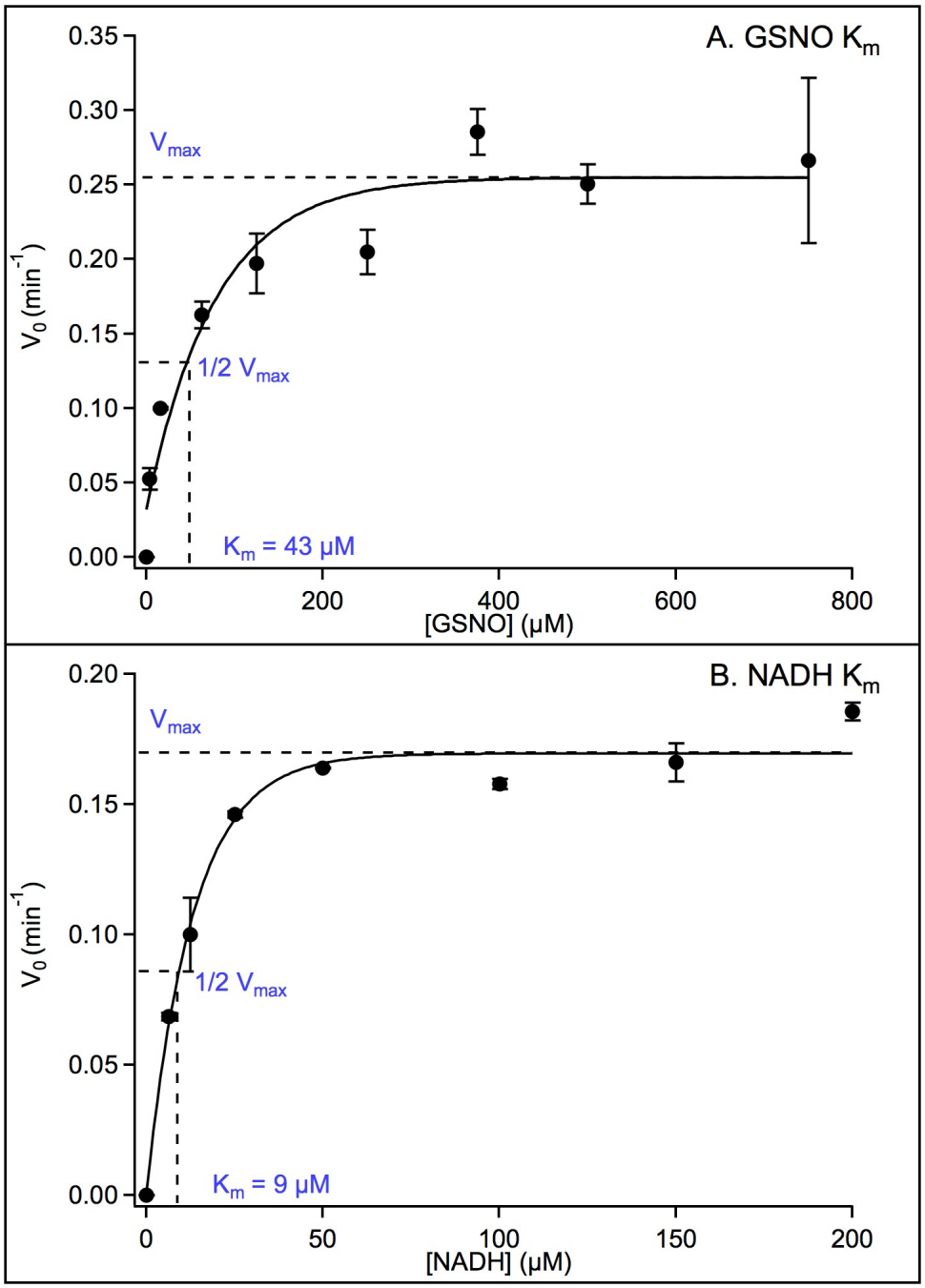

Figure 4-3. GSNOR enzyme kinetics. Initial velocity V_0 is calculated by NADH decay at 340 nm. Each point represents reactions with certain concentration of GSNO, NADH and 2 ug/ml GSNOR. A) K_m of GSNO. NADH concentration was fixed at 100 µM for all reactions. GSNO concentration was varied from 0 to 750 µM. Initial velocities were plotted and fitted to an exponential curve. B) K_m of NADH. GSNO concentration was fixed at 250 µM for all reaction. NADH concentration was varied from 0 to 200 µM. Initial velocities were plotted and fitted to an exponential curve.

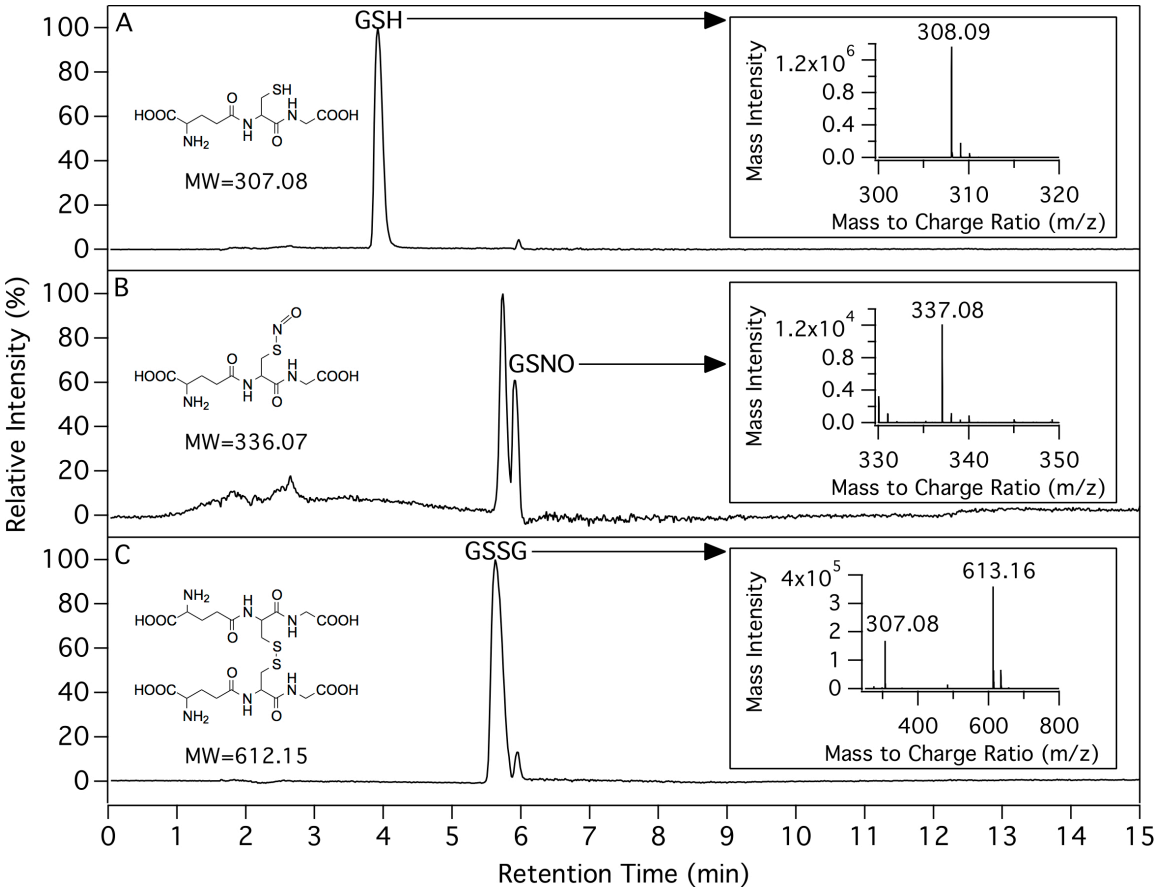

Figure 4-4. LC/MS standards. Relative intensity on the left axis shows the LC intensity relative to the highest peak. Sub-graphs show the extracted mass (positive mode) from arrow pointed peaks. A) reduced glutathione (GSH); B) s-nitrosoglutathione (GSNO); C) oxidized glutathione (GSSG).

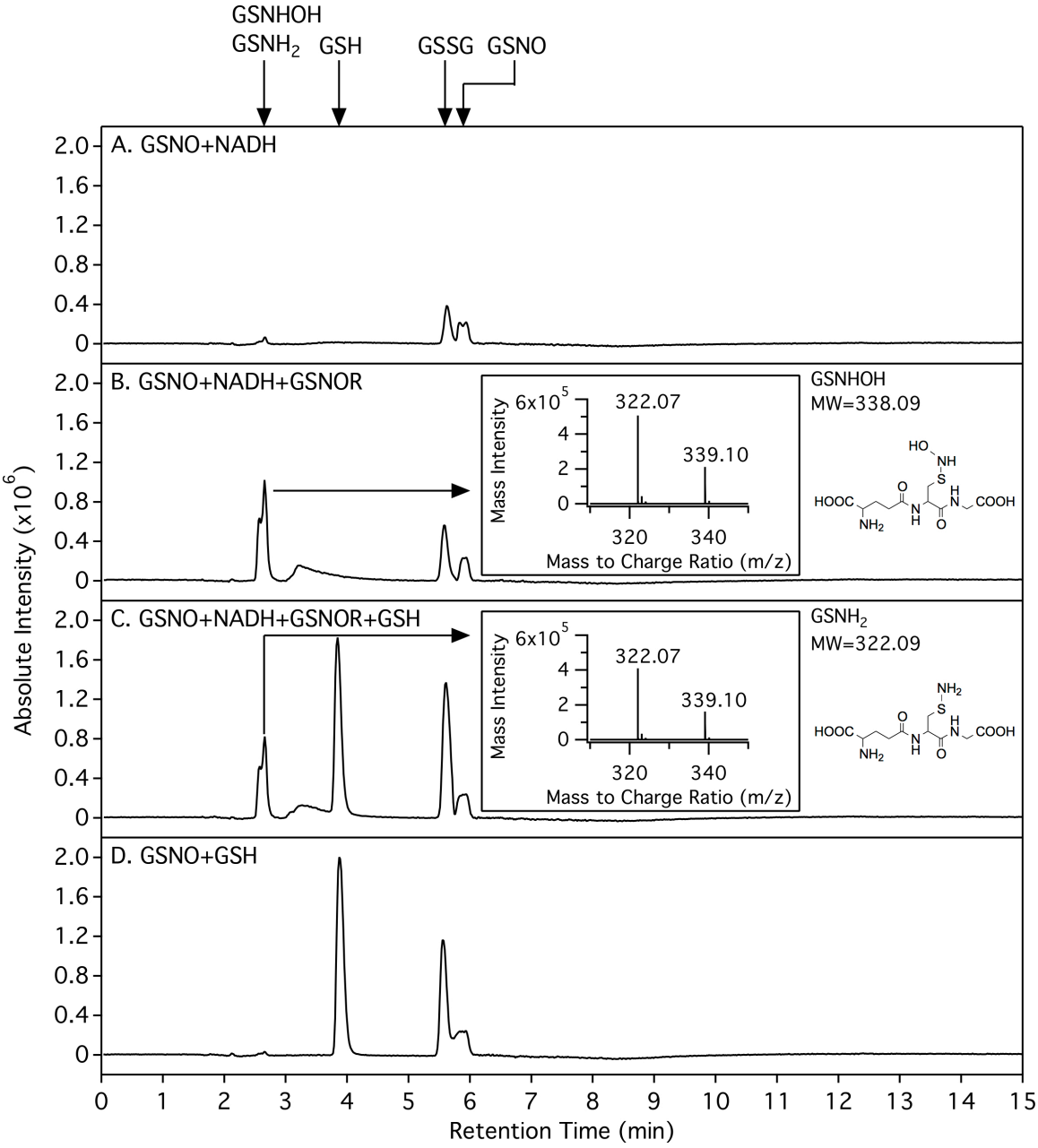

Figure 4-5. GNSOR produce analysis by LC/MS. Main graphs are LC intensities against retention time. A) negative control, 1 mM GSNO and 1 mM NADH. B) 1 mM GSNO, 1mM NADH with 2 µg/ml GSNOR. C) same as B, but added 1 mM GSH. D) negative control for C, 1 mM GSNO and 1 mM GSH. Sub-graphs show extracted mass (positive mode) for arrow pointed peaks. Products predicted from mass and their structures are shown on the right.

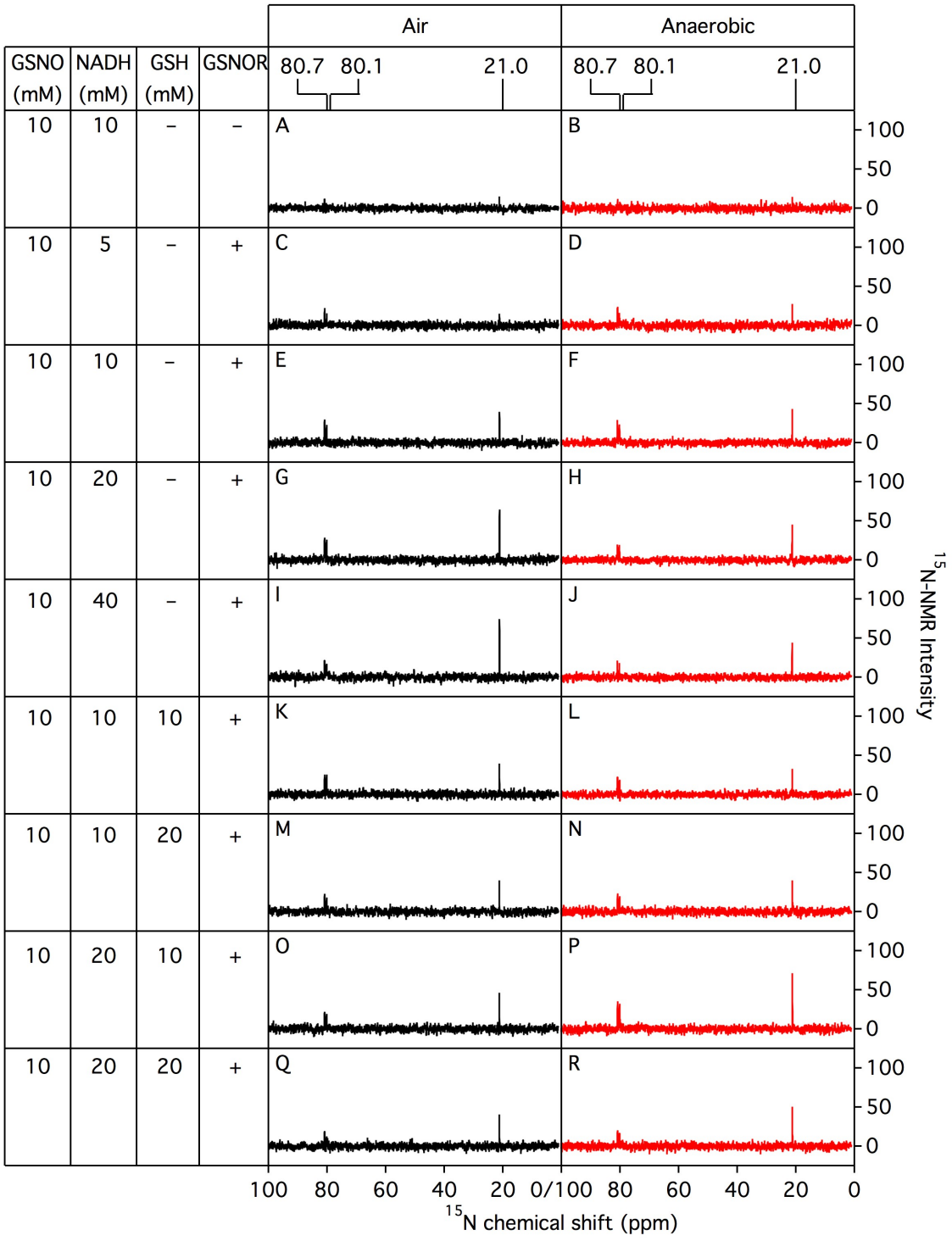

Figure 4-6. GSNOR product analysis by ^{15}N-NMR. ^{15}N labeled GSNO was used in all reactions. 1 ml reaction mixtures components and concentrations are listed in the table on left. Each reaction mixture was done twice, once in air (black), once in anaerobic chamber (red). All reactions were incubated for 1 hour after mixing and then ^{15}N-NMR spectrums were taken.

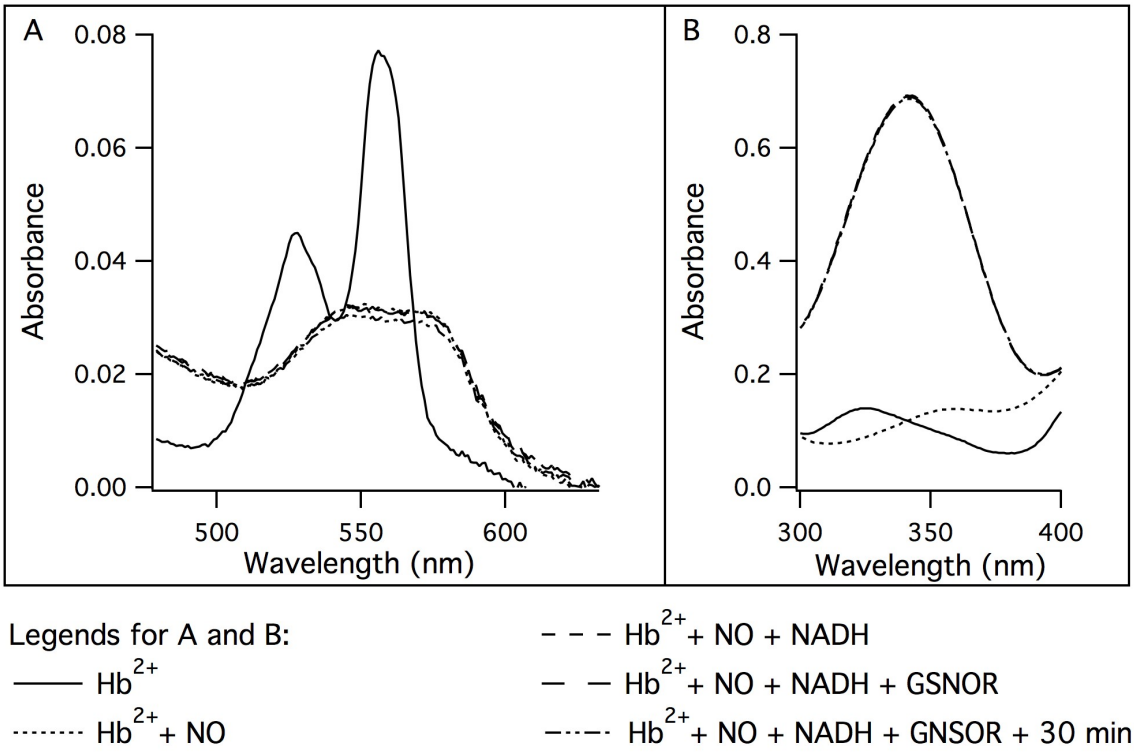

Figure 4-7. Test of hypothesis 1. A) and B) represents the spectrums at different wavelength for the same experiments. A) monitors heme peaks at visible range; B) monitors NADH peak at 340 nm. Legends are shown under graphs. Ferrous rice nsHb1 (Hb^{2+}) was first added in airtight cuvette in anaerobic chamber and its spectrum (solid line) was taken out side of chamber. Then NO saturated buffer was added into cuvette (dash line with small interval). Then 100 µM NADH was added (dash line with middle interval). Then 2 µg GSNOR was added (dash line with big interval). Then waited for 30 minutes and took the last spectrum (dash line with small/big intervals).

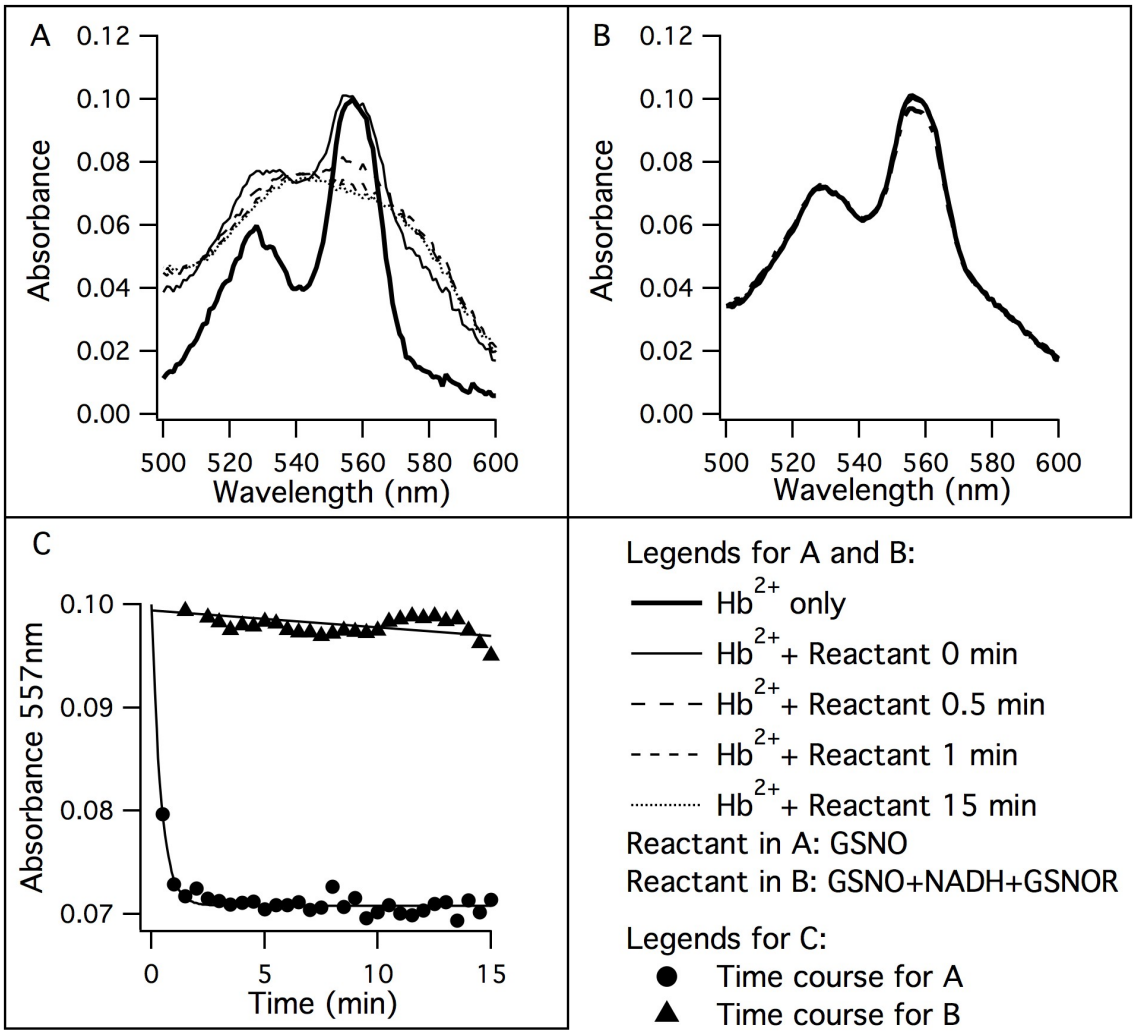

Figure 4-8. Test of hypothesis 2. Ferrous rice nsHb1 (Hb^{2+}) was first added in airtight cuvette in anaerobic chamber and its spectrum (bold solid lines) was taken out side of chamber. Then reactant was added to to Hb^{2+}. Right after adding reactant, spectrum was taken (thin solid lines). Reactant in A) was 100 μM GSNO; in B) was mixture of 100 μM GSNO, 200 μM NADH and 2 μg GSNOR, incubated in anaerobic chamber for 1h. Then after 0.5 minutes, 1 minute and 15 minutes, spectrums were taken, respectively represented by dash line with big, middle and small intervals. C) shows time courses of 557 nm for A (circle) and B (triangle).

CHAPTER 5

CONCLUSION

One physiological role of plant nonsymbiotic hemoglobins (nsHbs) was proposed to be nitric oxide (NO) scavenging via the NO dioxygenation (NOD) reaction with assistance of ascorbate (AA) and monodehydroascorbate reductase (MDHAR) [1]. This specific hypothesis was tested with two conclusions: 1) AA can slowly reduce nsHb, so potentially it can facilitate the reduction half of the NOD reaction for ferrous nsHb recycling. But the AA reduction of nsHb1 does not borrow a favor from MDHAR. 2) AA does not stimulate NO scavenging by nsHb under hypoxic conditions.

Under hypoxic or anoxic conditions, the NOD function of nsHb will be inhibited by low oxygen level. A more possible role of nsHb under such conditions is to reduce nitrite and produce NO. This is supported by the fact that plant nsHbs are much better nitrite reductases than other hemoglobins [2, 3]. At this point, dissimilatory NO reduction instead of NOD will be more beneficial for plants under hypoxia or anoxia pressure. However, the NO produced from nitrite reduction can form a very tight complex with ferrous nsHb and toxify it *in vitro*. But considering nsHbs are also efficient hydroxylamine reductases [4], it is still reasonable to hypothesize that nsHbs are dissimilatory nitrite reductases under hypoxic or anoxic conditions. If this is true, there has to be a mechanism *in vivo* for nsHb to over come the NO toxic effect. To find the possible factors involved in this mechanism, we need a proper biology screen. The *E.coli nirB* mutant (a nitrite reductase single gene knockout) was found to have a growth

deficient phenotype in glucose and nitrate minimal medium, therefor is a good screen for this purpose.

Plant s-nitrosoglutathione reductase (GSNOR) is potentially important for relieving hypoxic nitrosative stress [5, 6]. But our data proof that it does not facilitate plant nsHb to over come the NO toxic effect.

In the future, our priority is to use the *E.coli nirB* mutant to screen the plant root cDNA library and find possible cofactors for nsHb nitrite reduction under hypoxic or anoxic conditions.

References

1. Igamberdiev, A.U., N.V. Bykova, and R.D. Hill, *Nitric oxide scavenging by barley hemoglobin is facilitated by a monodehydroascorbate reductase-mediated ascorbate reduction of methemoglobin.* Planta, 2006. **223**(5): p. 1033-40.
2. Sturms, R., A.A. DiSpirito, and M.S. Hargrove, *Plant and cyanobacterial hemoglobins reduce nitrite to nitric oxide under anoxic conditions.* Biochemistry, 2011. **50**(19): p. 3873-8.
3. Tiso, M., et al., *Nitrite reductase activity of nonsymbiotic hemoglobins from Arabidopsis thaliana.* Biochemistry, 2012. **51**(26): p. 5285-92.
4. Sturms, R., et al., *Hydroxylamine reduction to ammonium by plant and cyanobacterial hemoglobins.* Biochemistry, 2011. **50**(50): p. 10829-35.
5. Valderrama, R., et al., *Nitrosative stress in plants.* FEBS Lett, 2007. **581**(3): p. 453-61.
6. Leterrier, M., et al., *Function of S-nitrosoglutathione reductase (GSNOR) in plant development and under biotic/abiotic stress.* Plant Signal Behav, 2011. **6**(6): p. 789-93.